Title
Identification of a function for the zinc coordination center of Shh and mechanisms of Smo inhibition by Ptch1/2 activity

Author
Jaegers, Carina Elena

Publication Date
2020

Peer reviewed|Thesis/dissertation

Identification of a function for the zinc coordination center of Shh and mechanisms of Smo inhibition by Ptch1/2 activity

By

Carina Elena Jaegers

A dissertation submitted in partial satisfaction of the

requirements for the degree of

Doctor of Philosophy

in

Molecular and Cell Biology

in the

Graduate Division

of the

University of California, Berkeley

Committee in charge:

Professor Henk Roelink, Chair
Professor Gian Garriga
Professor Helen Bateup
Professor David Bilder

Fall 2020

Abstract

Identification of a function for the zinc coordination center of Shh and mechanisms of Smo inhibition by Ptch1/2 activity

By

Carina Elena Jaegers

Doctor of Philosophy in Molecular and Cell Biology

University of California, Berkeley

Professor Henk Roelink, Chair

The Hedgehog (Hh) signaling pathway is critical for patterning during embryonic development in most animals. The three key components in mammals are the ligand Sonic Hedgehog (Shh), its receptors Patched1 and -2 (Ptch1/2), and the pathway activator Smoothened (Smo). In the absence of Shh, Smo is inhibited by a small antagonist that is thought to be transported across the cell membrane by Ptch1/2. In the genetic and functional analyses of single pathway components, three-dimensional aggregates of cells with varying genotypes pose a valuable proxy for the in vitro study of signaling events. I describe a protocol for the generation and analysis of such in vitro organoids where specific roles (like producing and responding cell) can be assigned to a fraction of the cells based on their genotype. Release of the ligand Shh from producing cells and the inhibition of Smo by Ptch1/2 in responding cells in the absence of Shh are central aspects of this thesis. I demonstrate a function for the zinc coordination center of Shh in the release of the protein from the cell into the extracellular matrix. Furthermore, I present the known Smo inhibitor 7-Dehydrocholesterol (7DHC) as a putative cargo for Ptch1/2. Ptch1/2 are not only required for 7DHC to be inhibitory but also exacerbate the Smo inhibitory effect of 7DHC.

Chapter 1

Introduction

Identification of the Hh signaling pathway

Embryonic development depends on the orchestration of signals to transform single cells into structured tissues and whole organisms. The central question is how genes, their temporal regulation, and subsequent molecular events result in the formation of an organism. The legendary forward genetic screen in *Drosophila melanogaster* conducted by Nüsslein-Volhard and Wieshaus in the late 1970s revealed a myriad of genes that played pivotal roles during development (Nüsslein-Volhard & Wieshaus, 1980). One of them was named *Hedgehog* (*Hh*), as incorrect function of this gene resulted in an embryo with widespread denticles, reminiscent of hedgehogs (Nüsslein-Volhard & Wieshaus, 1980). Other genes identified in this famed Heidelberg screen, *Patched (Ptc), Smoothened (Smo),* and *Cubitus interruptus (Ci)* were later assembled into a signaling network with Hh as the ligand, Ptc as a Hh receptor and suppressor of the response, Smo as the central signal transducer, and Ci as a transcription factor activating the expression of Hh target genes (Ingham, Taylor, & Nakano, 1991; Hepker et al., 1997; Alcedo et al., 1996).

Conservation

Perhaps one of the most remarkable findings following the Nüsslein-Volhard/Wieshaus screen was that nearly all genes essential for development in *Drosophila* had counterparts in all other bilaterians. As it is the case for most central developmental genes, the Hh pathway components and their function in signaling are well conserved throughout the animal kingdom as deep as the *Cnidaria* (Adamska et al., 2007). Whereas central components of the Hh signaling pathway are not found in porifera nor the pre-metazoan *Choanoflagellatae,* single components of the pathway are even present in bacteria (Roelink, 2018). Despite the remarkable conservation of components of the pathway, distinct parts and features have emerged in two widely studied organisms, *Drosophila melanogaster* and *Mus musculus*. Vertebrates have multiple paralogs coding for proteins in the central Hh pathway, and three Hh paralogs are present in mammals, Sonic hedgehog (Shh), Indian hedgehog (Ihh), and Desert hedgehog (Dhh) (Marigo et al., 1995). All ligand can activate the Hh response, but they differ in their location and timing of expression. Two paralogous receptors called Ptch1 and Ptch2 share overlapping functions and three Ci-homologs (Gli1, Gli2, and Gli3) each have specific properties in mammals. Of the three mammalian ligands, Shh has the most impactful contributions in embryonic development and is, therefore, most widely studied.

Shh as a morphogen that patterns the vertebrate developing neural tube

A morphogen, literally producer of shape, is a molecule that controls patterning of tissue development through non-uniform distribution. It is therefore of great interest to developmental biologists asking the question how patterns arise from a uniform group of cells. Although the underlying mechanisms of tissue patterning are conserved across different species, their organismal size varies quite drastically. A morphogen can provide size-invariant information so that patterns arise in proportion to the size of the organism, even when the system is perturbed (Almuedo-Castillo et al., 2018).

In a landmark paper from 1969, Wolpert introduced the French Flag Problem as a metaphor to address the necessary properties and communications of cells in one

dimension to form three distinct regions; the blue, white, and red portion of the French Flag (Wolpert, 1969). Every cell in a tissue is thought to have information about its global position in a field, called positional information. Wolpert postulated that positional information can not only be conveyed through temporal gradients or oscillating phases, but also through the formation and interpretation of a spatial gradient of a diffusible molecule, the morphogen. A spatial gradient has one area with the highest concentration, usually the site where the morphogen is synthesized, and ever decreasing concentrations away from the site of synthesis. The cells are able to detect their position in a gradient and translate it into a pattern of gene expression, resulting in the differentiation of the stereotypical cell types at the appropriate positions. The cells are thought to have a concentration-specific response to the morphogen with certain threshold levels for the induction of a class of cell fates, that in turn suppress the fates associated with lower Hh concentrations.

In the developing embryo, Shh and its receptor are largely expressed at complementary and adjacent sites, highlighting that, perhaps with a few exceptions, Shh signaling events are non-cell autonomous (Motoyama et al., 1998). Central developmental signaling events are orchestrated from several embryonic signaling centers called organizers, where originating signals influence the cell fate of surrounding cells (Spemann & Mangold, 1923). These cell populations with inducing activity were confirmed by transplantation experiments and mis-expression and genetic manipulation identified a central (but not unique) role for Shh in the orchestration of tissue patterning (Placzek, Tessier-Lavigne, Yamada, Jessell, & Dodd, 1990). Well-studied examples of "organizing" Shh signaling centers are the notochord, a structure involved in patterning of somites and the neural tube, and the zone of polarizing activity (ZPA), a structure central in limb and digit patterning along the anterior-posterior axis (Riddle, Johnson, Laufer, & Tabin, 1993).

The Shh-mediated induction of neural cell fates in the developing neural tube after neurulation is a classic example not only of non-cell autonomous Shh signaling from the mesoderm to the ectoderm, but also of the interpretation of a morphogen gradient by a tissue. After vertebrate gastrulation, cells from one of the three newly-formed germ layers, the ectoderm, are signaled to contribute to the nervous system by the underlying notochord of the mesoderm. The sheet of cells, also called the neural plate, begins to fold inwardly until the ends converge and close the now circular structure along the rostral-caudal axis with the notochord on the ventral and overlying ectoderm on the dorsal side of the embryo (Spemann & Mangold, 1923). The notochord and signals originating from this tissue are required and sufficient for the induction of ventral cell fates, as removal of the notochord abrogates the formation of the full repertoire of cell fates whereas notochord explants can induce ventral cell fates on transplanted tissue (Roelink et al., 1994; 1995). The contact-dependent inductive signal of ventral cell fates in the neural tube from the notochord was identified as Shh (Roelink et al., 1994). Shh is synthesized in the notochord and induces the formation of another organizer in the ventral midline of the neural tube, the floor plate (Placzek, 1995). The floor plate becomes a new site of synthesis for Shh and promotes the formation of a diffusible Shh gradient with the highest concentration at the floor plate. Besides floor plate cells, a specialized class of glia cells, two classes of motor- and interneurons are generated at slightly more dorsal positions (Jessell, 2000). The Shh

gradient along the ventral-dorsal axis is interpreted by cells in the neural tube via two classes of homeodomain proteins (Briscoe, Pierani, Jessell, & Ericson, 2000). The expression of class I transcription factors is repressed at certain thresholds of Shh signaling, whereas class II transcription factors are induced (Jessell, 2000). They act as intermediate factors in the interpretation of the Shh gradient and their combinatorial and cross-regulatory expression in the ventral neural tube eventually defines five progenitor cell domains. Both class I and II transcription factors have found wide acceptance as markers for cell fates in in vivo as well as in vitro experiments (Briscoe et al., 2000).

Mutations in the Hh pathway components have revealed its importance in development of all bilaterians. Reduced Hh signaling can lead to a number of severe birth defects in humans, among them holoprosencephaly, hypotelorism, and cleft palate (Roessler et al., 1996). Holoprosencephaly is the most common structural defect of the developing brain and characterized by a failure of formation of midline structures, resulting in an undivided forebrain. Mouse knock-out experiments have shown that complete absence of Shh or the signal transducer Smo are embryonically lethal at early developmental stages (Chiang et al., 1996; X. M. Zhang, Ramalho-Santos, & McMahon, 2001). *Shh*$^{-/-}$ mice have extensive defects affecting tissues adjacent to the normal sites of Shh expression, emphasizing the role of Shh as a central secreted signaling ligand (Chiang et al., 1996). Consistent with the idea that Smo is essential for all Hh signaling, *Smo*$^{-/-}$ mice are phenotypically similar to *Shh* and *Ihh* compound mutants that do not survive beyond 9.5 days post coitum (dpc) (X. M. Zhang et al., 2001).

Whereas developmental defects generally are caused by reduced Hh signaling, cancers usually arise due to increased activation of the Hh pathway. In pancreatic cancer for example, Shh is produced by tumor cells and activates the pathway in the neighboring stromal cells, thereby activating this compartment and creating a favorable environment for tumor cells (Bailey, Mohr, & Hollingsworth, 2009). Oncogenic Kras in the pancreatic cells promotes the aberrant production of Shh, which the pancreatic cells themselves do not respond to (H. Nakashima et al., 2006; Tian et al., 2009).

Other cancer driving mutations have been found in Ptch1/2, resulting in a loss of function of this tumor suppressor (Xie et al., 1997). Tumor-associated mutations in Smo either lock the protein in an active state or render it insensitive to inhibition (Unden et al., 1996; Xie et al., 1998; Yauch et al., 2009). Furthermore, some cases of Gallbladder cancer have underlying mutations in a specific area of the Shh ligand, presumably increasing its activity and providing an excellent opportunity to study the role of certain domains of the protein for normal Shh function (Dixit, Pandey, Tripathi, Dwivedi, & Shukla, 2017).

Hh signaling

Human Shh is synthesized as a 462 amino acid, 45 kDa protein that undergoes auto-processing mediated by the C-terminal domain. The result is the 20 kDa N-terminal mature signaling protein, covalently attached to a cholesterol at the C-terminal residue, and the C-terminal processing domain (Porter et al., 1995; Porter, Young, & Beachy, 1996). Subsequently, the acyltransferase skinny Hedgehog mediates lipidation of the of the N-terminal residue of the mature protein (Chamoun et al., 2001). This dual-lipidated molecule is commonly referred to as ShhNp and is thought to be membrane-bound (Peters,

Wolf, Wagner, Kuhlmann, & Waldmann, 2004). Release of ShhNp from the synthesizing cells into the environment – a crucial step in non-cell autonomous signaling – requires the function of the Ptch1 homolog Disp1, via a poorly understood mechanism (Etheridge, Crawford, Zhang, & Roelink, 2010). In addition, the release of ShhNp is facilitated by zinc-metalloproteases of the ADAM (a disintegrin and metalloprotase) family, glycosylated components of the extracellular matrix, and other scaffolding proteins like Scube2 (Dierker, Dreier, Petersen, Bordych, & Grobe, 2009; Jakobs et al., 2014). The inhibition of the signal transducer and GPCR Smoothened (Smo) in the absence of the ligand is non-stochiometric and mediated by a not yet unambiguously identified molecule, most likely a sterol (Taipale, Cooper, Maiti, & Beachy, 2002). Binding of Shh to the transmembrane transporter Ptch1 on responding cells blocks the transporter activity of Ptch1, leading to the release of Ptch1/2-mediated inhibition of Smo (Tukachinsky, Petrov, Watanabe, & Salic, 2016). Activation of Smo elicits an intracellular downstream transcriptional response mediated by the Gli family of transcription factors (Ruppert, Vogelstein, Arheden, & Kinzler, 1990). Gli transcription factors function as transcriptional repressors in the absence of the ligand due to post-translational processing that is inhibited upon Smo activation (Hynes et al., 1997). Target genes of the Gli transcription factors include Ptch1, creating a negative feedback loop (Hynes et al., 1997).

Components of the Hh signaling pathway in metazoans

All Hh ligands have two domains, a secreted N-terminus ("Hedge") and a "Hog" domain with autocatalytic activity (Bürglin, 2008). This setup is found in many protists and suggests that the Hog family of genes with different N-termini arose early in eukaryotic evolution. The structure of the auto-processing domain is homologous to that of self-splicing proteins (Hall et al., 1997): A reactive thio-sidechain of cysteine in the C-terminal "Hog" domain forms a thio-ester with the carbonyl carbon of the preceding glycine, an intermediate that is resolved via the nucleophilic attack of a lipophilic nucleophile (Porter et al., 1996). In case of Hhs, the hydroxyl group on the A ring of cholesterol can provide this nucleophilic center, resulting in the addition of cholesterol to Shh at the site of cleavage (Porter et al., 1996). Positioning a stop codon at the site of cleavage results in the form of Shh with a peptide structure identical to mature Shh but lacking the cholesterol moiety. This truncated version of Hh (usually referred to as HhN) is soluble and therefore commonly used in experiments, as production and harvesting of this form of ShhN is relatively straightforward. HhN retains signaling activity and even signals better in some assays (Casillas & Roelink, 2018). In mice expressing ShhN, the morphogenic gradient appears longer and flatter due to the altered physical properties. The response to the cholesterol-unmodified ligand, however, remains largely unchanged (Y. Li, Zhang, Litingtung, & Chiang, 2006). Nevertheless, this version remains a useful artificial proxy for the physiological ligand (Ingham & McMahon, 2001).

Another post-translational lipid modification is added to all Hhs in the Golgi before secretion from the cell: Hh acyltransferase (HHAT) or Skinny Hedgehog (Skn) catalyzes the amide linkage of palmitate to a conserved cysteine residue at the N-Terminus (Buglino & Resh, 2008; Chamoun et al., 2001). Neither autoprocessing nor cholesterol at the C-Terminus is required for palmitoylation. The importance of the C-Terminal lipid

modification becomes apparent again when it is absent: Mice lacking Hhat have severely disrupted Hh signaling, in particular long-range signaling, and restriction of Shh expression to the notochord (Dennis et al., 2012).

Lipid modifications at both the N- and C-Terminus of Shh tether it tightly into the cell membrane (Peters et al., 2004). Various models have emerged that aim to reconcile the insoluble properties of Hh ligands with signaling from the site of synthesis to recipient cells, oftentimes over considerable distances (Briscoe & Thérond, 2013). Shh can form multimers reminiscent of micelles with the hydrophobic lipid modifications in the center of the multimer, thereby rendering the proteins soluble (Chen, Li, Kawakami, Xu, & Chuang, 2004). Another way of solubilizing the protein is to enzymatically remove the lipid modifications, a process called "shedding" and involving members of a disintegrin and metalloprotease (ADAM) family and the scaffolding protein Scube2 (Tukachinsky, Kuzmickas, Jao, Liu, & Salic, 2012). Alternatively, carriers of Hh ligands like exosomes, liposomes, and cytonemes are harnessed to transport the signaling molecule from producing to recipient cells (Ohlig et al., 2012; Palm et al., 2013; Roy, Huang, Liu, & Kornberg, 2014). Exosomes are extracellular vesicular particles originating from endocytic multivesicular bodies or derived from apical microvilli (Tanaka, Okada, & Hirokawa, 2005). Liposomes are assembled from lipophorin apolipoproteins that can be recruited from the heparan sulfate sidechains of glypicans, an extracellular matrix protein that Shh interacts with (Eugster, Panáková, Mahmoud, & Eaton, 2007). Finally, cytonemes are specialized filopodia in both Drosophila and vertebrates. These highly dynamic basal filopodia can be decorated with Hh and deliver the signaling molecule over some distance to recipient cells (Roy et al., 2014). The cellular context and functional impact of each of these modes of transport, however, is contentious.

The structure of ShhN

The protein sequence of ShhN can be divided into three domains with distinct functions: 1) the N-terminal Ptch1/2-binding domain, 2) the calcium coordination domain encompassing the large alpha-helix, and 3) the zinc coordination domain. Structurally, Hh consists of five antiparallel beta-sheets that separate a large alpha-helix from the zinc coordination center (Hall, Porter, Beachy, & Leahy, 1995). Furthermore, two calcium ions can be coordinated in close proximity to the zinc coordination center. Three residues (H141, D148, and H183, mouse numbering) coordinate a zinc ion and occupancy of this coordination site by zinc is imperative to the structural integrity of Shh and increases the half-life of the protein (Day et al., 1999). Initial crystallographic studies recognized the overall structure of the bioactive Hh ligand to be similar to peptidases of the M15 family of D-Ala-D-Ala carboxypeptidases (DD peptidase) that, in addition to Zn^{2+} in their active center, also coordinate two calcium ions (Hall et al., 1995). The protein sequence of the Shh calcium and zinc coordination domains have a remarkable 65 % sequence identity with several bacterial proteins (Roelink, 2018). *Mesorhizobium* and *Bradyrhizobium* can code for a protein that has in which the identity to Shh includes all calcium and zinc coordinating residues and are thus referred to as "bacterial Hh" (BacHh) (Roelink, 2018). DD-peptidases initiate catalysis of their substrates with the abstraction of a proton from the catalytic water in close proximity to the zinc via the reactive sidechain of a glutamic

acid (the equivalent in murine Shh would be E177). This is followed by a nucleophilic attack of the resulting hydroxide on the carbonyl carbon of the peptide backbone. Two additional histidine residues (H135 and H181) then create a pentacoordinate intermediate state that is resolved into the hydrolyzation products (Cerdà-Costa & Gomis-Rüth, 2014).

The extracellular matrix and Shh distribution

Shh binds to heparan-sulfate via a series of positively charged lysines and arginines in an unstructured stretch of the N-Terminus, called the Cardin-Weintraub motif (Esko & Selleck, 2002; Farshi et al., 2011). This binding is crucial in the process of releasing Shh from the producing cell, the shedding (Jakobs et al., 2016). HS as well as another scaffolding protein, Scube2, guide Shh to metalloproteases that remove the N-terminal palmitoyl modification (Jakobs et al., 2017). Up to six Shh molecules binding a stretch of HS has been shown, a feature that has found wide popularity in the tag-free protein purification process of Shh using HS affinity columns (Whalen et al., 2013).

Heparan-sulfate proteoglycans (HSPGs) are cell-tethered or untethered components of the extracellular matrix and characterized by a protein core and O-linked heparan-sulfate side chains of varying lengths (Sarrazin, Lamanna, & Esko, 2011). As a member of the glycosaminoglycan family of carbohydrates, heparan sulfate consists of disaccharide units with varying sulfatations (Varki et al., 2009). The varying lengths of the HS side chains in combination with different glucosaminoglycan units produces a multitude of variations in the HS composition across different tissues, sometimes referred to as the "heparome" (Turnbull, Powell, & Guimond, 2001). Initial steps in the post-translational chain formation include the addition of xylose to a serine residue of the core protein by xylosyltransferase, followed by the addition of two galactose residues and glucuronic acid by galactosyltransferases I and II and glucuronosyltransferase (Almeida et al., 1997; Müller et al., 2005). Exostosin 1 and 2 (Ext1 and Ext2) are glycosyltransferases that act as heterodimers in the elongation of the side chains. As tumor suppressors, mutations in these genes cause developmental diseases as well as tumors (Lind et al., 1998).

Morphogenetic signaling by Shh is most easily explained by the graded distribution of Shh away from the sources of synthesis. The precise mechanisms of Shh transport away from the cells is unknown, but genetic evidence show an important role for HSPGs. In *Drosophila*, mutations in the Glypican orthologs *dally* and *dally-like* or the Ext1/2 orthologs *tout velu* and *brother of tout velu* reduce the signaling range of Hh due to disruption of Hh spread (Bellaiche, The, & Perrimon, 1998; Han et al., 2004). In mammals, both the HSPG core proteins, Glypicans, as well as the enzymes elongating the HS side chains, Ext1/2, are tumor suppressors. Additionally, the loss of Ext1/2 causes severe embryonic defects and effects embryonic Shh distribution and response in mice (Lin et al., 2000; Stickens, Zak, Rougier, Esko, & Werb, 2005), highlighted by a hypomorphic allele of Ext1 that increases the range of Ihh signaling (Koziel, Kunath, Kelly, & Vortkamp, 2004). In vitro experiments showed that the loss of Gpc5 or Ext1/2 in recipient cells results in the accumulation of extracellular Shh, indicating that HSPGs are involved in sequestration of extracellular Shh (Capurro et al., 2008; Guo & Roelink, 2019). HSPGs are also involved in the transport of Shh to the recipient cells. In in vitro experiments where *Ext1/2*$^{-/-}$ or *Gpc5*$^{-/-}$ cell were

assigned the role of "transporting cells", the non-cell autonomous response to Shh was increased in Ext1/2 or Gpc5 competent recipient cells (Guo & Roelink, 2019).

Is Shh a peptidase?

Although the sequence and structure of Shh is reminiscent of zinc-metalloprotease, functional studies rejected the idea of Shh having proteolytic activity and the zinc-coordination center was declared "pseudo-active" and a Ptch1-binding site (Fuse et al., 1999; Hall et al., 1995). In these studies, purified recombinant ShhNp elicited a Hh response when added to the medium of chicken intermediate neural plate explants, arguing against a role of the putative peptidase activity of Shh in the reception of the signal but not of earlier steps like the release of Shh from producing cells. Informed approaches with a variety of substrates, including known targets for DD-carboxypeptidases, failed to reveal any Shh peptidase activity (Fuse et al., 1999).

Bacterial operons are functional entities of genes under the control of a single promoter and the genes in one operon usually code for proteins with similar functions or proteins that function in the same pathway (Jacob, Perrin, Sanchez, & Monod, 1960). Therefore, operons are a useful tool to infer the function of an unknown protein by comparing the sequence and function of the gene product to those in the same operon. In *Mesorhizobium* and *Bradyrhizobium,* BacHh can be found in operons together with other genes that code for cell-wall degrading proteases like lysozyme, a peptidoglycan endopeptidase, N-acetylmuramoyl-L-alanine amidase, and several trypsin homologs, suggesting a role for BacHh in the degradation and/or remodeling of the bacterial cell wall (Roelink, 2018). A major component of the cell wall and the periplasmatic space are peptidoglycans or murein, a mesh-like structure consisting of long chains of carbohydrates and short (3-5 amino acids) peptide chains connecting the carbohydrate chains (Meroueh et al., 2006). As bacteria incorporate D-amino acids in peptidoglycan, DD-peptidases are predicted to specifically cleave bacterial peptidoglycans (Aliashkevich, Alvarez, & Cava, 2018).

Ptch1 and Ptch2 – Reconciling their roles as RND transporters, Smo inhibitors and Shh receptors

Mammals have two Ptch paralogs with largely complementary expression with Shh. In the vertebrate neural tube for example, Ptch1 is expressed in a gradient with the highest expression adjacent to the floor plate and notochord, both structures that express Shh. Once Shh-expressing floor plate cells are established, Ptch1 expression disappears from those cells (Goodrich, Johnson, Milenkovic, McMahon, & Scott, 1996). During epidermal development in the tooth and hair follicle on the other hand, Ptch2 and Shh are co-expressed in epithelial cells (Motoyama et al., 1998).

Concurrent biochemical studies revealed binding of vertebrate Shh to the second extracellular loop of the 12-pass transmembrane protein (Gong et al., 2018; Qi, Schmiege, Coutavas, Wang, & Li, 2018). An ancient, internal duplication of the gene presumably gave rise to a six-plus-six transmembrane structure with two large extracellular loops, producing an internal symmetry in the structure (Hausmann, Mering, & Basler, 2009). Although Ptch1 and Ptch2 share overlapping functions, Ptch1 is thought to be the main molecule regulating

the canonical Shh response. Ptch2, however, can substitute in the absence of Ptch1 (Alfaro, Roberts, Kwong, Bijlsma, & Roelink, 2014).

Ptch1/2, together with another component in Shh signaling, Dispatched, belong to the resistance-nodulation-division (RND) superfamily of transporters. Other members of this family include NPC1 and bacterial and archaeal proton-driven antiporters (Tseng et al., 1999). RND transporters are small-molecule efflux pumps that, in complexes with other structural proteins, span the inner and outer wall of gram-negative bacteria (Z. Wang et al., 2017). Protons accumulating in the periplasmatic or intermembrane space create an electrochemical pH gradient that is utilized by RND transporters to drive the transport of their cargo in exchange for a proton (Hausmann et al., 2009). As a proton gradient across the cell membrane does not exist in metazoans, Ptch1/2 has been suggested to use the naturally occurring sodium gradient at the cell membrane to efflux its cargo or function in acidified compartments like late endosomes and trans Golgi (Myers, Neahring, Zhang, Roberts, & Beachy, 2017). The cargos for bacterial RND transporters are in many cases not known and assumed to be diverse. Best studied members of the RND family transport beta-lactam antibiotics, thereby providing antibiotic resistance and posing a grave challenge in modern medicine. In the quest of identifying the cargo for Ptch1/2, functional counterparts in bacteria have been consulted. Hopanoid biosynthesis genes are located directly adjacent to a subfamily of RND transporters, therefore presumably forming co-transcribed functional entities (Perzl et al., 1998). Hopanoid is a structural and functional analog to sterols and the cargo for a bacterial transporter with remarkably high sequence similarity to Ptch1, suggesting that the Ptch1/2 cargo is a sterol (Hausmann et al., 2009). Other evidence that the Ptch1/2 cargo is a sterol comes from a conserved domain in RND transporters, the sterol-sensing domain (SSD). This domain formed in 5 of the transmembrane regions of Ptch1/2 is able to bind cholesterol and is present in proteins that have functions in cholesterol signaling and metabolism (V. Martin, Carrillo, Torroja, & Guerrero, 2001). A definitive experiment showing the transport of cholesterol (or another molecule) by Ptch1/2, however, has not been performed, leaving this aspect as one of the main open questions in the field.

RND transporters are understood to function as obligate homotrimers, a feature that has been shown to be true for Disp1 as well (Etheridge et al., 2010). Crystallographic studies on AcrB, an RND transporter in *Escherischia coli (E. coli)*, together with its cargos suggested that RND transporters function as "peristaltic pumps", where each monomer of the trimer is in different conformations at a time (Murakami, Nakashima, Yamashita, Matsumoto, & Yamaguchi, 2006). Ptch1/2 might also function in this fashion, as mutations in the membrane-spanning pore are dominant negative, presumably leaving the complex stalled. The variety of cargos for RND transporters can be explained with different entry routes for the cargo. Besides the central transmembrane pore created by the trimer, an opening at the side of the protein in the periplasmic space can be a point of entry (Murakami et al., 2006; Seeger et al., 2006). Although Ptch1/2 lacks the periplasm-spanning accessory proteins of RND transporters, alternative entry points for cargos have been speculated as well, in particular a site adjacent to the SSD and in the extracellular loops. Furthermore, evidence was presented that Ptch1, as some prokaryotic RND

transporters, might function as a lipid flippase, influencing the lipid composition of the inner membrane leaflet (Y. Zhang et al., 2018).

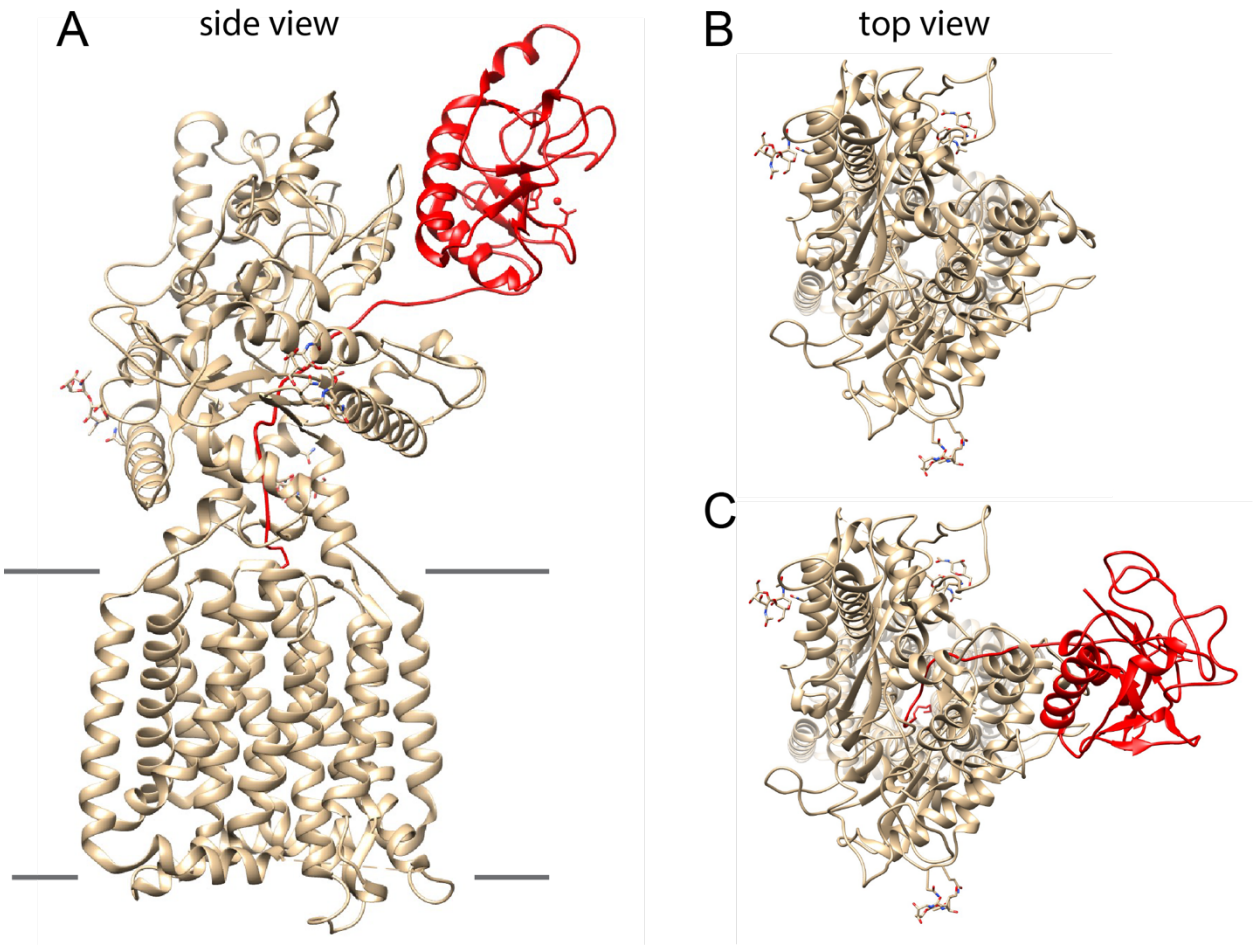

Figure 1. Structure of Ptch1 bound to ShhN. A: Side view: Shh is shown in red., Ptch1 in beige. Note the insertion of the N-terminal domain deep into Ptch1, close to the transmembrane region. Lines indicate the position of the membrane. **B: Top view.** The putative proton channel runs straight through the center of the molecule. **C:** as in B, but with Shh shown as well. Note that the N-terminus of Shh resides inside the putative proton channel, likely preventing proton-driven antiporter activity.

Another member of the RND superfamily might provide insight into the function and cargo for Ptch1/2. Genetic studies in mice revealed mutations in a transporter of the RND superfamily that was given the same name as an autosomal recessive disorder in humans, Niemann-Pick Type C1 (NPC1) (Karten, Peake, & Vance, 2009; Loftus et al., 1997). In the absence of the transporter, cholesterol homeostasis is impaired and lipids like cholesterol and sphingomyelin accumulate in acidic cellular compartments like endosomes and lysosomes (Karten et al., 2009). NPC1 normally regulates the cellular uptake of cholesterol from the extracellular space to the cytoplasm via endosomes and it can bind cholesterol at its SSD with nanomolar affinity, suggesting that its cargo is a sterol and that it functions in

a compartment with a proton gradient (Infante et al., 2008). This further suggests that the cargo of Ptch1/2 is a sterol.

Ptch1/2 is an inhibitory component of the pathway in the absence of the ligand. This inhibition can be reversed upon binding of Hh to Ptch1/2, and two distinct sites have been described. Biochemical and cryo-EM studies show the palmitoylated N-terminus of Shh inserting into the ion pore of Ptch1, close to its transmembrane domains and the N-terminus suffices to regulate Ptch1 activity (Figure 1) (Qi et al., 2018; Tukachinsky et al., 2016). An additional binding site was identified in the extracellular loops of Ptch1 and is more likely involved in the internalization of Ptch1/2 and Shh, thereby only indirectly affecting the response (Incardona et al., 2000; Rudolf et al., 2019).

Smoothened

Smoothened (Smo) is a 7-pass transmembrane G-protein coupled receptor (GPCR) of the class F and most conserved with Frizzled, the receptor for Wnt (van den Heuvel & Ingham, 1996). Smo is the sole transducer of the Hh signal, but a binding interaction between Smo and Ptch1/2 has not been shown. Instead, Smo is subject to a catalytic negative regulation by Hh-unbound Ptch1/2 in a sub-stochiometric fashion (Taipale et al., 2002). Sequestration of a Smo agonist by Ptch1/2 has been discussed as a possible mechanism for Smo inhibition by Ptch1/2, but the prevailing model in the field remains that Ptch1/2 utilizes the transport of a small molecule inhibitor to regulate Smo activity (Sharpe, Wang, Hannoush, & de Sauvage, 2015). Besides this canonical model of Smo inhibition and activation, evidence exists for cell autonomous Smo activation by Shh in the absence of Ptch1/2. (Casillas & Roelink, 2018)

An antenna-like cellular compartment called the primary cilium constitutes an important cellular compartment for many Shh pathway components in vertebrates. Ptch1 resides in primary cilia in the absence of the Shh ligand and switches places with Smo upon Shh binding (Rohatgi, Milenkovic, & Scott, 2007). Smo re-localization to the primary cilium is essential for activation of the downstream intracellular signaling response, as many components of this cascade can also be found in this organelle (Corbit et al., 2005). Thus, localization of Smo at the primary cilium has become a widely-used assay for transcriptional Hh pathway activation.

Besides the transcriptional response initiated by Smo from the primary cilium, activated Smo can be found in other intracellular locations like the endosome (Bijlsma, Damhofer, & Roelink, 2012). Shh is a cellular chemoattractant guiding commissural axons and retinal ganglion axons (Bijlsma, Borensztajn, Roelink, Peppelenbosch, & Spek, 2007). The chemotactic response is mediated by Smo outside of the primary cilium without requiring any *de novo* transcription or Gli proteins. *Drosophila* cells, notably, do not have primary cilia and Smo function, therefore, seems to have diverged between species. While *Drosophila* Smo cannot activate a transcriptional response in mouse cells, chemotactic signaling is even more efficient with *Drosophila* Smo than with mouse Smo, suggesting that the chemotactic function is evolutionarily more conserved than transcriptional activation (Bijlsma et al., 2012).

Smo is a potent oncogene and has therefore received tremendous attention aiming to find small molecule inhibitors as a therapeutic approach. A panel of synthetic and

naturally occurring small molecules has been classified into two categories based on the localization of binding (Sharpe et al., 2015). Smo possesses the typical architecture of GPCRs with 7 transmembrane helices that bundle together and an N-terminal extracellular domain that is rich in cysteine residues (cysteine rich domain, CRD) (C. Wang et al., 2013). Both the CRD and the heptahelical bundle in the transmembrane domain (TMD) are sites where small molecules can bind. The localization does not, however, predict the effect of small molecules on Smo, as both agonists and antagonist can bind to the CRD and TMD. The intracellular C-terminal tail constitutes a small helix closely associated with the membrane and thought to induce a small conformational change upon activation (Zhao, Tong, & Jiang, 2007). Co-crystallizations with Smo and bound agonists or antagonists were utilized to shed light on Smo dynamics and the dimerization of the cytoplasmic tails in particular.

Small molecules inhibiting the CRD or TMD

The first small molecule regulating Smo was discovered following a series of serious birth defects in lambs in Idaho (Keeler & Binns, 1968). The phenotype of lambs whose mothers consumed the wild plant *Veratum californicum* during gestation resembled those seen in congenital Shh perturbations and led eventually to the conclusion that the sterol-like molecule cyclopamine produced by the plant inhibits Shh signaling via binding to Smo at the heptahelical bundle (Chiang et al., 1996; Roessler et al., 1996; Taipale et al., 2000). Even within the class of small molecules binding to the TMD, different binding sites have been identified. Cyclopamine binds Smo relatively superficially and predominantly to the extracellular loops linking the transmembrane helices, therefore sometimes referred to as the "cyclopamine-binding pocket", whereas another antagonist, SANT-1, deeply inserts into the hydrophobic transmembrane region (C. Wang et al., 2014; Weierstall et al., 2014). Despite eliciting opposing effect on Smo, the Smo agonist SAG binds at a similar location and even shares many binding contacts with cyclopamine in the TMD (C. Wang et al., 2014).

The CRD of Smo is required for chemotactic response through regulating ciliary localization as well as cell-autonomous and Ptch1/2-independent transcriptional response (Aanstad et al., 2009). Wnts can bind Frz receptors via a hydrophobic groove in the CRD, but no such interaction of Smo with a ligand has been shown (Janda, Waghray, Levin, Thomas, & Garcia, 2012). Instead, the CRD of Smo can bind a variety of sterols with activating consequences (Myers et al., 2013; Nedelcu, Liu, Xu, Jao, & Salic, 2013). Of particular interest are oxysterols, oxidized derivatives of cholesterol, that occur naturally in the cell membrane and promote ciliary accumulation and activation of Smo (Dwyer et al., 2007; Rohatgi et al., 2007). The CRD is thought to be an allosteric binding site for small molecule Smo modulators like oxysterols, and the endogenous Smo inhibitor(s) could use both the TM and the CRD for optimal regulation of the Hh response (Sharpe et al., 2015).

The cholesterol synthesis pathway and Hh signaling – a way to find the Smo inhibitory molecule?

Hedgehog signaling and other important signaling networks rely on cholesterol, which is why cholesterol homeostasis, too, is critical for proper growth and development. *De novo*

synthesis of cholesterol from Acetyl-CoA requires a multitude of enzymatically catalyzed steps and can broadly be divided into the pre- and post-squalene pathway (Porter & Herman, 2011). In the first step of the post-squalene pathway, the linear squalene is cyclized to lanosterol, which represents a commitment to sterol synthesis. The following enzymatic reactions include reduction and isomerization of double bonds and reduction of methyl groups (Bloch, 1965). The linear pathway of cholesterol synthesis is named after the researchers that contributed significantly to the elucidation of the mechanism and were awarded a Nobel Prize for their work, Konrad Bloch and Feodor Lynen (Bloch, 1965). Shortly after, a parallel pathway was proposed by Kandutsch and Russell, arguing that the reduction of a double bond in the aliphatic side chain of cholesterol can be catalyzed by 3β-hydroxysterol Δ24-reductase (DHCR24) in between any step (Kandutsch & Russell, 1960). This depiction of two parallel pathways, referred to as the "Bloch" and "Kandutsch and Russell" pathways.

The extent of cholesterol contribution to normal development becomes particularly apparent in congenital malformations with underlying mutations in the cholesterol biosynthesis pathway. The most common malformation syndrome with underlying mutations in cholesterol synthesis genes is the Smith-Lemli-Opitz syndrome (SLOS), named after the physicians that first delineated it in 1964 (Smith, Lemli, & Opitz, 1964). SLOS is an autosomal recessive disorder caused by mutations in the gene coding for the 7-dehydrocholesterol reductase (DHCR7) (Waterham et al., 1998). This enzyme catalyzes the last step of cholesterol synthesis, the reduction of the immediate cholesterol precursor 7-dehydrocholesterol (7DHC) to cholesterol. Hence, mutations in the DHCR7 cause an increase in 7DHC and a decrease of cholesterol levels (Irons, Elias, Salen, Tint, & Batta, 1993). The spectrum of phenotypes in SLOS is broad and can range from mild symptoms like minor physical abnormalities and behavioral problems to lethal malformations (Ryan et al., 1998). The most common anatomical anomaly is a syndactyly of the second and third digit and craniofacial anomalies include microcephaly and cleft palate (Ryan et al., 1998).

Given the numerous biological functions of cholesterol as a component of cellular membranes, structural element of lipid rafts, and precursor of steroid hormones, oxysterols, and neuroactive steroids, it is self-evident that the pathogenesis of SLOS cannot be traced to a single pathogenic mechanism. In addition to its various functions in cellular homeostasis, cholesterol has many shown and suspected functions in Hh signaling that could contribute to SLOS pathogenesis. The resemblance of malformations seen in SLOS with those of developmentally impaired Shh signaling led researchers to the conclusion that Shh could be malfunctioning in patients with SLOS (Roessler et al., 1996; Ryan et al., 1998). Although the exact mechanism of Shh signaling impairment is not known, several models exist. The most obvious hypothesis, that a lack of cholesterol prevents Shh auto-processing and the simultaneous covalent addition of cholesterol to the new C-Terminus, however, could be refuted with studies showing the possibility of substitution of cholesterol with other sterols, yielding a functional morphogen (Cooper et al., 2003; Zhao et al., 2019). Instead, reduced total sterol levels were shown to inhibit Smo in mouse fibroblasts, causing impaired Shh signal transduction in the responding cell (Cooper et al., 2003). Other studies demonstrated an inhibitory effect of vitamin D3, a metabolic product of 7DHC, and oxysterols on Smo (Bijlsma et al., 2006). A less pursued hypothesis stipulates

that the disturbance of lipid rafts in the cell membrane could alter Shh signaling (Keller, Arnold, & Fliesler, 2004). Lipid rafts are discrete domains in the cell membrane with a distinct lipid composition and play a major role in signal transduction (Lingwood & Simons, 2010). Alterations in their composition and therefore physiochemical properties can have grave consequences for the dispatching and reception of signals, Shh among others. Shh enriches in lipid rafts before it is secreted, presumably in a potent form acting at a long range (Long, Winterbottom, & Robbins, 2015).

Two other congenital malformation syndromes with underlying mutations in genes coding for enzymes involved in cholesterol synthesis, lathosterolosis and desmosterolosis, are less well characterized and oftentimes confused with SLOS, presumably due to their rarity and overlapping phenotypic appearances in patients (Porter & Herman, 2011).

In vitro modeling of the developing neural tube

The complexity of developing organisms gives rise to certain limitations when studying developmental processes in model organisms, especially on a molecular level. Two-dimensional tissue culture experiments have shed light on numerous aspects of Shh signaling, but the advent of three-dimensional tissue culture systems and organoids enabled studying intercellular cell signaling events in a more physiological setting that is amenable to genetic manipulation. In particular, experiments investigating aspects of gradient formation and interpretation as well as cell-migration events benefit from more complex experimental setups. The generation of in vitro organoids from pluripotent stem-cells is established to date for numerous tissues like the brain, kidneys, intestine, and skin. When modeling the brain, three-dimensional organoids can be cultured for an extended period of time and develop defined brain regions reminiscent of human cortical development by culture day 30 (Lancaster et al., 2013). With the appropriate culture conditions, mouse embryonic stem cells (mESCs) can acquire embryonic lineages in organoids, or embryoid bodies, from their undifferentiated state in a two-dimensional tissue culture (G. R. Martin, 1981). In this process, addition of the endogenous patterning molecule retinoic acid aids in the acceptance of a pro-neural fate (Bain, Kitchens, Yao, Huettner, & Gottlieb, 1995). These organoids mimic the neural tube and are therefore referred to as spinal cord organoids (SCOs). While the “default” state of the cells in SCOs is the expression of markers of dorsal neural cell fates, ventral cell fates can be induced by activation of the Shh response in the cells (Alfaro et al., 2014; Meinhardt et al., 2014; Wichterle, Lieberam, Porter, & Jessell, 2002).

The Hh pathway is complex and many details are not well understood. There are several obvious observations that are still waiting to be reconciled with the canonical interpretation of the Hh pathway. In this thesis I will provide evidence that addresses the function of Ptch1 as a member of a large family of proton-driven antiporters in its role to inhibit Smo, and the apparent nature of Shh as a zinc metallopeptidase related to bacterial peptidoglycan peptidases.

References

Aanstad, P., Santos, N., Corbit, K. C., Scherz, P. J., Trinh le, A., Salvenmoser, W., et al. (2009). The extracellular domain of Smoothened regulates ciliary localization and is required for high-level Hh signaling. *Curr Biol*, *19*(12), 1034–1039.

Adamska, M., Matus, D. Q., Adamski, M., Green, K., Rokhsar, D. S., Martindale, M. Q., & Degnan, B. M. (2007). The evolutionary origin of hedgehog proteins. *Curr Biol*, *17*(19), R836–7.

Alcedo, J., Ayzenzon, M., Ohlen, Von, T., Noll, M., & Hooper, J. E. (1996). The Drosophila smoothened gene encodes a seven-pass membrane protein, a putative receptor for the hedgehog signal. *Cell*, *86*(2), 221–232.

Alfaro, A. C., Roberts, B., Kwong, L., Bijlsma, M. F., & Roelink, H. (2014). Ptch2 mediates the Shh response in Ptch1-/- cells. *Development*, *141*(17), 3331–3339. http://doi.org/10.1242/dev.110056

Aliashkevich, A., Alvarez, L., & Cava, F. (2018). New Insights Into the Mechanisms and Biological Roles of D-Amino Acids in Complex Eco-Systems. *Frontiers in Microbiology*, *9*, 683. http://doi.org/10.3389/fmicb.2018.00683

Almeida, R., Amado, M., David, L., Levery, S. B., Holmes, E. H., Merkx, G., et al. (1997). A family of human beta4-galactosyltransferases. Cloning and expression of two novel UDP-galactose:beta-n-acetylglucosamine beta1, 4-galactosyltransferases, beta4Gal-T2 and beta4Gal-T3. *Journal of Biological Chemistry*, *272*(51), 31979–31991. http://doi.org/10.1074/jbc.272.51.31979

Almuedo-Castillo, M., Bläßle, A., Mörsdorf, D., Marcon, L., Soh, G. H., Rogers, K. W., et al. (2018). Scale-invariant patterning by size-dependent inhibition of Nodal signalling. *Nat Cell Biol*, *20*(9), 1032–1042. http://doi.org/10.1038/s41556-018-0155-7

Bailey, J. M., Mohr, A. M., & Hollingsworth, M. A. (2009). Sonic hedgehog paracrine signaling regulates metastasis and lymphangiogenesis in pancreatic cancer. *Oncogene*, *28*(40), 3513–3525.

Bain, G., Kitchens, D., Yao, M., Huettner, J. E., & Gottlieb, D. I. (1995). Embryonic stem cells express neuronal properties in vitro. *Developmental Biology*, *168*(2), 342–357. http://doi.org/10.1006/dbio.1995.1085

Bellaiche, Y., The, I., & Perrimon, N. (1998). Tout-velu is a Drosophila homologue of the putative tumour suppressor EXT-1 and is needed for Hh diffusion. *Nature*, *394*(6688), 85–88. http://doi.org/10.1038/27932

Bijlsma, M. F., Spek, C. A., Zivkovic, D., van de Water, S., Rezaee, F., & Peppelenbosch, M. P. (2006). Repression of smoothened by patched-dependent (pro-)vitamin D3 secretion. *PLoS Biol*, *4*(8), e232.

Bijlsma, M. F., Borensztajn, K. S., Roelink, H., Peppelenbosch, M. P., & Spek, C. A. (2007). Sonic hedgehog induces transcription-independent cytoskeletal rearrangement and migration regulated by arachidonate metabolites. *Cell Signal*, *19*(12), 2596–2604. http://doi.org/10.1016/j.cellsig.2007.08.011

Bijlsma, M. F., Damhofer, H., & Roelink, H. (2012). Hedgehog-stimulated chemotaxis is mediated by smoothened located outside the primary cilium. *Science Signaling*, *5*(238), ra60. http://doi.org/10.1126/scisignal.2002798

Bloch, K. (1965). The biological synthesis of cholesterol. *Science*, *150*(3692), 19–28. http://doi.org/10.1126/science.150.3692.19

Briscoe, J., & Thérond, P. P. (2013). The mechanisms of Hedgehog signalling and its roles in development and disease. *Nature Reviews. Molecular Cell Biology*, *14*(7), 416–429. http://doi.org/10.1038/nrm3598

Briscoe, J., Pierani, A., Jessell, T. M., & Ericson, J. (2000). A homeodomain protein code specifies progenitor cell identity and neuronal fate in the ventral neural tube. *Cell*, *101*(4), 435–445.

Buglino, J. A., & Resh, M. D. (2008). Hhat is a palmitoylacyltransferase with specificity for N-palmitoylation of Sonic Hedgehog. *J. Biol. Chem.*, *283*(32), 22076–22088.

Bürglin, T. R. (2008). Evolution of hedgehog and hedgehog-related genes, their origin from Hog proteins in ancestral eukaryotes and discovery of a novel Hint motif. *BMC Genomics*, *9*(1), 127–27. http://doi.org/10.1186/1471-2164-9-127

Capurro, M. I., Xu, P., Shi, W., Li, F., Jia, A., & Filmus, J. (2008). Glypican-3 inhibits Hedgehog signaling during development by competing with patched for Hedgehog binding. *Dev Cell*, *14*(5), 700–711. http://doi.org/10.1016/j.devcel.2008.03.006

Casillas, C., & Roelink, H. (2018). Gain-of-function Shh mutants activate Smo cell-autonomously independent of Ptch1/2 function. *Mech Dev*, *153*, 30–41. http://doi.org/10.1016/j.mod.2018.08.009

Cerdà-Costa, N., & Gomis-Rüth, F. X. (2014). Architecture and function of metallopeptidase catalytic domains. *Protein Sci*, *23*(2), 123–144. http://doi.org/10.1002/pro.2400

Chamoun, Z., Mann, R. K., Nellen, D., Kessler, von, D. P., Bellotto, M., Beachy, P. A., & Basler, K. (2001). Skinny hedgehog, an acyltransferase required for palmitoylation and activity of the hedgehog signal. *Science*, *293*(5537), 2080–2084.

Chen, M. H., Li, Y. J., Kawakami, T., Xu, S. M., & Chuang, P. T. (2004). Palmitoylation is required for the production of a soluble multimeric Hedgehog protein complex and long-range signaling in vertebrates. *Genes Dev*, *18*(6), 641–659.

Chiang, C., Litingtung, Y., Lee, E., Young, K. E., Corden, J. L., Westphal, H., & Beachy, P. A. (1996). Cyclopia and defective axial patterning in mice lacking Sonic hedgehog gene function. *Nature*, *383*(6599), 407–413.

Cooper, M. K., Wassif, C. A., Krakowiak, P. A., Taipale, J., Gong, R., Kelley, R. I., et al. (2003). A defective response to Hedgehog signaling in disorders of cholesterol biosynthesis. *Nat Genet*, *33*(4), 508–513.

Corbit, K. C., Aanstad, P., Singla, V., Norman, A. R., Stainier, D. Y., & Reiter, J. F. (2005). Vertebrate Smoothened functions at the primary cilium. *Nature*, *437*(7061), 1018–1021.

Day, E. S., Wen, D., Garber, E. A., Hong, J., Avedissian, L. S., Rayhorn, P., et al. (1999). Zinc-dependent structural stability of human Sonic hedgehog. *Biochemistry*, *38*(45), 14868–14880. http://doi.org/10.1021/bi9910068

Dennis, J. F., Kurosaka, H., Iulianella, A., Pace, J., Thomas, N., Beckham, S., et al. (2012). Mutations in Hedgehog acyltransferase (Hhat) perturb Hedgehog signaling, resulting in severe acrania-holoprosencephaly-agnathia craniofacial defects. *PLoS Genet*, *8*(10), e1002927. http://doi.org/10.1371/journal.pgen.1002927

Dierker, T., Dreier, R., Petersen, A., Bordych, C., & Grobe, K. (2009). Heparan sulfate-modulated, metalloprotease-mediated sonic hedgehog release from producing cells. *J. Biol. Chem.*, *284*(12), 8013–8022. http://doi.org/10.1074/jbc.M806838200

Dixit, R., Pandey, M., Tripathi, S. K., Dwivedi, A. N. D., & Shukla, V. K. (2017). Comparative Analysis of Mutational Profile of Sonic hedgehog Gene in Gallbladder Cancer. *Digestive Diseases and Sciences*, *62*(3), 708–714. http://doi.org/10.1007/s10620-016-4438-1

Dwyer, J. R., Sever, N., Carlson, M., Nelson, S. F., Beachy, P. A., & Parhami, F. (2007). Oxysterols are novel activators of the hedgehog signaling pathway in pluripotent mesenchymal cells. *Journal of Biological Chemistry*, *282*(12), 8959–8968. http://doi.org/10.1074/jbc.M611741200

Esko, J. D., & Selleck, S. B. (2002). Order out of chaos: assembly of ligand binding sites in heparan sulfate. *Annu. Rev. Biochem.*, *71*(1), 435–471. http://doi.org/10.1146/annurev.biochem.71.110601.135458

Etheridge, L. A., Crawford, T. Q., Zhang, S., & Roelink, H. (2010). Evidence for a role of vertebrate Disp1 in long-range Shh signaling. *Development*, *137*(1), 133–140. http://doi.org/10.1242/dev.043547

Eugster, C., Panáková, D., Mahmoud, A., & Eaton, S. (2007). Lipoprotein-heparan sulfate interactions in the Hh pathway. *Dev Cell*, *13*(1), 57–71. http://doi.org/10.1016/j.devcel.2007.04.019

Farshi, P., Ohlig, S., Pickhinke, U., Höing, S., Jochmann, K., Lawrence, R., et al. (2011). Dual roles of the Cardin-Weintraub motif in multimeric Sonic hedgehog. *J. Biol. Chem.*, *286*(26), 23608–23619. http://doi.org/10.1074/jbc.M110.206474

Fuse, N., Maiti, T., Wang, B., Porter, J. A., Hall, T. M., Leahy, D. J., & Beachy, P. A. (1999). Sonic hedgehog protein signals not as a hydrolytic enzyme but as an apparent ligand for patched. *Proceedings of the National Academy of Sciences of the United States of America*, *96*(20), 10992–10999.

Gong, X., Qian, H., Cao, P., Zhao, X., Zhou, Q., Lei, J., & Yan, N. (2018). Structural basis for the recognition of Sonic Hedgehog by human Patched1. *Science*, *112*, eaas8935. http://doi.org/10.1126/science.aas8935

Goodrich, L. V., Johnson, R. L., Milenkovic, L., McMahon, J. A., & Scott, M. P. (1996). Conservation of the hedgehog/patched signaling pathway from flies to mice: induction of a mouse patched gene by Hedgehog. *Genes Dev*, *10*(3), 301–312.

Guo, W., & Roelink, H. (2019). Loss of the Heparan Sulfate Proteoglycan Glypican5 facilitates long-range Shh signaling. *Stem Cells*. http://doi.org/10.1002/stem.3018

Hall, T. M., Porter, J. A., Beachy, P. A., & Leahy, D. J. (1995). A potential catalytic site revealed by the 1.7-A crystal structure of the amino-terminal signalling domain of Sonic hedgehog. *Nature*, *378*(6553), 212–216. http://doi.org/10.1038/378212a0

Hall, T. M., Porter, J. A., Young, K. E., Koonin, E. V., Beachy, P. A., & Leahy, D. J. (1997). Crystal structure of a Hedgehog autoprocessing domain: homology between Hedgehog and self-splicing proteins. *Cell*, *91*(1), 85–97.

Han, C., Belenkaya, T. Y., Khodoun, M., Tauchi, M., Lin, X., & Lin, X. (2004). Distinct and collaborative roles of Drosophila EXT family proteins in morphogen signalling and gradient formation. *Development*, *131*(7), 1563–1575. http://doi.org/10.1242/dev.01051

Hausmann, G., Mering, von, C., & Basler, K. (2009). The hedgehog signaling pathway: where did it come from? *PLoS Biol*, *7*(6), e1000146. http://doi.org/10.1371/journal.pbio.1000146

Hepker, J., Wang, Q. T., Motzny, C. K., Holmgren, R., & T, O., V. (1997). Drosophila cubitus interruptus forms a negative feedback loop with patched and regulates expression of Hedgehog target genes. *Development*, *124*, 549–558.

Hynes, M., Stone, D. M., Dowd, M., Pitts-Meek, S., Goddard, A., Gurney, A., & Rosenthal, A. (1997). Control of cell pattern in the neural tube by the zinc finger transcription factor and oncogene Gli-1. *Neuron*, *19*, 15–26.

Incardona, J. P., Lee, J. H., Robertson, C. P., Enga, K., Kapur, R. P., & Roelink, H. (2000). Receptor-mediated endocytosis of soluble and membrane-tethered Sonic hedgehog by Patched-1. *Proceedings of the National Academy of Sciences of the United States of America*, *97*(22), 12044–12049. http://doi.org/10.1073/pnas.220251997

Infante, R. E., Wang, M. L., Radhakrishnan, A., Kwon, H. J., Brown, M. S., & Goldstein, J. L. (2008). NPC2 facilitates bidirectional transfer of cholesterol between NPC1 and lipid bilayers, a step in cholesterol egress from lysosomes. *Proc. Natl. Acad. Sci. U. S. a.*, *105*(40), 15287–15292. http://doi.org/10.1073/pnas.0807328105

Ingham, P. W., & McMahon, A. P. (2001). Hedgehog signaling in animal development: paradigms and principles. *Genes and Development*, *15*(23), 3059–3087.

Ingham, P. W., Taylor, A. M., & Nakano, Y. (1991). Role of the Drosophila patched gene in positional signalling. *Nature*, *353*(6340), 184–187.

Irons, M., Elias, E. R., Salen, G., Tint, G. S., & Batta, A. K. (1993). Defective cholesterol biosynthesis in Smith-Lemli-Opitz syndrome. *Lancet*, *341*(8857), 1414. http://doi.org/10.1016/0140-6736(93)90983-n

Jacob, F., Perrin, D., Sanchez, C., & Monod, J. (1960). [Operon: a group of genes with the expression coordinated by an operator]. *Comptes Rendus Hebdomadaires Des Seances De l'Academie Des Sciences*, *250*, 1727–1729.

Jakobs, P., Exner, S., Schürmann, S., Pickhinke, U., Bandari, S., Ortmann, C., et al. (2014). Scube2 enhances proteolytic Shh processing from the surface of Shh-producing cells. *Journal of Cell Science*, *127*(Pt 8), 1726–1737. http://doi.org/10.1242/jcs.137695

Jakobs, P., Schulz, P., Ortmann, C., Schürmann, S., Exner, S., Rebollido-Rios, R., et al. (2016). Bridging the gap: heparan sulfate and Scube2 assemble Sonic hedgehog release complexes at the surface of producing cells. *Scientific Reports*, *6*(1), 26435–14. http://doi.org/10.1038/srep26435

Jakobs, P., Schulz, P., Schürmann, S., Niland, S., Exner, S., Rebollido-Rios, R., et al. (2017). Ca2+ coordination controls sonic hedgehog structure and its Scube2-regulated release. *Journal of Cell Science*, *130*(19), 3261–3271. http://doi.org/10.1242/jcs.205872

Janda, C. Y., Waghray, D., Levin, A. M., Thomas, C., & Garcia, K. C. (2012). Structural basis of Wnt recognition by Frizzled. *Science*, *337*(6090), 59–64. http://doi.org/10.1126/science.1222879

Jessell, T. M. (2000). Neuronal specification in the spinal cord: inductive signals and transcriptional codes. *Nat Rev Genet*, *1*(1), 20–29.

Kandutsch, A. A., & Russell, A. E. (1960). Preputial gland tumor sterols. 3. A metabolic pathway from lanosterol to cholesterol. *Journal of Biological Chemistry*, *235*, 2256–2261.

Karten, B., Peake, K. B., & Vance, J. E. (2009). Mechanisms and consequences of impaired lipid trafficking in Niemann-Pick type C1-deficient mammalian cells. *Biochim. Biophys. Acta*, *1791*(7), 659–670. http://doi.org/10.1016/j.bbalip.2009.01.025

Keeler, R. F., & Binns, W. (1968). Teratogenic compounds of Veratrum californicum (Durand). V. Comparison of cyclopian effects of steroidal alkaloids from the plant and structurally related compounds from other sources. *Teratology*, *1*(1), 5–10.

Keller, R. K., Arnold, T. P., & Fliesler, S. J. (2004). Formation of 7-dehydrocholesterol-containing membrane rafts in vitro and in vivo, with relevance to the Smith-Lemli-Opitz syndrome. *J. Lipid Res.*, *45*(2), 347–355. http://doi.org/10.1194/jlr.M300232-JLR200

Koziel, L., Kunath, M., Kelly, O. G., & Vortkamp, A. (2004). Ext1-dependent heparan sulfate regulates the range of Ihh signaling during endochondral ossification. *Dev Cell*, *6*(6), 801–813.

Lancaster, M. A., Renner, M., Martin, C.-A., Wenzel, D., Bicknell, L. S., Hurles, M. E., et al. (2013). Cerebral organoids model human brain development and microcephaly. *Nature*, *501*(7467), 373–379. http://doi.org/10.1038/nature12517

Li, Y., Zhang, H., Litingtung, Y., & Chiang, C. (2006). Cholesterol modification restricts the spread of Shh gradient in the limb bud. *Proceedings of the National Academy of Sciences of the United States of America*, *103*(17), 6548–6553. http://doi.org/10.1073/pnas.0600124103

Lin, X., Wei, G., Shi, Z., Dryer, L., Esko, J. D., Wells, D. E., & Matzuk, M. M. (2000). Disruption of gastrulation and heparan sulfate biosynthesis in EXT1-deficient mice. *Dev. Biol.*, *224*(2), 299–311. http://doi.org/10.1006/dbio.2000.9798

Lind, T., Tufaro, F., McCormick, C., Lindahl, U., & Lidholt, K. (1998). The putative tumor suppressors EXT1 and EXT2 are glycosyltransferases required for the biosynthesis of heparan sulfate. *Journal of Biological Chemistry*, *273*(41), 26265–26268. http://doi.org/10.1074/jbc.273.41.26265

Lingwood, D., & Simons, K. (2010). Lipid rafts as a membrane-organizing principle. *Science*, *327*(5961), 46–50. http://doi.org/10.1126/science.1174621

Loftus, S. K., Morris, J. A., Carstea, E. D., Gu, J. Z., Cummings, C., Brown, A., et al. (1997). Murine model of Niemann-Pick C disease: mutation in a cholesterol homeostasis gene. *Science*, *277*(5323), 232–235.

Long, J., Winterbottom, E., & Robbins, D. J. (2015). Sonic Hedgehog: a lipid speciated hormone? *Oncotarget*, *6*(23), 19340–19341. http://doi.org/10.18632/oncotarget.4969

Marigo, V., Roberts, D. J., Lee, S. M., Tsukurov, O., Levi, T., Gastier, J. M., et al. (1995). Cloning, expression, and chromosomal location of SHH and IHH: two human homologues of the Drosophila segment polarity gene hedgehog. *Genomics*, *28*(1), 44–51. http://doi.org/10.1006/geno.1995.1104

Martin, G. R. (1981). Isolation of a pluripotent cell line from early mouse embryos cultured in medium conditioned by teratocarcinoma stem cells. *Proceedings of the National Academy of Sciences of the United States of America*, *78*(12), 7634–7638. http://doi.org/10.1073/pnas.78.12.7634

Martin, V., Carrillo, G., Torroja, C., & Guerrero, I. (2001). The sterol-sensing domain of Patched protein seems to control Smoothened activity through Patched vesicular trafficking. *Curr Biol*, *11*(8), 601–7.

Meinhardt, A., Eberle, D., Tazaki, A., Ranga, A., Niesche, M., Wilsch-Bräuninger, M., et al. (2014). 3D reconstitution of the patterned neural tube from embryonic stem cells. *Stem Cell Reports*, *3*(6), 987–999. http://doi.org/10.1016/j.stemcr.2014.09.020

Meroueh, S. O., Bencze, K. Z., Hesek, D., Lee, M., Fisher, J. F., Stemmler, T. L., & Mobashery, S. (2006). Three-dimensional structure of the bacterial cell wall peptidoglycan. *Proceedings of the National Academy of Sciences of the United States of America*, *103*(12), 4404–4409. http://doi.org/10.1073/pnas.0510182103

Motoyama, J., Heng, H., Crackower, M. A., Takabatake, T., Takeshima, K., Tsui, L. C., & Hui, C. (1998). Overlapping and non-overlapping Ptch2 expression with Shh during mouse embryogenesis. *Mech Dev*, *78*(1-2), 81–84. http://doi.org/10.1016/s0925-4773(98)00149-x

Murakami, S., Nakashima, R., Yamashita, E., Matsumoto, T., & Yamaguchi, A. (2006). Crystal structures of a multidrug transporter reveal a functionally rotating mechanism. *Nature*, *443*(7108), 173–179. http://doi.org/10.1038/nature05076

Müller, S., Schöttler, M., Schön, S., Prante, C., Brinkmann, T., Kuhn, J., et al. (2005). Human xylosyltransferase I: functional and biochemical characterization of cysteine residues required for enzymic activity. *Biochem. J.*, *386*(Pt 2), 227–236. http://doi.org/10.1042/BJ20041206

Myers, B. R., Neahring, L., Zhang, Y., Roberts, K. J., & Beachy, P. A. (2017). Rapid, direct activity assays for Smoothened reveal Hedgehog pathway regulation by membrane cholesterol and extracellular sodium. *Proc. Natl. Acad. Sci. U. S. a.*, *114*(52), E11141–E11150. http://doi.org/10.1073/pnas.1717891115

Myers, B. R., Sever, N., Chong, Y. C., Kim, J., Belani, J. D., Rychnovsky, S., et al. (2013). Hedgehog pathway modulation by multiple lipid binding sites on the smoothened effector of signal response. *Dev Cell*, *26*(4), 346–357. http://doi.org/10.1016/j.devcel.2013.07.015

Nakashima, H., Nakamura, M., Yamaguchi, H., Yamanaka, N., Akiyoshi, T., Koga, K., et al. (2006). Nuclear factor-kappaB contributes to hedgehog signaling pathway activation through sonic hedgehog induction in pancreatic cancer. *Cancer Res*, *66*(14), 7041–7049. http://doi.org/10.1158/0008-5472.CAN-05-4588

Nedelcu, D., Liu, J., Xu, Y., Jao, C., & Salic, A. (2013). Oxysterol binding to the extracellular domain of Smoothened in Hedgehog signaling. *Nat Chem Biol*. http://doi.org/10.1038/nchembio.1290

Nüsslein-Volhard, C., & Wieshaus, E. (1980). Mutations affecting segment number and polarity in Drosophila. *Nature*, *287*, 795–801.

Ohlig, S., Pickhinke, U., Sirko, S., Bandari, S., Hoffmann, D., Dreier, R., et al. (2012). An emerging role of Sonic hedgehog shedding as a modulator of heparan sulfate interactions. *J. Biol. Chem.*, *287*(52), 43708–43719. http://doi.org/10.1074/jbc.M112.356667

Palm, W., Swierczynska, M. M., Kumari, V., Ehrhart-Bornstein, M., Bornstein, S. R., & Eaton, S. (2013). Secretion and signaling activities of lipoprotein-associated hedgehog and non-sterol-modified hedgehog in flies and mammals. *PLoS Biol*, *11*(3), e1001505. http://doi.org/10.1371/journal.pbio.1001505

Perzl, M., Reipen, I. G., Schmitz, S., Poralla, K., Sahm, H., Sprenger, G. A., & Kannenberg, E. L. (1998). Cloning of conserved genes from Zymomonas mobilis and Bradyrhizobium japonicum that function in the biosynthesis of hopanoid lipids.

Biochim. Biophys. Acta, *1393*(1), 108–118. http://doi.org/10.1016/s0005-2760(98)00064-2

Peters, C., Wolf, A., Wagner, M., Kuhlmann, J., & Waldmann, H. (2004). The cholesterol membrane anchor of the Hedgehog protein confers stable membrane association to lipid-modified proteins. *Proc. Natl. Acad. Sci. U. S. a.*, *101*(23), 8531–8536.

Placzek, M. (1995). The role of the notochord and floor plate in inductive interactions. *Curr. Opin. in Genet. Dev.*, *5*, 499–506.

Placzek, M., Tessier-Lavigne, M., Yamada, T., Jessell, T., & Dodd, J. (1990). Mesodermal control of neural cell identity: floor plate induction by the notochord. *Science*, *250*(4983), 985–988.

Porter, J. A., von, K. D., Ekker, S. C., Young, K. E., Lee, J. J., Moses, K., & Beachy, P. A. (1995). The product of hedgehog autoproteolytic cleavage active in local and long-range signalling. *Nature*, *374*(6520), 363–366.

Porter, J. A., Young, K. E., & Beachy, P. A. (1996). Cholesterol modification of hedgehog signaling proteins in animal development. *Science*, *274*(5285), 255–259.

Porter, F. D., & Herman, G. E. (2011). Malformation syndromes caused by disorders of cholesterol synthesis. *J. Lipid Res.*, *52*(1), 6–34. http://doi.org/10.1194/jlr.R009548

Qi, X., Schmiege, P., Coutavas, E., Wang, J., & Li, X. (2018). Structures of human Patched and its complex with native palmitoylated sonic hedgehog. *Nature*, *15*, 3059. http://doi.org/10.1038/s41586-018-0308-7

Riddle, R. D., Johnson, R. L., Laufer, E., & Tabin, C. (1993). Sonic hedgehog mediates the polarizing activity of the ZPA. *Cell*, *75*(7), 1401–1416.

Roelink, H. (2018). Sonic Hedgehog Is a Member of the Hh/DD-Peptidase Family That Spans the Eukaryotic and Bacterial Domains of Life. *Journal of Developmental Biology*, *6*(2), 12. http://doi.org/10.3390/jdb6020012

Roelink, H., Augsburger, A., Heemskerk, J., Korzh, V., Norlin, S., Ruiz i Altaba, A., et al. (1994). Floor plate and motor neuron induction by vhh-1, a vertebrate homolog of hedgehog expressed by the notochord. *Cell*, *76*(4), 761–775.

Roelink, H., Porter, J. A., Chiang, C., Tanabe, Y., Chang, D. T., Beachy, P. A., & Jessell, T. M. (1995). Floor plate and motor neuron induction by different concentrations of the amino-terminal cleavage product of sonic hedgehog autoproteolysis. *Cell*, *81*(3), 445–455.

Roessler, E., Belloni, E., Gaudenz, K., Jay, P., Berta, P., Scherer, S. W., et al. (1996). Mutations in the human Sonic Hedgehog gene cause holoprosencephaly. *Nat Genet*, *14*(3), 357–360.

Rohatgi, R., Milenkovic, L., & Scott, M. P. (2007). Patched1 regulates hedgehog signaling at the primary cilium. *Science*, *317*(5836), 372–376.

Roy, S., Huang, H., Liu, S., & Kornberg, T. B. (2014). Cytoneme-Mediated Contact-Dependent Transport of the Drosophila Decapentaplegic Signaling Protein. *Science*. http://doi.org/10.1126/science.1244624

Rudolf, A. F., Kinnebrew, M., Kowatsch, C., Ansell, T. B., Omari, El, K., Bishop, B., et al. (2019). The morphogen Sonic hedgehog inhibits its receptor Patched by a pincer grasp mechanism. *Nat Chem Biol*, *15*(10), 975–982. http://doi.org/10.1038/s41589-019-0370-y

Ruppert, J. M., Vogelstein, B., Arheden, K., & Kinzler, K. W. (1990). GLI3 encodes a 190-kilodalton protein with multiple regions of GLI similarity. *Mol Cell Biol*, *10*(10), 5408–5415.

Ryan, A. K., Bartlett, K., Clayton, P., Eaton, S., Mills, L., Donnai, D., et al. (1998). Smith-Lemli-Opitz syndrome: a variable clinical and biochemical phenotype. *J Med Genet*, *35*(7), 558–565. http://doi.org/10.1136/jmg.35.7.558

Sarrazin, S., Lamanna, W. C., & Esko, J. D. (2011). Heparan sulfate proteoglycans. *Cold Spring Harbor Perspectives in Biology*, *3*(7), a004952–a004952. http://doi.org/10.1101/cshperspect.a004952

Seeger, M. A., Schiefner, A., Eicher, T., Verrey, F., Diederichs, K., & Pos, K. M. (2006). Structural asymmetry of AcrB trimer suggests a peristaltic pump mechanism. *Science*, *313*(5791), 1295–1298.

Sharpe, H. J., Wang, W., Hannoush, R. N., & de Sauvage, F. J. (2015). Regulation of the oncoprotein Smoothened by small molecules. *Nat Chem Biol*, *11*(4), 246–255. http://doi.org/10.1038/nchembio.1776

Smith, D. W., Lemli, L., & Opitz, J. M. (1964). A Newly Recognized Syndrome of Multiple Congenital Anomalies. *J. Pediatr.*, *64*(2), 210–217. http://doi.org/10.1016/s0022-3476(64)80264-x

Spemann, H., & Mangold, H. (1923). Induction of embryonic primordia by implantation of organizers from a different species. *The International journal of developmental biology* (Vol. 45, pp. 13–38). Int J Dev Biol.

Stickens, D., Zak, B. M., Rougier, N., Esko, J. D., & Werb, Z. (2005). Mice deficient in Ext2 lack heparan sulfate and develop exostoses. *Development*, *132*(22), 5055–5068. http://doi.org/10.1242/dev.02088

Taipale, J., Chen, J. K., Cooper, M. K., Wang, B., Mann, R. K., Milenkovic, L., et al. (2000). Effects of oncogenic mutations in Smoothened and Patched can be reversed by cyclopamine. *Nature*, *406*(6799), 1005–9.

Taipale, J., Cooper, M. K., Maiti, T., & Beachy, P. A. (2002). Patched acts catalytically to suppress the activity of Smoothened. *Nature*, *418*(6900), 892–897.

Tanaka, Y., Okada, Y., & Hirokawa, N. (2005). FGF-induced vesicular release of Sonic hedgehog and retinoic acid in leftward nodal flow is critical for left-right determination. *Nature*, *435*(7039), 172–177.

Tian, H., Callahan, C. A., DuPree, K. J., Darbonne, W. C., Ahn, C. P., Scales, S. J., & de Sauvage, F. J. (2009). Hedgehog signaling is restricted to the stromal compartment during pancreatic carcinogenesis. *Proc. Natl. Acad. Sci. U. S. a.*, *106*(11), 4254–4259. http://doi.org/10.1073/pnas.0813203106

Tseng, T. T., Gratwick, K. S., Kollman, J., Park, D., Nies, D. H., Goffeau, A., & Saier, M. H. J. (1999). The RND permease superfamily: an ancient, ubiquitous and diverse family that includes human disease and development proteins. *J Mol Microbiol Biotechnol*, *1*(1), 107–125.

Tukachinsky, H., Kuzmickas, R. P., Jao, C. Y., Liu, J., & Salic, A. (2012). Dispatched and scube mediate the efficient secretion of the cholesterol-modified hedgehog ligand. *Cell Reports*, *2*(2), 308–320. http://doi.org/10.1016/j.celrep.2012.07.010

Tukachinsky, H., Petrov, K., Watanabe, M., & Salic, A. (2016). Mechanism of inhibition of the tumor suppressor Patched by Sonic Hedgehog. *Proc. Natl. Acad. Sci. U. S. a.*, *113*(40), E5866–E5875. http://doi.org/10.1073/pnas.1606719113

Turnbull, J., Powell, A., & Guimond, S. (2001). Heparan sulfate: decoding a dynamic multifunctional cell regulator. *Trends Cell Biol*, *11*(2), 75–82. http://doi.org/10.1016/s0962-8924(00)01897-3

Unden, A. B., Holmberg, E., Lundh-Rozell, B., Stähle-Bäckdahl, M., Zaphiropoulos, P. G., Toftgard, R., & Vorechovsky, I. (1996). Mutations in the human homologue of Drosophila patched (PTCH) in basal cell carcinomas and the Gorlin syndrome: different in vivo mechanisms of PTCH inactivation. *Cancer Res*, *56*(20), 4562–4565.

van den Heuvel, M., & Ingham, P. W. (1996). Smoothened encodes a receptor-like serpentine protein required for hedgehog signalling. *Nature*, *382*(6591), 547–551.

Varki, A., Cummings, R. D., Esko, J. D., Freeze, H. H., Stanley, P., Bertozzi, C. R., et al. (2009). Proteoglycans and Sulfated Glycosaminoglycans.

Wang, C., Wu, H., Evron, T., Vardy, E., Han, G. W., Huang, X.-P., et al. (2014). Structural basis for Smoothened receptor modulation and chemoresistance to anticancer drugs. *Nature Communications*, *5*(1), 4355–11. http://doi.org/10.1038/ncomms5355

Wang, C., Wu, H., Katritch, V., Han, G. W., Huang, X.-P., Liu, W., et al. (2013). Structure of the human smoothened receptor bound to an antitumour agent. *Nature*, *497*(7449), 338–343. http://doi.org/10.1038/nature12167

Wang, Z., Fan, G., Hryc, C. F., Blaza, J. N., Serysheva, I. I., Schmid, M. F., et al. (2017). An allosteric transport mechanism for the AcrAB-TolC multidrug efflux pump. *eLife*, *6*, 11103. http://doi.org/10.7554/eLife.24905

Waterham, H. R., Wijburg, F. A., Hennekam, R. C., Vreken, P., Poll-The, B. T., Dorland, L., et al. (1998). Smith-Lemli-Opitz syndrome is caused by mutations in the 7-dehydrocholesterol reductase gene. *Am J Hum Genet*, *63*(2), 329–338.

Weierstall, U., James, D., Wang, C., White, T. A., Wang, D., Liu, W., et al. (2014). Lipidic cubic phase injector facilitates membrane protein serial femtosecond crystallography. *Nature Communications*, *5*(1), 3309–6. http://doi.org/10.1038/ncomms4309

Whalen, D., Malinauskas, T., Gilbert, R. J. C., Siebold, C. (2013). Structural insights into proteoglycan-shaped Hedgehog signaling. *Proc. Natl. Acad. Sci. U. S. a.*, *110*(41), 16420–16425. http://doi.org/10.1073/pnas.1310097110

Wichterle, H., Lieberam, I., Porter, J. A., & Jessell, T. M. (2002). Directed differentiation of embryonic stem cells into motor neurons. *Cell*, *110*(3), 385–397.

Wolpert, L. (1969). Positional information and the spatial pattern of cellular differentiation. *J Theor Biol*, *25*(1), 1–47.

Xie, J., Johnson, R. L., Zhang, X., Bare, J. W., Waldman, F. M., Cogen, P. H., et al. (1997). Mutations of the PATCHED gene in several types of sporadic extracutaneous tumors. *Cancer Res*, *57*(12), 2369–2372.

Xie, J., Murone, M., Luoh, S. M., Ryan, A., Gu, Q., Zhang, C., et al. (1998). Activating Smoothened mutations in sporadic basal-cell carcinoma. *Nature*, *391*(6662), 90–92. http://doi.org/10.1038/34201

Yauch, R. L., Dijkgraaf, G. J., Alicke, B., Januario, T., Ahn, C. P., Holcomb, T., et al. (2009). Smoothened mutation confers resistance to a Hedgehog pathway inhibitor in medulloblastoma. *Science*, *326*(5952), 572–574.

Zhang, X. M., Ramalho-Santos, M., & McMahon, A. P. (2001). Smoothened mutants reveal redundant roles for Shh and Ihh signaling including regulation of L/R asymmetry by the mouse node. *Cell*, *105*(6), 781–792.

Zhang, Y., Bulkley, D. P., Xin, Y., Roberts, K. J., Asarnow, D. E., Sharma, A., et al. (2018). Structural Basis for Cholesterol Transport-like Activity of the Hedgehog Receptor Patched. *Cell*, *175*(5), 1352–1364.e14. http://doi.org/10.1016/j.cell.2018.10.026

Zhao, Y., Tong, C., & Jiang, J. (2007). Hedgehog regulates smoothened activity by inducing a conformational switch. *Nature*, *450*(7167), 252–258. http://doi.org/10.1038/nature06225

Zhao, J., Ciulla, D. A., Xie, J., Wagner, A. G., Castillo, D. A., Zwarycz, A. S., et al. (2019). General Base Swap Preserves Activity and Expands Substrate Tolerance in Hedgehog Autoprocessing. *Journal of the American Chemical Society*, *141*(46), 18380–18384. http://doi.org/10.1021/jacs.9b08914

Chapter 2

Generation and analysis of mosaic spinal cord organoids derived from mouse embryonic stem cells

Carina Jägers and Henk Roelink
Department of Molecular and Cell Biology, University of California, Berkeley

Manuscript to be published in "Methods in Molecular Biology - Hedgehog Signaling: Methods and Protocols", Springer Nature (2021)

Abstract

Three central cell populations play roles in morphogen action – the cells that produce, the cells that distribute, and the cells that respond to the morphogen. Taking advantage of the properties of embryonic stem cells to aggregate and readily differentiate into neural progenitor tissue, we describe an approach using genetically modified murine stem cell lines to individually address the contribution of these cells in the establishment and response to a morphogenetic gradient in mosaic spinal cord organoids.

Key Words: Non-cell autonomous Sonic Hedgehog signaling, Genetic mosaicism, Spinal cord organoids, Embryonic stem cells, Neural development

1 Introduction

Sonic Hedgehog (Shh) is a morphogen. Morphogens are critical signaling molecules that induce the formation of a pattern in a homogeneous cell population in a concentration dependent manner (Andrews, Kong, Novitch, & Butler, 2019). The morphogen concentration is proposed to be established by the distribution away from the sites of synthesis, resulting in high morphogen concentrations close to the source, and even lower concentrations away from the source. Combining this graded distribution of the morphogen with certain threshold levels for induction of specific cell types in the responding tissue would result in a stereotypic pattern (Kerszberg & Wolpert, 1998). The mechanism by which morphogens are distributed remains contentious, as this might not be achieved solely by diffusion. For example, many aspects of morphogenetic signaling in *Drosophila* can be explained by the detection of morphogen on the source cells via cellular processes (cytonemes) sent out by the responding cells (Kornberg, 2014). As more distal cells are expected to have fewer processes that reach the source than proximal cells, a pattern can be generated by a stereotypic response in each cell possibly determined by the number of processes that contact the source.

In the developing vertebrate embryo, Shh is thought to move away from the sites of synthesis, thus establishing a gradient away from its site of synthesis. This Shh gradient is interpreted by local cells that differentiate into a stereotypic pattern. The mechanism by which Shh is transported along the morphogenetic gradient to induce a measured response at a distance away from the source field remains poorly understood. Perhaps not surprisingly, several molecular interactions have been described that affect Shh release from the source, as well as subsequent distribution and response. Dedicated molecules are required for the correct release of Shh from the source cells and several components of the extracellular matrix interact with Shh to facilitate or inhibit its distribution as well as affect Shh binding to its cognate receptors.

The establishment of a morphogenetic gradient involves three central events: 1) the production of the signaling molecule, 2) the distribution of the morphogen in a gradient away from the source, and 3) the graded response that results in patterning. In a morphogenetic field cells might be involved in more than one of these events simultaneously. The independent interrogation of these populations of cells that mediate production and transport of, and the response to Shh is critical in the mechanistic study of Shh-mediated morphogenesis. In vitro approaches can address the mechanism how cells respond to different concentrations of added morphogen, while in vivo approaches are useful in addressing the sufficiency and requirements of signaling molecules in morphogenetic signaling. However, both approaches are limited in addressing all aspects of the three central functions in parallel. Here, we describe an experimental approach that allows the interrogation of cell populations for their role in either production or transport of, or the response to Shh.

Using mosaic spinal cord organoids to assess Shh morphogenesis

We use an approach that employs mosaic spinal cord organoids (SCOs) made by aggregating cells with distinct genotypes. Formation of SCOs starts with the generation of

embryoid bodies (EBs), each an aggregate of around 10^4 embryonic stem cells. In a completely defined and serum free medium these aggregates are differentiated into tissues resembling the developing spinal cord, a classic model for Shh morphogenesis (Wichterle, Lieberam, Porter, & Jessell, 2002). A wealth of markers is available that define many cells types that appear at stereotypical positions in relation to the Shh source in response to distinct Shh concentrations.

The aggregation of around 10^4 cells into an EB allows us to mix ESCs with distinct genotypes, and even cells with a specific genotype present at only a few percent are reliably incorporated into the EBs. In general, this approach allows us to assess the patterning consequences of changing the properties of the Shh source cells, the Shh transporting cells, and the cells that respond to Shh.

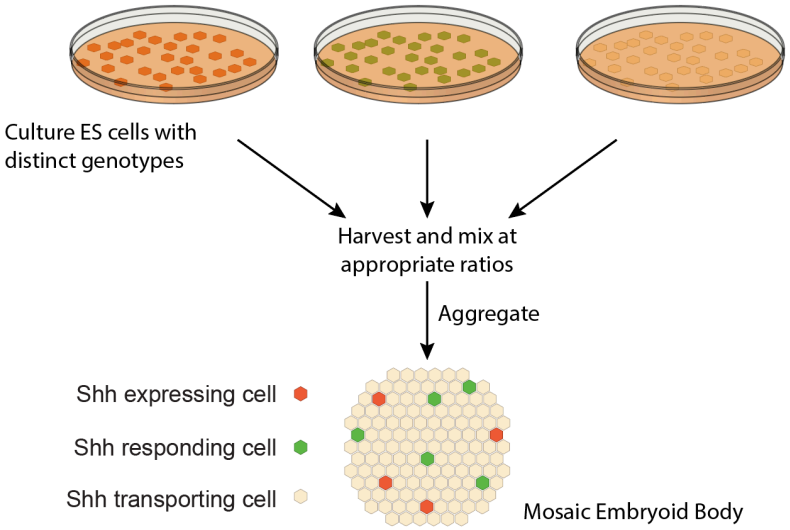

Figure 1: Diagram of experimental approach. Embryonic stem (ES) cells with distinct genotypes are harvested and mixed at appropriate ratios. The resulting aggregates, called mosaic embryoid bodies, contain Shh expressing, responding, and transporting cells, and can be differentiated into tissue resembling that of the developing spinal cord.

2 Materials

All tissue culture media should be prepared under sterile conditions in a biosafety cabinet.

2.1 Adherent Embryonic stem cell culture

Culture of ES cells is performed under standard conditions. We have used several lines of ES cells without noticeable difference in these aggregation and differentiation procedures.

1. Mouse embryonic stem cells.
2. Embryonic stem cell medium: DMEM, 20% FBS, 2 mM L-Glutamine, 1X MEM non-essential amino acids, 1X nucleosides for ES cells, 1 nM Leukemia Inhibitory Factor (LIF), and 0.55 µM 2-Mercaptoethanol.
3. Standard humidified incubator at 37° C and 5% CO_2. Culture conditions can be adjusted for specific cell lines as needed (see **Notes 1**).
4. Before use, Tissue Culture dishes are treated for at least 10 min with 0.1% w/v Gelatin in PBS. This solution is aspirated right before adding cells to the wet dish.
5. 0.25% trypsin with EDTA.

2.2 Generation of spinal cord organoids

1. Sterile PBS.
2. Cell counter or hemocytometer.
3. Sterile bacterial grade Petri dishes, or any other "low adherence/hydrophobic" type of dish.
4. DFNB medium: 25% DMEM, 25% HAMF12 and 50% Neurobasal medium, supplemented with 1.5 mM L-Glutamine and 2% (volume) B27 supplement.
5. Retinoic Acid in DMSO (10 mM). Stock is stable at -20°C.
6. Rotating platform in incubator, rotation speed of about 60 rpm (1Hz)
7. *Optional*: Lineage tracer like DiI/DiO or CMFDA
8. Conical tubes.
9. 60mm petri dish or 6-well plate.

2.3 Immunostaining for neural markers

1. PBS with 0.1% Triton X-100 (PBS-T).
2. Fixation solution: 4% Paraformaldehyde in PBS.
3. Heat-inactivated goat or donkey serum.
4. Antibody dilution solution: 10% Heat-inactivated goat or donkey serum in PBS-T.
5. Primary antibody solution: Primary antibody of choice diluted at the recommended concentration in antibody dilution solution.
6. Secondary antibody solution: Secondary antibody directed against the host species of the primary antibody and coupled to a fluorophore, diluted at the recommended concentration in antibody dilution solution.
7. Mounting medium of choice (see **Notes 2**).
8. Microscope slides and cover slips.
9. 1.5 ml centrifuge tubes.

10. P1000 pipet.
11. Pipet tips.
12. *Optional:* Nail polish.

2.4 LacZ reporter assay for transcriptional response

1. Galacton^{TM} Light Detection System or other system to measure *Ptch1:LacZ* (Goodrich, Milenkovic, Higgins, & Scott, 1997) expression.
2. Lysis buffer: 100 mM potassium phosphate pH 7.8, 0.2 % Triton X-100.
3. PBS.
4. Microcentrifuge tubes.
5. Centrifuge.
6. Bradford reagent diluted 1:5 with ultrapure water.
7. Protein standards (e.g. 0.1 – 0.5 mg/ml BSA).
8. 96 well assay plates.
9. Luminometer.
10. Spectrophotometer.

3 Methods

3.1 Embryonic stem cell culture

1. Plate approximately $2x10^4$ – $3x10^4$ mES cells/cm^2 in tissue culture plates coated with gelatin.
2. Exchange medium every 1-2 days.
3. Passage cells every other day into a new tissue culture plate (see **Notes 3**)

3.2 Generation of spinal cord organoids

1. Remove cells with the desired genotypes from the tissue culture plates by incubating with trypsin for 5-10 min, followed by trituration until a single cell suspension (assessed by microscopy) is obtained.
2. Collect the cells in separate conical tubes and wash at least twice with sterile PBS to remove any residual medium. Do so by centrifuging (<201 x g), aspirating the supernatant, resuspending in 4-5 ml PBS, and centrifuging again.
3. After washing resuspend the cells in DNFB.
4. Determine the cell number with a hemocytometer or cell counter.
5. *Optional*: Lineage tracing (see **Notes 4**)
6. Pipet the desired cell number the desired genotypes in the desired ratio into a sterile Petri dish (see **Table 1**). We recommend a total cell number of 500,000 for a 60 mm dish and 200,000 per well of an uncoated (suspension culture) 6 well plate (see **Notes 5**). This will yield around 100 EBs.
7. Add DFNB to a total volume of 5 ml for 60 mm dishes and 2 ml per well of a 6 well plate.
8. Place the dish on a rotating platform inside an incubator and rotate at 0.8 to 1 Hz (see **Notes 6**).
9. Incubate on the rotating platform for 48h. Small aggregates should be visible under the microscope after one night of incubation (see **Notes 7**).
10. *Optional*: If the medium turns yellow, carefully remove about half of the medium and replenish with fresh medium. In order to prevent removal of embryoid bodies when removing medium, the embryoid bodies can be collected in the middle of the plate by gentle swirling. This requires some practice, but collection of the EBs in the center of the plate can be easily observed against a black background.
11. Add 2 µM of Retinoic Acid (5000x dilution of 10mM stock) 48 h after aggregation.
12. Return plates back on the rotating platform (see **Notes 8**).
13. Incubate until the mosaic SCOs are collected for analysis. Exchange the medium (including RA) whenever it turns peach/yellow. Genetically encoded transcriptional reporter systems like *Ptch1:LacZ* expression can be measured 24h-48h after the addition of RA and immunostaining for neural progenitors 48h-72h after the addition of RA (see **Table 2**).

Table 1: Composition of mosaic SCOs. Cells in mosaic SCOs can exert desired functions (left column) according to their genotype (middle column). The percentages of cells with a specific genotype or function in the mosaic SCO is shown in the right column.

type	genotype	percentage of cells in mosaic SCO
source	Shh transgene	3-5 %
reporter	*HB9::GFP*	5-10 %
	Sim1::mCherry	10 %
	Ptch1$^{LacZ/LacZ}$	20-50 %
intermediate	any genotype of interest	50-90 %

3.3 Immunostaining for neural progenitor markers

1. Incubate the mosaic SCO according to expression time points specified in **Table 2**.
2. Collect the mosaic SCO in the middle of the plate by gentle swirling and transfer them to a 1.5 ml centrifuge tube with a p1000 pipet.
3. Let the SCOs settle at the bottom of the tube by gravity for 1-2 min and carefully aspirate the supernatant (see **Notes 9**).
4. Add 1 ml of PBS, let SCOs settle, and aspirate supernatant.
5. Fix SCOs with 4% fixation solution in a fume hood for 10 min on ice. The volume of fixation solution depends on the number of SCOs but 100 µl should suffice to cover the SCOs.
6. Gently flick the tube after addition of the fixation solution and after 5 min of incubation. Do not invert the tube to avoid SCOs being stuck at the wall of the tube!
7. Remove fixation solution and wash twice with PBS-T. At this point 0.1% goat serum can be added to prevent sticking and clumping of the SCOs
8. To block non-specific epitopes, add 100 µl antibody dilution solution and incubate at room temperature for 30 min.
9. Remove blocking solution and add 100 µl of primary antibody solution. Incubate for at least 1 h at room temperature; an incubation overnight at 4° C is recommended.
10. Remove primary antibody solution and wash 3 times with PBS-T. Each wash step should be 5-10 min.
11. Add secondary antibody solution and incubate for at least 1 h at room temperature in the dark; an incubation overnight at 4° C is recommended.
12. Remove secondary antibody solution and wash 3 times with PBS-T. Each wash step should be 5-10 min, and one long wash (> 6h) is recommended.
13. Wash one last time with PBS, ideally for 30 min to 1h (see **Notes 10**).
14. Before mounting, make sure microscope slides are clean and free of dust. Pipet 12 µl of mounting medium in a circle on the microscope slide to form a donut shape.

15. "Wash" a pipet tip in heat-inactivated goat/donkey serum to prevent the organoids from sticking to the tip. This reduces the number of SCOs getting stuck inside the pipet tip while pipetting.
16. Transfer 30-50 SCOs into the center of the prepared donut shape of mounting medium using the "washed" tip. The volume of transferred PBS should not exceed 15 µl.
17. Gently place a cover slip on top (see **Notes 11**).
18. Remove excessive liquid from the sides of the cover slip.
19. *Optional*: Seal the cover slips onto the microscope slide with nail polish. This reduces evaporation and enables long-term storage of the slides.
20. Let the prepared slides dry overnight in a slide folder at room temperature prior to microscopy.

Table 2: Examples of neural markers for immunostaining of SCOs. SCOs start expressing either ventral or dorsal markers of neural progenitor cells depending on their genotype and environment. These markers can be stained with fluorescently labeled antibodies (or fluorescent reporters) at the indicated recommended time points of in vitro culture.

identity	neural marker	recommended SCO incubation time
ventral	Nkx2.2	4 days
	Olig2	4 days
	Isl1/2	4-5 days
	Hb9	5 days
	Sox2	3 days
dorsal	Pax7	4 days

3.4 LacZ reporter assay for transcriptional response

1. Incubate the mosaic SCOs for 3-4 days.
2. Collect the SCOs in the middle of the plate by gently swirling and transfer them to a 1.5 ml centrifuge tube with a p1000 pipet.
3. Let SCOs settle by gravity, aspirate supernatant, and add 1 ml PBS. Let SCOs settle again and aspirate supernatant (see **Notes 9**).
4. Add 100 µl lysis buffer and break up cells by vigorously pipetting up and down.
5. Clear lysate of cell debris by centrifugation at maximum speed for 3 min in a microcentrifuge. Transfer supernatant to a new tube (see Notes).
6. For total protein measurement, pipet 1-3 µl of lysate or protein standard into a well of a 96 well plate and add 100 µl of diluted Bradford Reagent.

7. Read the absorbance of each sample and protein standard at 595 nm. The amount of total protein per sample can be calculated with the help of the protein standard curve.
8. For quantification of *Ptch1:LacZ* expression, follow instructions of the Galacton Light Detection Kit for suspension cells and measure *Ptch1:LacZ* expression levels in a luminometer.
9. The obtained values should be divided by total protein measurement of the same sample for normalization.

3.5 Examples of mosaic SCOs

We have successfully used mosaic SCOs to investigate aspects of Shh signaling. We showed that cells lacking Ptch1 and Ptch2 facilitate signaling between small fractions of Shh producing cells and Shh responding cells (Roberts, Casillas, Alfaro, Jägers, & Roelink, 2016). Similarly, we showed that the loss of Glypican5 in the Shh-transporting cells facilitates signaling between fractions of Shh producing cells and Shh responding cells (Guo & Roelink, 2019). When using lineage tracing to assess the extent of mosaicism, we found that mosaic aggregates had a typical "salt and pepper" distribution of cells. In most instances this patter was maintained throughout the experiments, but in some cases cells with the same genotype clustered over time (Figure 2B, 24h). In this example *Shh*$^{-/-}$ cells that also lacked the gene coding for an enzyme involved in cholesterol synthesis (*Sc5d*$^{-/-}$) clustered in a background of *Ptch1*$^{LacZ/LacZ}$;*Ptch2*$^{-/-}$;*Shh*$^{-/-}$ cells over a 24h period.

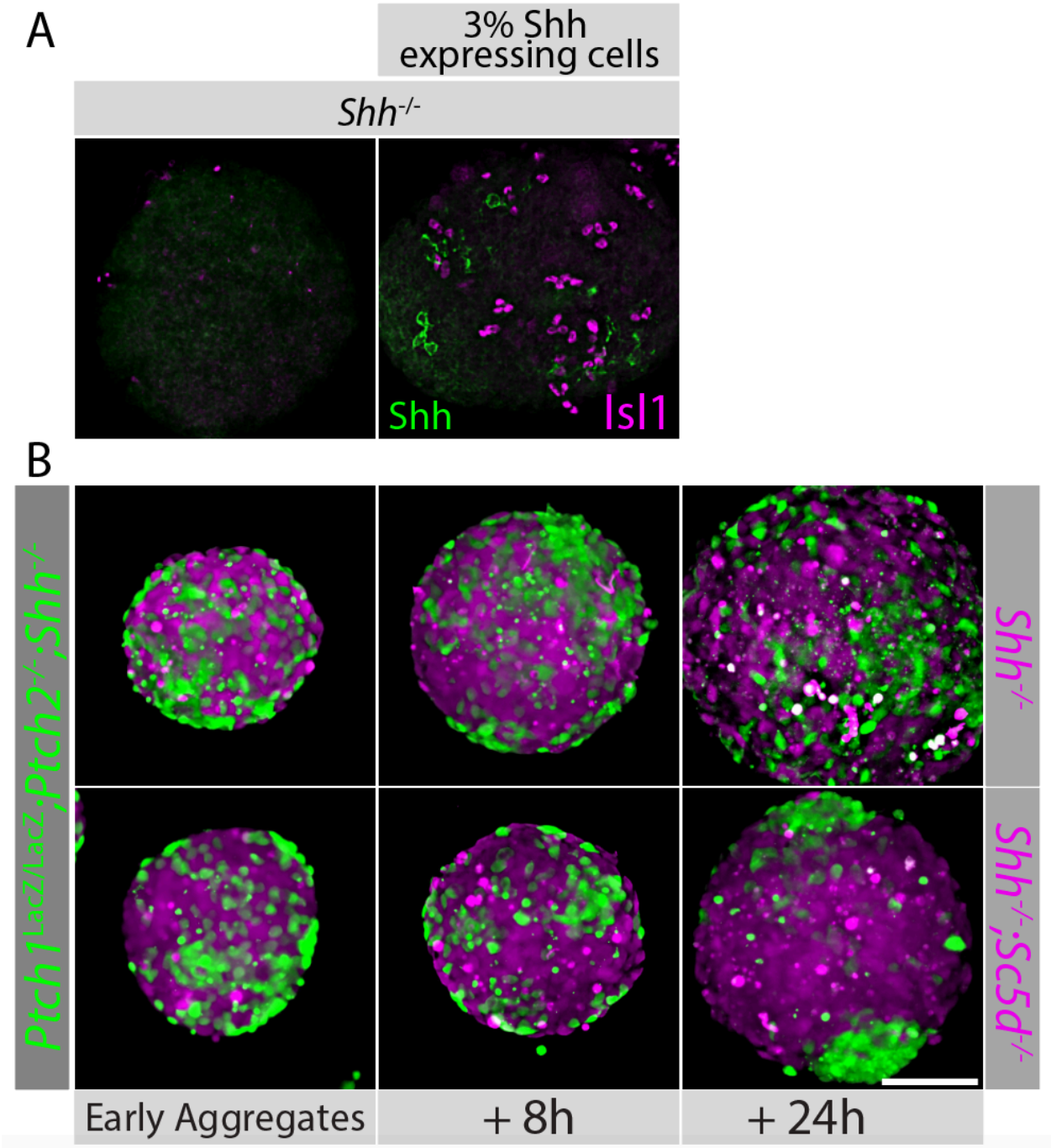

Figure 2: Examples of mosaic SCOs. A: *Shh*$^{-/-}$ SCOs were generated with or without 3% of Shh-expressing cells (indicated). The presence of the Shh expressing cells (labeled for Shh in green) induces the localized expression of the motor neuron marker Isll (magenta). **B:** *Ptch1*$^{LacZ/LacZ}$;*Ptch2*$^{-/-}$;*Shh*$^{-/-}$ mES cells were loaded with CellTracker™ CMFDA (green) dye and *Shh*$^{-/-}$ (left panel) or *Shh*$^{-/-}$;*Sc5d*$^{-/-}$ (bottom row) mES cells with CellTracker™ CMAC (magenta) prior to aggregation. Images were taken at the indicated time points of aggregation. Earliest aggregates can be observed approximately 15 h after cells were mixed and placed on a rotating platform.

4 Notes

1. If possible EB culture is performed without antibiotics.
2. Mounting medium containing DAPI is not recommended. ESCs have a high nucleus:cytoplasm ratio, so staining DNA usually provides little information. Furthermore, exposure of DAPI to UV light causes it to fluoresce at longer wavelengths, often interfering with green fluorescent dyes.
3. In general, mES cells deposit low amounts of extracellular matrix. We find that re-plating the cells into the same tissue culture dish for up to 5 passages can help in adhering the cells.
4. Lineages should be traced to ensure that cells with different genotypes do not grow disproportionally in the SCOs. Ideal are genetically encoded (fluorescent) markers but we have achieved satisfactory results with DiI/DiO or short-term CellTracker™ (Thermo Fisher) dyes. Cells can be loaded separately with the dye of choice prior to aggregation (between steps 4 and 6). Cells should be incubated at 37°C with DiI/DiO for 5 min and with CellTracker™ dyes for 30 min and washed at least twice with PBS. Re-count cells if necessary.
5. The total number of cells can be reduced if embryoid bodies clump together or form aggregates that are too big.
6. The frequency of rotation affects clumping and the size of aggregates. Optimization is empirical. Larger culture dishes should generally be rotated at a lower frequency than smaller ones.
7. It frequently happens that embryoid bodies clump together or form networks after one or two days of incubation. These bigger aggregates can be broken up by pipetting up and down or using a razor blade without negatively impacting downstream analysis. For prevention of clumps/networks forming see **Notes 5** and **6**.
8. If needed, embryoid bodies can be incubated without rotation after one night. EBs should, however, be dispersed throughout the dish and agitated regularly to prevent adhesion to the culture dish and outgrowth of cells.
9. The “pellet” in the tube is fragile and easily aspirated. Careful removal of medium using a disposable transfer pipette is recommended. Centrifugation to collect SCOs in a more stable “pellet” is not recommended as this promotes clumping.
10. As SCOs are three-dimensional objects, antibody diffusivity through the tissue is decreased. Longer wash times are therefore recommended to reduce background staining. In general, the bigger the SCOs, the longer the washing step should be. It is suggested to do the final wash overnight.
11. Mounted SCOs are easily flattened. For normal analysis this is desired as it significantly improves microscopic analysis. However, if analysis of spherical SCOs is necessary, use coverslip standoffs, or analyze without coverslips.

5 References

Andrews, M. G., Kong, J., Novitch, B. G., & Butler, S. J. (2019). New perspectives on the mechanisms establishing the dorsal-ventral axis of the spinal cord. *Curr Top Dev Biol*, *132*, 417–450. http://doi.org/10.1016/bs.ctdb.2018.12.010

Goodrich, L. V., Milenkovic, L., Higgins, K. M., & Scott, M. P. (1997). Altered neural cell fates and medulloblastoma in mouse patched mutants. *Science*, *277*, 1109–1113.

Guo, W., & Roelink, H. (2019). Loss of the Heparan Sulfate Proteoglycan Glypican5 facilitates long-range Shh signaling. *Stem Cells*. http://doi.org/10.1002/stem.3018

Kerszberg, M., & Wolpert, L. (1998). Mechanisms for positional signalling by morphogen transport: a theoretical study. *J Theor Biol*, *191*(1), 103–114.

Kornberg, T. B. (2014). Cytonemes and the dispersion of morphogens. *Wiley Interdisciplinary Reviews. Developmental Biology*, *3*(6), 445–463. http://doi.org/10.1002/wdev.151

Roberts, B., Casillas, C., Alfaro, A. C., Jägers, C., & Roelink, H. (2016). Patched1 and Patched2 inhibit Smoothened non-cell autonomously. *eLife*, *5*, e17634. http://doi.org/10.7554/eLife.17634

Wichterle, H., Lieberam, I., Porter, J. A., & Jessell, T. M. (2002). Directed differentiation of embryonic stem cells into motor neurons. *Cell*, *110*(3), 385–397.

Chapter 3

Association of Sonic Hedgehog with the extracellular matrix requires its zinc-coordination center

Carina Jägers and Henk Roelink
Department of Molecular and Cell Biology, University of California, Berkeley

Manuscript submitted to Biomed Central (BMC) Molecular and Cell Biology
Available on BioRxiv (uploaded on September 15th, 2020)
https://doi.org/10.1101/2019.12.17.880039

Abstract

Background: Sonic Hedgehog (Shh) has a catalytic cleft characteristic for zinc metallopeptidases and has significant sequence similarities with some bacterial peptidoglycan metallopeptidases defining a subgroup within the M15A family that, besides having the characteristic zinc coordination motif, can bind two calcium ions. Extracellular matrix (ECM) components in animals include heparan-sulfate proteoglycans, which are analogs of bacterial peptidoglycan and are involved in the extracellular distribution of Shh.
Results: We found that the zinc-coordination center of Shh is required for its association to the ECM as well as for non-cell autonomous signaling. Association with the ECM requires the presence of at least 0.1 µM zinc and is prevented by mutations affecting critical conserved catalytical residues. Consistent with the presence of a conserved calcium binding domain, we find that extracellular calcium inhibits ECM association of Shh.
Conclusions: Our results indicate that the putative intrinsic peptidase activity of Shh is required for non-cell autonomous signaling, possibly by enzymatically altering ECM characteristics.

Background

The *Hedgehog* (*Hh*) gene was first identified in the *Drosophila melanogaster* screen performed by Christiane Nüsslein-Volhard and Eric Wieshaus in the late 1970s (Nüsslein-Volhard & Wieshaus, 1980). Like other segment polarity genes found in this screen, *Hh* genes are widely conserved among animals, and mammals have three Hh paralogs that play roles in development (Echelard et al., 1993). Like all other Hhs, Sonic Hedgehog (Shh) is synthesized as a pro-protein that undergoes autoproteolytic cleavage mediated by the C-terminal part yielding an N-terminal part (ShhNp) that is the active ligand. Structural analysis of ShhN revealed its similarity to zinc-peptidases and Shh coordinates a zinc ion with residues H141, D148, and H183 (Hall, Porter, Beachy, & Leahy, 1995). The notion that Shh signaled through a peptidase activity was quickly rejected by demonstrating that mutation of a critical residue involved in catalysis (E177) did not impair the ability of Shh to activate the Hh response (Fuse et al., 1999), and consequently the zinc coordination center of Shh is often referred to as its "pseudo active" site (Bosanac et al., 2009; Maun et al., 2010). Still, a role for the zinc coordination center is supported by the finding that Shh-E177A is unable to mediate non-cell autonomous long-range signaling from the notochord to the overlying neural plate (Himmelstein et al., 2017). Perhaps unsurprisingly, the zinc-coordination motif is found mutated in some individuals with the Shh signaling-related birth defect holoprosencephaly (Roessler et al., 1996; Traiffort et al., 2004), further indicating that the zinc-coordination center of Shh is important for normal function. This is consistent with structures of Shh complexed with its receptor Patched1 (Ptch1), showing that the N-terminal 22 residues of Shh that are not part of the zinc-coordination motif, mediate binding to Ptch1 (Gong et al., 2018; Qi, Schmiege, Coutavas, & Li, 2018a; Qi, Schmiege, Coutavas, Wang, & Li, 2018b) and suffice to regulate Ptch1 activity (Tukachinsky, Petrov, Watanabe, & Salic, 2016).

Some bacterial species have conserved genes coding for peptidases that coordinate zinc and calcium identically to Shh (Rebollido-Rios et al., 2014; Roelink, 2018). These bacterial peptidases (members of the M15A subfamily of zinc D-Ala-D-Ala carboxypeptidases) cleave murein peptidoglycans, suggesting that Shh too might cleave a glycan-modified protein, possibly a matrix heparan sulfate proteoglycan (HSPGs). HSPG are an integral part of the extracellular matrix (ECM) and play in important role in the transport and presentation of several morphogens, including Hhs (Yan & Lin, 2009). Several HSPGs bind Shh and can both negatively and positively affect the Shh response (Capurro et al., 2008; Carrasco, Olivares, Faunes, Oliva, & Larraín, 2005; Guo & Roelink, 2019; Witt et al., 2013). Furthermore, mutations in *Ext1* and *-2* coding for glycosyltransferases that catalyze glycosaminoglycan addition to the core proteins, disrupt Hh signaling in vertebrates (Guo & Roelink, 2019; Siekmann & Brand, 2005) and insects (Bellaiche, The, & Perrimon, 1998).

By mutating residues in the zinc-coordination center that are conserved between bacterial Hh-like peptidases and Shh, we provide evidence that this center is required for the association of ShhN to the ECM and for non-cell autonomous signaling. Release of Shh into the ECM is enhanced in the presence of μM amounts of zinc indicating that this ion is

an agonist of Shh. The ECM-associated Shh is active in signaling, indicating that the zinc-coordination center of Shh mediates its release into the ECM to facilitate non-cell autonomous signaling, possibly through an intrinsic metallopeptidase activity of Shh.

Results

ShhN associates with the extracellular matrix

Due to its very high sequence similarity to bacterial murein peptidases (Roelink, 2018), a conceivable function for the Shh zinc-coordination center could be to modify proteoglycans, thereby affecting its extracellular matrix (ECM) association. Cultured cells condition their substrate with functional ECM proteins like fibronectin and collagen, at least some of which is retained by the substrate after removal of the cells (Hellewell, Rosini, & Adams, 2017). Shh has a Cardin-Weintraub motif that mediates binding to heparan sulfate in the ECM (Farshi et al., 2011; Ohlig et al., 2012), and we assessed ECM-bound Shh in the fraction of macromolecules that remain on the tissue culture plate after non-lysing cell removal. Hek293t cells were transfected with *Shh* (mutant) constructs and after two days the cells were removed by washing with PBS and mild agitation. The cells were then collected and lysed with RIPA buffer for protein gel and Western Blot analysis. The tissue culture dishes were extensively washed with PBS and remaining material was collected in hot SDS using a scraper for further analysis (Hellewell et al., 2017). We will refer to this as the ECM fraction. Using gel electrophoresis followed by SYPRO Ruby protein staining, we detected overall fewer proteins in the fraction remaining in the tissue culture dish (ECM) compared to the cell-only fraction (lysate) with a pattern distinct from the lysate indicating recovery of extracellular molecules (Figure 1A). Here, we are focusing on the association of Shh with the ECM, and in order to circumvent the complexities of Shh maturation and secretion (Tian, Jeong, Harfe, Tabin, & McMahon, 2005), we used Shh-C199* (ShhN). This form of Shh is active and secreted independent of Disp1 function (Tukachinsky, Kuzmickas, Jao, Liu, & Salic, 2012), and lacks the C-terminal sterol modification. We found that ShhN could readily be detected in the ECM extracted from decellularized tissue culture plates. (Figure 1B). Visualizing Shh-C199* by staining of the decellularized plates with the anti-Shh mAb5E1, "footprints" of Shh producing cells were observed (Figure 1B). Shh-C199* is commonly thought of as a "soluble" protein and also accumulates in the supernatant of ShhN-producing cells. The non-homogeneous association with the ECM indicates that upon secretion ShhN enters adjacent ECM directly and not via an intermediate soluble form as this would result in a homogeneous Shh distribution in the ECM. More ShhN could be detected in the ECM than in the cell-only fraction of *Shh-C199** transfected Hek293t cells (Figure 1B), showing that entry of ShhN into the ECM is robust. Shh-responsive LightII cells plated on the decellularized and ShhN-conditioned ECM showed that it is able to elicit a transcriptional Hh pathway response similar to that of ShhN-conditioned medium (Figure 1C). Furthermore, wild-type Shh bound to the ECM also activated the Hh pathway response in LightII cells (Figure 1D).

Mutations in the Zinc-coordination motif reduce the stability of Shh-C199*

Mutating the residues directly involved in the coordination of zinc are obvious candidates to assess a role for the zinc-coordination center. However, Shh mutants in the zinc coordination motif could barely be detected as the N-terminal processed form (ShhNp) on Western Blots, despite normal detection of the Shh pro-protein (Casillas & Roelink, 2018).

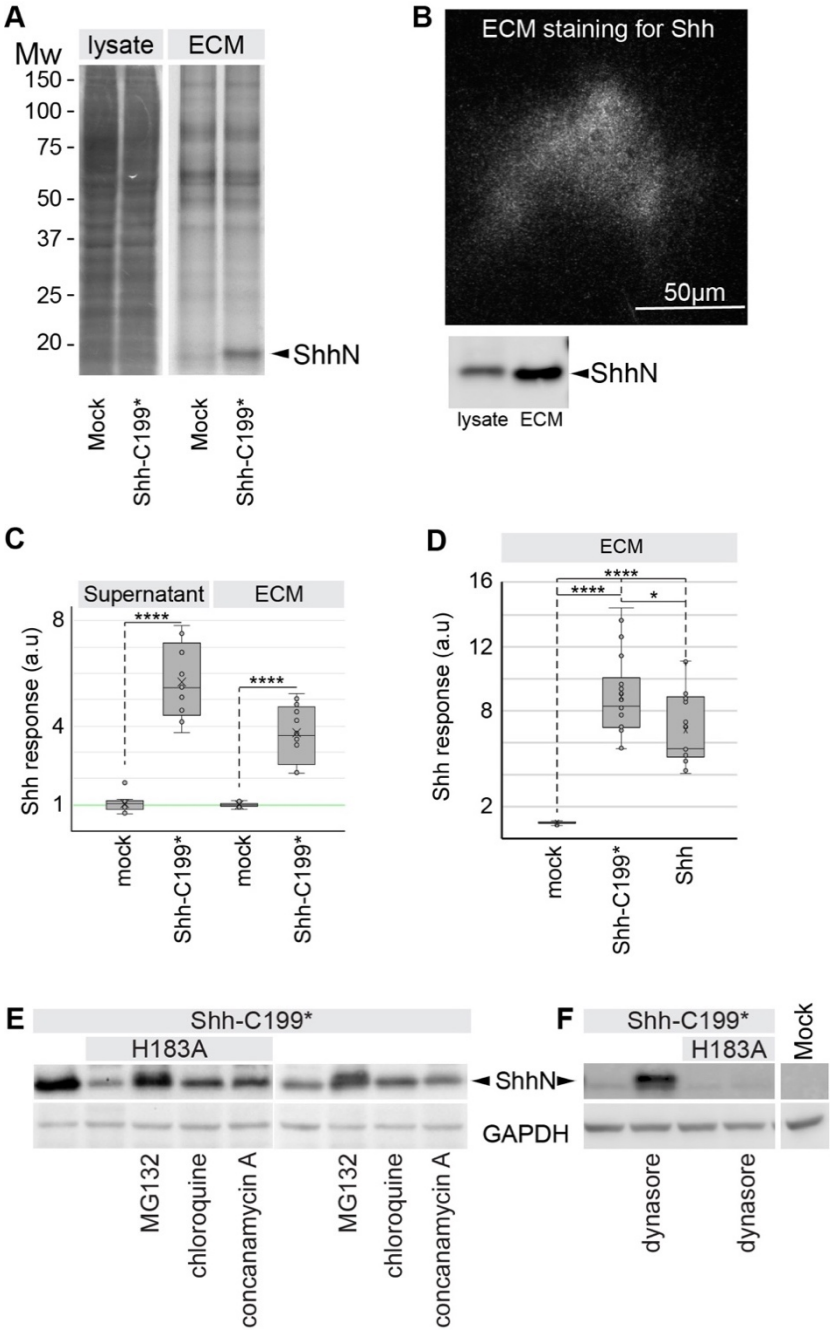

Figure 1: Active ShhN associates with the extracellular matrix. **A:** Lysate and ECM deposited by mock and *Shh-C199**-transfected Hek293t cells analyzed by SDS-PAGE and SYPRO-Ruby staining. ShhN is indicated. **B:** *Shh-C199**-transfected Hek293t cells were plated on glass slides and removed after 24h. The slides were stained with mAb5E1, showing the presence of ShhN. Scale bar is 50µm. **C:** Supernatant and ECM conditioned by *Shh-C199**-transfected Hek293t cells. LightII cells were either grown on mock or ShhN conditioned ECM. Cells grown on ECM deposited by mock transfected cell were grown in the absence or presence of mock or Shh-C199* conditioned supernatant. Box and whisker plots, n ≥ 3. *p<0.05, ****p<0.0001. **D:** Hh response in LightII cells grown on the decellularized ECM of mock-, *Shh-C199**-, or *Shh*-transfected Hek293t cells. ****p<0.0001. **E:** Western blot analysis of HEK293t cells transfected with the indicated Shh mutants. 100 nM MG-132 (proteasome inhibitor), 100 nM Chloroquine and 100 nM Concanamycin A (inhibitors of endosome acidification) were assessed for their ability to affect Shh accumulation. **F:** Western blot analysis of HEK293t cells transfected with the indicated Shh mutants, and the effects of the dynamin inhibitor Dynasore (50 µM) was assessed for its effect on Shh accumulation.

We and others (Traiffort et al., 2004) initially incorrectly interpreted this as a failure of auto-processing, but the same low levels were observed analyzing these mutants in Shh-C199*. Addition of the proteasome inhibitor MG132 (Lee & Goldberg, 1998) or the inhibitor of endosome acidification chloroquine resulted in ShhN accumulation of Shh-C199*/H183A (ShhN/H183A), possibly indicating a misfolded protein-induced degradation of this mutant (Figure 1E). The Dynamin inhibitor Dynasore (that inhibits endocytosis) (Macia et al., 2006) causes strong accumulation of Shh-C199*, but not of Shh-C199*/H183A, further indicating that the destabilization of Shh-C199*/H183A occurs before it reaches the plasma

membrane (Figure 1F). We found that other zinc coordination mutations as well as several holoprosencephaly-associated point mutations in Shh cause its destabilization, indicating a role for increased ShhN degradation in this birth defect (Casillas & Roelink, 2018). In general, we will not use these mutants with a reduced half-life.

The zinc-coordination center of Shh is required for association with the ECM

BacHh belongs to a family of metallopetidases that coordinate zinc, and consistent with the absolute conservation of the zinc-coordination center, zinc was found in the catalytic cleft of Shh (Figure 2A, grey sphere). We hypothesized that occupancy of the zinc-coordination center is required for normal Shh function. The K_d for zinc binding to Shh in the absence of calcium appears to be low (Day et al., 1999), but DMEM tissue culture

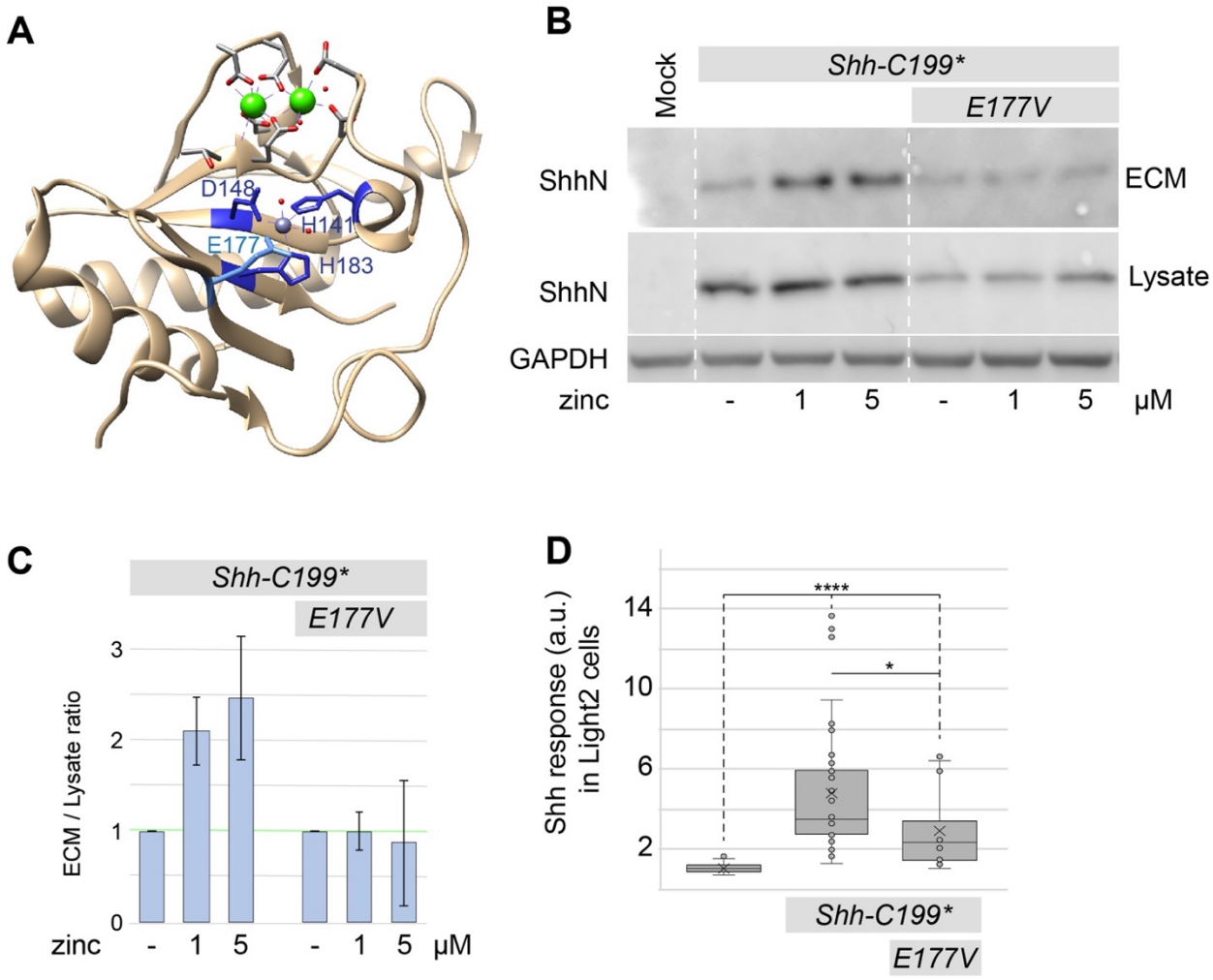

Figure 2: ECM-association of ShhN requires zinc and the catalytic E177V residue. A: Diagram of the Shh structure (PDB: 3D1M) with relevant residues indicated. **B:** Western blot analysis of the lysate and ECM of HEK293t cells transfected with *Shh-C199** and *Shh-C199*/E177V* and cultured in DMEM containing 0.18 mM calcium and the indicated concentrations of zinc. **C:** Quantification of band intensities shown in C as a fraction of ECM over lysate, normalized to the respective mock treatment. n=2. **D:** Hh response in LightII cells grown on the conditioned and decellularized ECM of Hek293t cells transfected with *Shh-C199** or *Shh-C199*/E177V*. n ≥ 3, *p<0.05, ****p<0.0001.

medium has no added zinc and is thus expected to have only very small amounts of it. While the amount of protein in the lysate of Hek293t cells transfected with *Shh-C199** remained relatively unchanged with increasing zinc concentrations, the amount of ECM-bound Shh-C199* increased approximately two and a half times with an EC_{50} between 0.1 and 1 μM zinc (Figure 2B, C). This indicates that there is little effect of zinc on Shh synthesis and intracellular stability, but that occupancy of the zinc coordination center enhances ECM association. Divalent copper and magnesium failed to increase the amount of ShhN in the ECM (Figure S2). Calcium, however, did have an effect consistent with its ability to bind to ShhN, and is further addressed below.

Besides the zinc coordinating residues, the glutamic acid residue at position 177 (E177, mouse numbering) is well-conserved and in close proximity to the zinc-coordinating residues (Figure 2A). In Shh-related peptidases the E177 equivalent is required for catalytic activity as it strips a proton from water yielding a reactive hydroxide. The mutants Shh-C199*/E177A and -/E177V are predicted to be able to coordinate zinc but lack the putative catalytic activity. Unlike the zinc coordination mutants, we found the Shh-C199*/E177A and -/E177V mutants to be stable in the lysate (Figure 2B). Shh-C199*/E177V in decellularized ECM activated the Hh response in LightII cells to a smaller extend than Shh-C199* (Figure 2D). This was likely was caused by lower protein amounts of Shh-C199*/E177V in the ECM, as we found that the amount of Shh-C199*/E177V in the ECM was similar to that of Shh-C199* under low zinc concentrations but failed to further accumulate in the ECM under increasing zinc concentrations. This demonstrates that ShhE177 is required for ECM association (Figure 2B, C), and importantly that the zinc effects are not primarily mediated by a Shh-independent zinc sensitive event. These observation supports the notion that a catalytic activity intrinsic to Shh is required for its association with the ECM.

Mutating residues in the zinc-coordination motif of Shh affect association with the ECM

A second group of conserved residues in the zinc-coordination motif are two histidine residues with stacking sidechains, H135 and H181 (Figure 3A). These two histidine residues are conserved between Shh and BacHhs, but either one can be a tyrosine residue in M15A peptidases, and a tyrosine residue is present in the position homologous to H181 in butterfly and moth Hhs (e.g. NCBI PCG69308.1). We mutated either or both histidine residues 135/181 into alanine or tyrosine residues (*Shh-C199*/H135Y*or*A*, *Shh-C199*/H181Y*or*A*) and found that these forms of Shh process normally and are stable in the lysate (Figure 3C). Substituting one or two histidines with tyrosines had little effect on the mutant's ability to elicit a Hh response in LightII cells from conditioned ECM (Figure 3B). Alanine substitutions reduced the Hh response in the LightII compared to Shh-C199* (Figure 3B). Similar to Shh-C199*/E177V, the reduced Hh response coincided with lower protein levels in the ECM. Mutants with one or two tyrosine substitutions as well as single alanine substitutions could be rescued under high zinc conditions (1, 10 μM) suggesting that tyrosine residues, as they are found in butterfly and moth Hhs, are largely synonymous mutations. Only *Shh-C199*/H135A/H181A* poorly associated with the ECM in the presence of zinc. We found that all H135 and H181 mutants have a similar EC_{50} for zinc (Figure 3D),

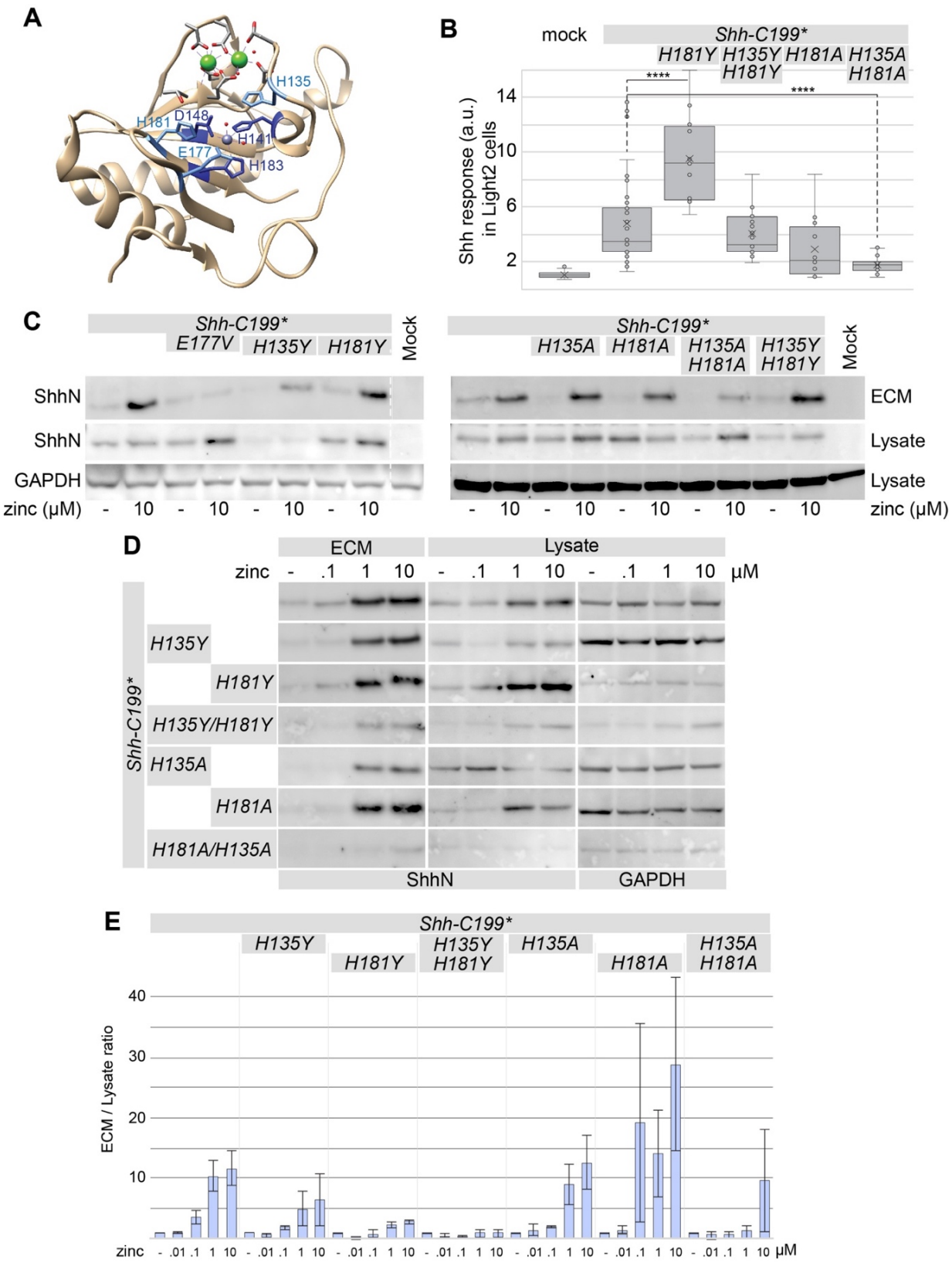
A
H135
H181
D148
H141
E177
H183
B
mock
Shh-C199*
H181Y
H135Y H181Y
H181A
H135A H181A
****
****
Shh response (a.u.) in Light2 cells
14
10
6
2
C
Shh-C199*
E177V
H135Y
H181Y
Mock
H135A
H181A
H135A H181A
H135Y H181Y
Mock
ShhN
ShhN
GAPDH
ECM
Lysate
Lysate
zinc (μM) - 10 - 10 - 10 - 10
- 10 - 10 - 10 - 10 - 10
zinc (μM)
D
ECM
Lysate
zinc - .1 1 10 - .1 1 10 - .1 1 10 μM
Shh-C199*
H135Y
H181Y
H135Y/H181Y
H135A
H181A
H181A/H135A
ShhN
GAPDH
E
Shh-C199*
H135Y
H181Y
H135Y H181Y
H135A
H181A
H135A H181A
ECM / Lysate ratio
40
30
20
10
zinc - .01 .1 1 10 - .01 .1 1 10 - .01 .1 1 10 - .01 .1 1 10 - .01 .1 1 10 - .01 .1 1 10 - .01 .1 1 10 - .01 .1 1 10 μM

Figure 3: Stacking histidines of the zinc coordination center affect ECM association. A: Diagram of the Shh structure (PDB: 3D1M) with relevant residues indicated. **B:** Hh response in LightII cells grown on the conditioned and decellularized ECM of Hek293t cells transfected with the indicated *Shh-C199** constructs. n ≥ 2, *p<0.05, ****p<0.0001. **C:** The effect of mutations of the transition state-stabilizing residues H135 and H181 to alanine (A) or tyrosine (Y) on the zinc-dependent accumulation in the ECM was analyzed on a Western Blot of the extracted ECM from transfected HEK293t cells cultured in 0.18 mM calcium with or without 10 µM zinc. **D:** zinc dose-response analysis of H135 and H181 mutations assessed by Western blot of the lysate and ECM of HEK293t cells transfected with the indicated mutants and cultured in 0.18 mM calcium and increasing concentrations of zinc (0.1, 1, 10 µM). **E:** Quantification of band intensities shown in D as a fraction of ECM over lysate, normalized to the respective mock treatment. n=2.

consistent with the notion that these residues are not directly involved in zinc coordination. Together with *Shh-C199*/E177V*, our findings using *Shh-C199*/H135A/H181A* further support the notion that the zinc-coordination center of Shh is required for ECM association.

The peptidase domain of a BacHh is unable to facilitate ECM association

The protein sequences of bacterial Hhs (BacHh) are highly similar Shh and all residues of the zinc coordination motif are identical. As BacHhs are predicted to be peptidoglycan peptidases we tested if this bacterial peptidase activity could substitute for the putative peptidase activity intrinsic to ShhN. The conservation between BacHhs and Shh involves the calcium and zinc binding motifs, but neither the N-terminal domain that binds to Ptch1 and Heparan Sulfate (Farshi et al., 2011), nor the 10 amino acids that follow this domain in ShhN. Therefore, we made a construct coding for a chimeric protein consisting of the N-terminal 65 residues of Shh, the conserved calcium and zinc binding motifs of *Bradyrhizobium paxllaeri* BacHh (codon optimized for expression in mammalian cells), followed by an HA tag replacing the bacterial stop codon, followed by the last 10 residues of Shh up to G198 (Shh/BacHh^{HA}, Figure 4A diagram). As a control, we positioned an HA tag at the same distance (10 residues) from the C-terminus of Shh-C199* (Shh^{HA}-C199*). We found that Shh^{HA}-C199* behaved indistinguishable from Shh-C199* and entered into the ECM and the medium in a zinc-dependent manner (Figure 4A). In contrast, although readily detected in the lysate, no Shh/BacHh^{HA} was detected in the ECM or the medium (Figure 4A). We detected similar amounts of GAPDH in the medium as in the cell lysate. GAPDH is commonly used as a loading control for intracellular proteins but has also been described as a soluble form found in the extracellular compartment (Kunjithapatham et al., 2015). Cell lysis in the tissue culture as an explanation for GAPDH in the medium seems unlikely, as no Shh/BacHh^{HA} was detectable in the soluble fraction. As ShhN can be internalized by several Shh-binding proteins (Incardona et al., 2000; McCarthy, Barth, Chintalapudi, Knaak, & Argraves, 2002; Wilson & Chuang, 2010), we assessed whether the chimeric proteins accumulates on the outside of cells with detergent-free, live staining with an α-HA antibody prior to fixation of transfected receptor-less (*Ptch1*$^{LacZ/LacZ}$;*Ptch2*$^{-/-}$;*Boc*$^{-/-}$;*Cdo*$^{-/-}$;*Gas1*$^{-/-}$) fibroblasts. We found no difference in staining between Shh^{HA}-C199* and Shh/BacHh^{HA}, indicating that Shh/BacHh^{HA}, similarly to Shh^{HA}-C199*, is being trafficked to the plasma membrane (Figure 4B). It is not, however, being released from the cell, indicating that the bacterial zinc-coordination domain is not sufficient for entry into the

ECM. *Bradyrhizobium paxllaeri* BacHh presumably lacks the specificity for an ECM binding partner that is recognized by Shh. These results suggest that the observed presence of Shh and ShhN in the decellularized tissue culture plate is due to a precise property of Shh rather than simple cell lysis or ShhN-containing cell debris.

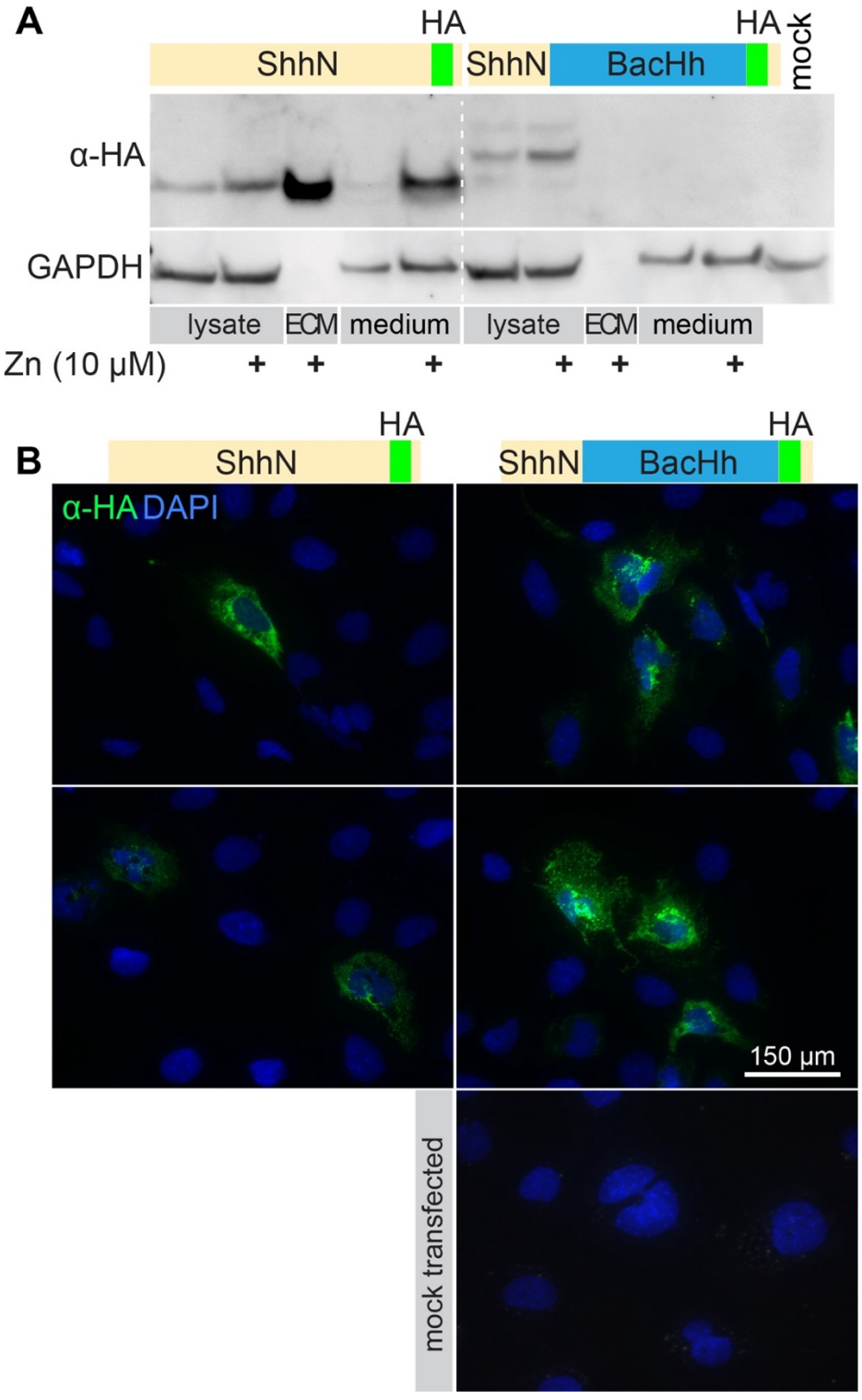

Figure 4: **The zinc-coordination domain of BacHh is not sufficient for association with the ECM. A:** Western Blot analysis of the lysate, ECM, and supernatant of *ShhN-HA* or *Shh-BacHh-HA* (diagrams) transfected HEK293t cultured in the indicated zinc concentrations. **B:** Detergent-free live staining with an α-HA antibody (3F10) of transfected *Ptch1*$^{LacZ/LacZ}$;*Ptch2*$^{-/-}$;*Boc*$^{-/-}$;*Cdo*$^{-/-}$;*Gas1*$^{-/-}$ cells. Nuclei were stained with DAPI.

Shh-C199* mutants unable to bind calcium remain sensitive to zinc

The overall structure of ShhN and BacHhs indicate that they consist of a regulatory calcium-binding and a catalytic zinc coordinating center (Rebollido-Rios et al., 2014), making up most of ShhN outside the extreme N-terminal Ptch1-binding domain. With the exception of BacHhs, bacterial M15A metallopeptidases lack the Hh/BacHh-type calcium coordination center, and this part is thus unlikely to be required for catalytic function *per se*. We made a Shh-C199* mutant that lacked all calcium-coordinating residues (Shh-C199*/E90A/E91D/D96A/E127A/D130N/D132L, Shh-C199*-Ca^{Free}) and this form of Shh should be unable to bind calcium. After transfection, more ShhN was detected in lysates of cells cultured in the presence of higher calcium levels, but that was also observed in the Shh-C199*-Ca^{Free} expressing cells, and thus unlikely a direct effect of calcium on Shh (Figure 5A). Increased amounts of ShhN in the lysate at higher calcium concentrations complicated the interpretation of the effects of calcium on ShhN accumulation in the ECM. Sill, while ShhN accumulation in the ECM varied with calcium concentrations, that of the Shh-C199*-Ca^{Free} mutant remained at the same level, indicating that this mutant is insensitive to extracellular calcium as measured by ECM association (Figure 5A).

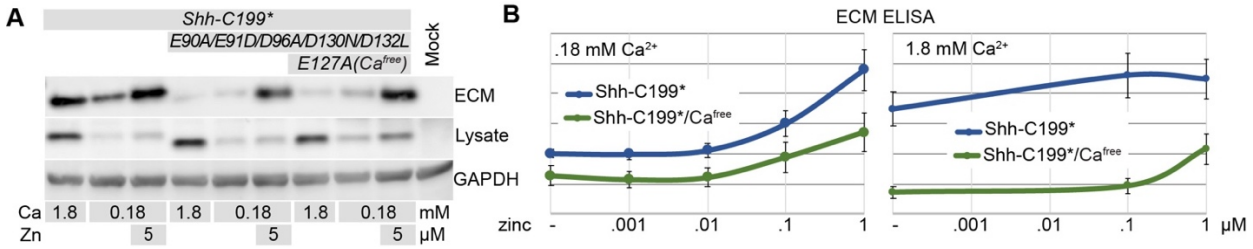

Figure 5: Calcium alters the sensitivity of Shh to zinc. A: Western blot analysis of lysates and ECM of HEK293t cells transfected with *Shh-C199**, *Shh-C199*/E90A/E91D/D96AD130N/D132L*, or *Shh-C199*/E90A/E91D/D96A/E127A/D130N/D132L* (*Ca*^{Free}), cultured in the presence of 0.18 or 1.8 mM calcium, and in the absence or presence of 5 µM added zinc. **B:** ECM-associated Shh-C199*N or Shh-C199*/Ca^{Free} deposited by transfected HEK293t cells was assessed by ELISA in the presence of .18 mM calcium (left panel) or 1.8 mM calcium (right panel) and increasing zinc concentrations as indicated. Shown are means and standard errors, n=6.

One possible mechanism of calcium regulating the transition from a cell- to an ECM-bound state would be by affecting zinc coordination, thereby changing its K_d for zinc. We therefore tested if the EC_{50} of zinc is different under high (1.8 mM, the concentration in regular DMEM) and low (0.18 mM, the lowest concentration the cultured cells appeared normal) calcium. Under low calcium conditions, the addition of 5 µM zinc to the medium resulted in increased accumulation of ShhN in the ECM both of Shh-C199*-Ca^{Free} and Shh-C199* (Figure 5A). This indicates that Shh-C199*-Ca^{Free} is still active and supports the notion that calcium binding is not required for Shh distribution. E127 is located at the

interface between the calcium and zinc-binding centers of Shh, and we tested if restauration of this residue in Shh-C199*-Ca^{Free} affects ECM localization but found little or no difference (Figure 5A). To better quantify the effect of calcium and zinc on Shh-C199* and Shh-C199*-Ca^{Free} in their ability to accumulate in the ECM we used an indirect ELISA protocol directly on the decellularized ECM. HEK293t cells were cultured and transfected in 96 well plates and washed off with PBS to allow for subsequent detection of ShhN with HRP-linked antibodies. Under low calcium conditions we found that the response to increasing zinc concentrations was similar between Shh-C199* and Shh-C199*-Ca^{Free} (Figure 5B). For both versions of Shh-C199*, the EC_{50} for zinc appeared to be around 0.1 µM. Instantiated in Figure 5A and quantified over multiple experiments in Figure 5B, it appears that Shh-C199*-Ca^{Free} is less efficient in entering the ECM than Shh-C199*. This effect was more profound in the presence of 1.8 mM calcium, and much more Shh-C199* was detected in the ECM than Shh-C199*-Ca^{Free} in the absence of added zinc. The addition of zinc had a bigger effect on Shh-C199*-Ca^{Free} than on Shh-C199*. These results indicate that Shh-C199*-Ca^{Free} behaves similarly in high and low calcium and resembles Shh-C199* under low calcium. Thus, whereas the behavior of Shh-C199* changes as a function of calcium, that of Shh-C199*-Ca^{Free} does not, indicating that binding of calcium to Shh alters its intrinsic properties as measured by its ECM association. The calcium concentration in the endoplasmic reticulum and the Golgi apparatus is variable, with values ranging from 0.2-1 mM (Alonso, Rojo-Ruiz, Navas-Navarro, Rodríguez-Prados, & García-Sancho, 2017). These concentrations that Shh encounters in these organelles are within the range in which we observe changes in zinc sensitivity of ShhN, consistent with the notion that the activity of ShhN could be regulated by calcium.

Distribution of cholesterol-modified ShhNp in the ECM differs from cholesterol-unmodified ShhN but remains zinc sensitive

While ShhN could readily be detected in the ECM of Hek293t cells, ShhNp was poorly detectable on Western Blots of the ECM fraction of Hek293t cells. We therefore turned to staining of decellularized ECM of our line of fibroblasts lacking Shh binding partners (*Ptch1*$^{LacZ/LacZ}$;*Ptch2*$^{-/-}$;*Boc*$^{-/-}$;*Cdo*$^{-/-}$;*Gas1*$^{-/-}$) that were found to accumulate ShhNp in the ECM to comparable levels as ShhN, presumably due to a failure to re-internalize ShhN(p) (Figure 6A and B). Staining for Shh on decellularized plates showed that ShhN was present in small puncta that gave a cloudy appearance at lower magnifications, whereas cholesterol-modified ShhNp was detected in larger puncta in more restricted areas (Figure 6A). 5 µM zinc increased ShhN and ShhNp association with the ECM as measured by fluorescence intensity across the entire image area (Figure 6B). The effects of zinc on Shh distribution in the presence of 1.8 mM calcium was much less pronounced, further supporting the finding that high calcium negatively affects the zinc-dependent activity of Shh.

To assess if the observed effects require the zinc-coordination center of Shh we tested Shh-E177V, and -H181Y for their ability to associate with the ECM. Consistent with the biochemical observations using Shh-C199* (Figures 1, 2, 3), we could barely visualize ShhE177V in the ECM (Figure 6B). In contrast, ShhH181Y distribution into the ECM was

indistinguishable from Shh, further indicating that this "butterfly version" of Shh is functional (Figure 6B).

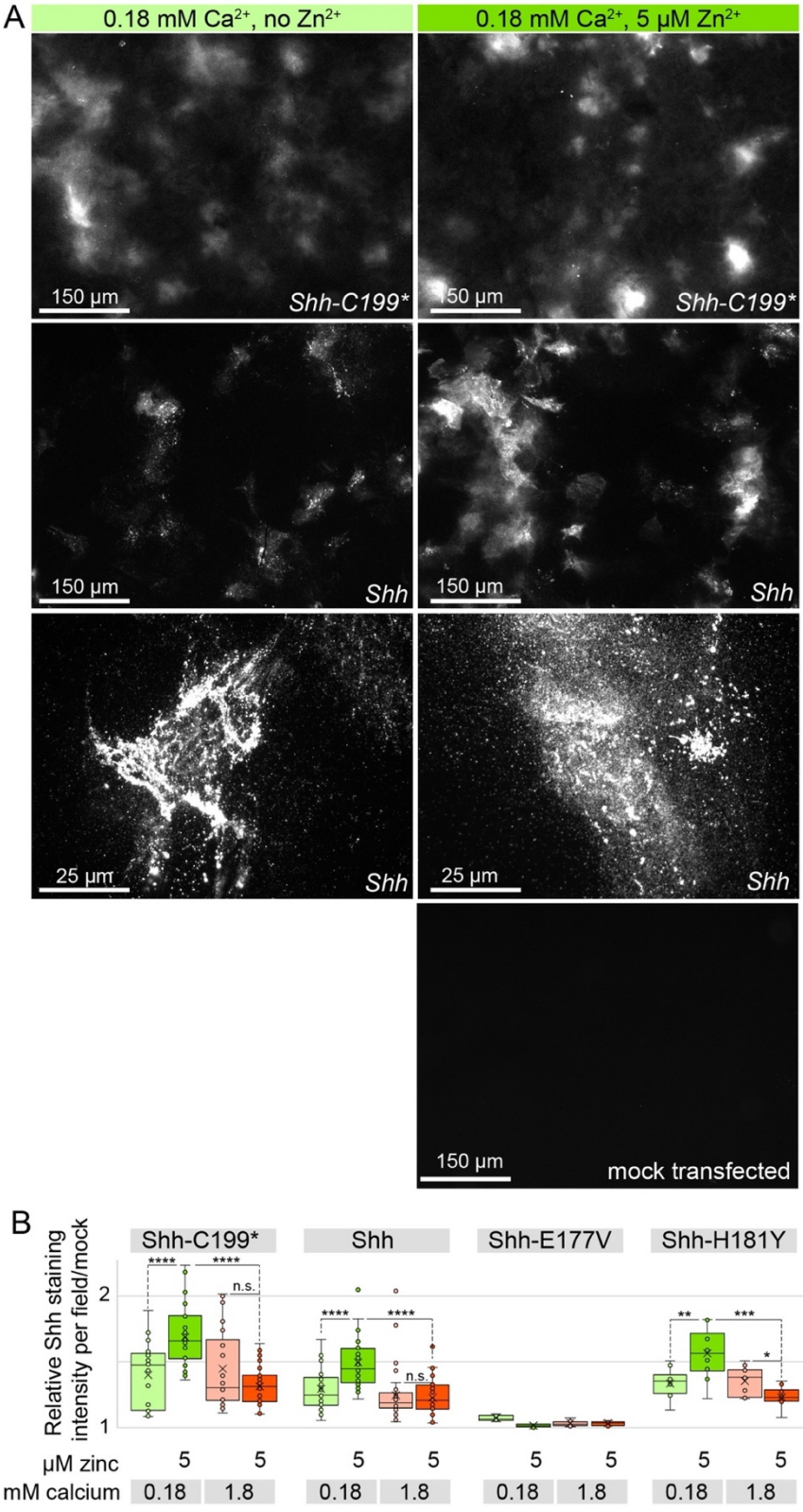

Figure 6: Cholesterol-modified ShhNp associates with the ECM in a zinc and peptidase-dependent manner. A: *In situ* staining with anti ShhN mAb5E1 of ECM deposited by *Ptch1*$^{LacZ/LacZ}$;*Ptch2*$^{-/-}$;*Boc*$^{-/-}$;*Cdo*$^{-/-}$;*Gas1*$^{-/-}$ cells that were transfected with *Shh* or *Shh-C199** in the presence or absence of 5 µM zinc and presence of 0.18 mM calcium. **B:** Quantification of ECM-bound Shh shown in A. Box and whisker plots of mean fluorescence intensity per image of 10 microscope fields per experiment was measured in ImageJ and normalized to the ECM of mock transfected cells. n=3, ****p<0.0001.). **C:** LightII cells co-cultured with *Shh-C199** and *Shh-C199*/E177V* transfected *Ptch1*$^{LacZ/LacZ}$;*Ptch2*$^{-/-}$ fibroblasts in the presence of 0.18 calcium and the indicated zinc concentrations. Responses were normalized to Shh-C199* with 1.8 mM calcium and no zinc. Shown are means and standard errors of 3 independent experiments. *p<0.05, **p<0.01. **D:** HEK293t cells transfected with *Shh-C199** and *Shh-C199*/H135A/H181A* were incorporated into spinal cord organoids otherwise consisting of *Ptch1*$^{+/LacZ}$;*Shh*$^{-/-}$ stem cells were assessed for LacZ induction. n=4, ****p<0.0001.

Mutations in the putative peptidase domain reduce non-cell autonomous signaling

To test if the increased accumulation of Shh in the ECM is correlated with the non-cell autonomous signaling efficacy, we assessed the signaling activity of ShhN expressing cells embedded in three-dimensional cell aggregates of responding cells (Figure 7A). Live staining with 5E1 prior to fixation and cell permeabilization showed that ShhNp and ShhC199* were detected around a large proportion of cells in transfected Hek293t aggregates. In mixed aggregates consisting of 80% Hh-responsive *Ptch1*$^{LacZ/+}$;*Shh*$^{-/-}$ mouse embryonic stem cell (mESC) reporter cells and 20% transfected Hek293t cells, we observed that both Hek293t-derived ShhNp and Shh-C199* induced the Shh response (Figure 7B). Shh peptidase mutants (Shh-E177V and Shh-H135A/H181A) failed to elicit a Hh-response, further supporting the notion that the peptidase activity is required for non-cell autonomous signaling. The pattern of Shh extracellular distribution was similar for Shh and Shh-E177V as seen in detergent-free live staining with 5E1, although slightly weaker staining for Shh-E177V was observed. In a more stringent non-cell autonomous assay, aggregated of transfected Hek293t cells were co-cultured with 3D spinal cord organoids (SCOs) derived from the mESC *Ptch1*$^{LacZ/+}$;*Shh*$^{-/-}$ reporter cells. Whereas the Hh response to ShhNp was below detection level in this assay, Shh-C199* induced the Shh response in reporter cells (Figure 7C), likely via a soluble form of ShhN. Putative peptidase mutants failed to show any activity in this assay, further supporting the idea that an intact zinc-coordination center of Shh is necessary to mediate the release from Shh-producing cells and consequently, the facilitation of long-range signaling.

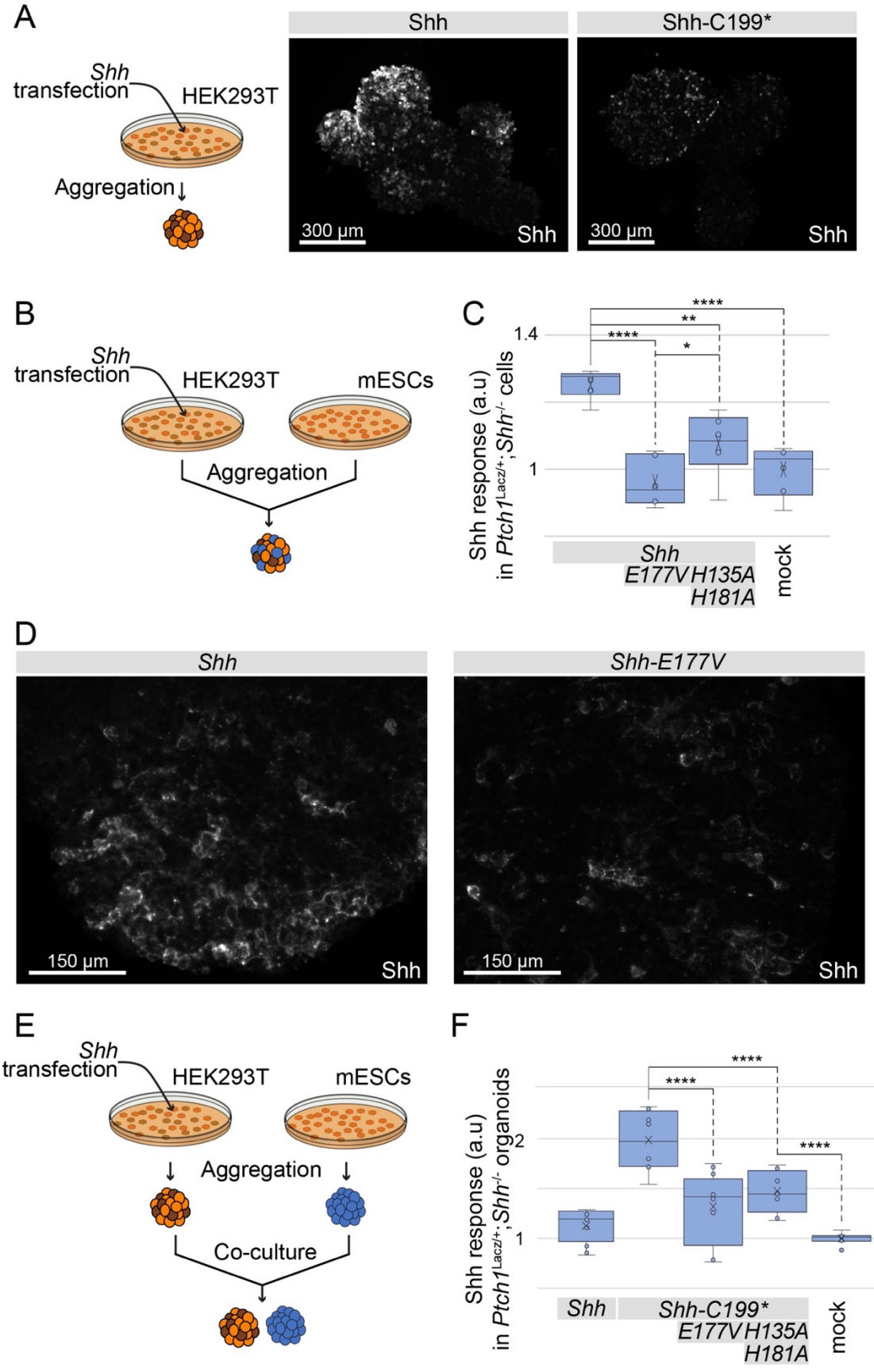
A
Shh
transfection
HEK293T
Aggregation
Shh
Shh-C199*
300 µm
Shh
300 µm
Shh
B
Shh
transfection
HEK293T
mESCs
Aggregation
C
Shh response (a.u)
in Ptch1Lacz/+;Shh-/- cells
1.4
1
****
**
****
*
Shh
E177V
H135A
H181A
mock
D
Shh
Shh-E177V
150 µm
Shh
150 µm
Shh
E
Shh
transfection
HEK293T
mESCs
Aggregation
Co-culture
F
Shh response (a.u)
in Ptch1Lacz/+;Shh-/- organoids
2
1
****
****
****
Shh
Shh-C199*
E177V
H135A
H181A
mock

Figure 7: **The zinc coordination center of Shh is required for long-range signaling. A**: Experimental setup and immunofluorescent staining of Shh-expressing Hek293t aggregates. Hek293t cells were transfected with *Shh* or *Shh-C199**, washed off the culture dish with PBS and placed on a rotating platform in DMEM without serum for 2 days, followed by live staining with 5E1. **B:** Experimental setup: Hek293t cells were transfected with Shh-constructs, washed off the culture dish with PBS, and mixed with mESC *Ptch1*$^{LacZ/+}$;*Shh*$^{-/-}$ reporter cells in a 1:4 ratio. Chimeric aggregates were then formed on a rotating platform in the absence of serum. The Ptch1:LacZ expression was measured after 3 days and normalized to total protein content. **C:** Ptch1:LacZ expression in chimeric aggregates in response to the indicated versions of Shh expressed by Hek293t cells. Box-and-Whisker plot, n=2. **p*<0.05, ***p*<0.01, *****p*<0.0001. **D:** 5E1 live staining of Shh in the chimeric aggregates described in B and C. **E:** Experimental setup: Hek293t cells were transfected with Shh-constructs, washed off the culture dish with PBS, and incubated on a rotating platform. Separate mESC *Ptch1*$^{LacZ/+}$;*Shh*$^{-/-}$ reporter aggregates were added to the dish in a 1:4 ratio and Ptch1:LacZ expression in mESCs was measured after 3 days. **F:** Ptch1:LacZ expression normalized to total protein in mESC aggregates co-cultured with Shh-expressing Hek293t aggregates. Box-and-Whisker plot, n=4, *****p*<0.0001.

Discussion

Here, we provide evidence for a function of the zinc-coordination center of Shh for the association of Shh to the ECM and non-cell autonomous signaling. The zinc coordination domain of Shh appears to be involved as μM amounts of zinc are required for ECM association, while mutants in the zinc coordination domain are insensitive to zinc in the medium and have reduced activity in non-cell autonomous signaling. The observation that Shh-E177A is unable to mediate signaling from the notochord to the overlying neural tube (a textbook example of non-cell autonomous Shh signaling), but is fully capable to induce the Hh response when expressed in the developing neural tube (likely cell-autonomously) (Himmelstein et al., 2017), provides in vivo evidence that the zinc-coordination domain of Shh is required for non-cell autonomous signaling, although not for the productive binding of Shh to its cognate receptors. The initial experiments that demonstrated that E177 is dispensable for the activation of the Hh response is easily explained as this mutant ligand was added to the responding cells as a purified and soluble fraction (Fuse et al., 1999), thus bypassing the requirement for the function of the zinc-coordination domain. This is further supported by structural analysis of the Ptch1/Shh complex demonstrating that the extreme N-terminus of Shh interacts with Ptch1 (Gong et al., 2018; Qi, Schmiege, Coutavas, & Li, 2018a; Qi, Schmiege, Coutavas, Wang, & Li, 2018b) and suffices to alter Ptch1 activity (Tukachinsky et al., 2016). These observations further demonstrate the dispensability of the zinc-coordination domain to activate the Shh response in the responding cell.

Do Bacterial Hhs and Shh share a peptidase activity?

Our observations indicate that Shh distribution away from the sites of synthesis and non-cell autonomous Shh signaling can be enhanced under low-calcium and high zinc conditions. The surprising sequence similarity between bacterial and mammalian Hedgehog proteins strongly suggest they have similar functions. The organization of bacterial genomes into operons helps in the assignment of possible functions of unknown proteins. The suggested role of BacHh (as a M15A peptidase (Rawlings & Barrett, 2013)) in the modification of the bacterial peptidoglycans is further supported by the observation that in *Mesorhizobium* and *Bradyrhizobium* the *BacHh* gene is surrounded by genes (likely constituting an operon) that code for proteases, including lysozyme, N-acetylmuramoyl-L-alanine amidase, a peptidoglycan endopeptidase (peptidase M23A), several Trypsin homologs (peptidase S1), a zinc Matrix Metalloprotease (MMP) homolog (peptidase M54), an endonuclease, peptidase S53, and possibly a Phytase (DUF3616). This complex of enzymes might be involved in bacterial feeding or scavenging. BacHhs in *Rhizobiacea* are not part of the core genome (González et al., 2019), as the majority of these bacteria do not carry *BacHh*, a further indication that BacHhs provide a niche-specific specialized function.

Possible mechanisms of catalysis of zinc peptidases have been elucidated with the help of structural models of enzyme-inhibitor complexes. Thermolysin is a well-studied zinc metallopeptidase structurally related to Shh (Hall et al., 1995; Rebollido-Rios et al., 2014). Shh and Thermolysin coordinate zinc via two histidine and an aspartic acid residue. A

catalytic glutamic acid residue initiates catalysis (E177 in mouse Shh) by accepting a proton from water to form the nucleophilic hydroxide that attacks the carbonyl carbon, further stabilized by the coordinated zinc. With the two stacking histidine (or occasionally tyrosine) residues a pentacoordinate transition state is formed and resolved into the hydrolyzation products (Matthews, 2002; Tronrud, Roderick, & Matthews, 1992).

M15 peptidases cleave peptidoglycans, the major component of the bacterial periplasmic space, and a major component of detritus. Peptidoglycans are analogs of proteoglycans that are common in extracellular matrix (ECM) of animals. Therefore, it is possible that functional conservation between BacHhs and Shh is reflected in the ability of Shh to cleave or modify proteoglycans, thus affecting the Shh response and/or distribution, independent of its binding to the canonical Hh receptors. Although any Shh antagonist could be a possible target for the putative Shh peptidase activity, the Hh-interacting protein (Hhip) is an unlikely candidate as it binds to Shh via the zinc ion, thereby replacing the catalytic water. This mode of binding is akin to that of a metalloprotease/inhibitor interaction (Bosanac et al., 2009), and thus likely to inhibit the putative catalytic function of Shh instead of being a substrate. The targets for penicillin and related antibiotics are peptidoglycan peptidases, leaving open the development of nM drugs that inactivate the peptidase activity of Shh, and thus be powerful inhibitors of non-autonomous Shh signaling that underlies several cancers.

Are Hhs proteoglycan peptidases?

Hedglings and Hedglets are related to Hhs, and the conserved domains possibly homologous. All animals that have Hedglet also have a *Hh* gene and it is thus plausible that Hedglets are derived from Hh. Hhs are not found in any eukaryote except *cnidarians* and bilaterians. The distribution of Hedgling and Hhs only overlaps in *cnidarians*, but Hedgling can also be found in sponges and choanoflagellates (Figure S1). This suggests two evolutionary events giving rise to these proteins; one occurring in a *Choanoflagellate* ancestor that originated the gene coding for Hedgling, and an independent event in a *Cnidarian* ancestor that gave rise to modern Hh. The absence of both Hedgling and Hh from algae, plants, fungi, in addition to almost all unicellular eukaryotes makes it unlikely that both Hh and Hedgling linearly evolved from a BacHh protein that could have been present in the Ur-eukaryote, but more likely are products of more recent gene transfers from bacteria. The distribution among eukaryotes of Glypicans and Hs is overlapping, and both are first observed in *Cnidarians* and present in all bilaterians. A more recent evolutionary relationship between BacHh and Hhs is further supported by the observation that the C-terminal residue of many BacHhs perfectly aligns with the exon 2 splice donor site in *Hh* genes, thereby providing a parsimonious explanation how a *BacHh* gene was incorporated in a eukaryotic genome giving rise to *Hh*. This is in contrast to the much less conserved Hh domain in Hedgling that is encoded within a single large exon. Given the central role of Gpcs in the distribution of and response to Hhs (including Shh), Glypicans and Hhs might have co-evolved possibly as a peptidase/substrate combination, co-opting the peptidoglycan activity of BacHhs to cleave the proteoglycan Glypican. Shh binds heparan sulfate (HS), the O-linked glycosaminoglycan sidechain of Gpcs and other

proteoglycans (Esko & Selleck, 2002), via the N-terminal Cardin-Weintraub motif, which plays a crucial role in the release of Shh from the producing cell (Farshi et al., 2011). Although HS is thought to merely aid in scaffolding of a release complex (Jakobs et al., 2016; 2017), our results could hint to an additional role for HS in guiding Shh to its peptidase target.

Hh-like bacterial peptidases (M15A) are predicted to be carboxy(trans)peptidases, cleaving adjacent to the D-ala that is linked to the murein glycans (Bochtler, Odintsov, Marcyjaniak, & Sabala, 2004; Vollmer & Bertsche, 2008). By analogy, Shh might cleave an unusually modified C-terminal residue. It is intriguing that the C-termini of Glypicans are linked to the GPI anchor that restricts them to the cell surface (Filmus, Shi, Wong, & Wong, 1995). Solubilization of Shh-sequestering glypicans by GPI removal would elegantly reconcile the observed peptidase-dependent entry of Shh into the ECM with the important effects of glypicans on Shh signaling and distribution. If Shh remains attached to its potential substrate after cleavage and enters the ECM in a complex or alone remains unresolved.

Drosophila is the exception

It is perhaps unfortunate that Hh was discovered in *Drosophila,* as of all animals sequenced, only Hh in *Drosophilids* is divergent for two of the three residues that coordinate zinc and has a valine residue at the equivalent position of the critical E177. The predicted lack of peptidase activity in *Drosophilid* Hhs is remarkable and further supports the observation that the putative peptidase activity is not required for the Hh/receptor interaction. Perhaps stricter reliance on cytonemes in *Drosophila* that detect Hh at its source (Huang, Liu, & Kornberg, 2019) renders the ancestral peptidase activity obsolete. Nevertheless, this loss of the putative peptidase activity is unique to *Drosophilids*, as all other (sequenced) animals retain the typical zinc coordination motif and the associated E177 equivalent that are required for catalytic activity. Based on the loss-of-function of several mutants, this intrinsic property is likely a zinc metallopeptidase activity, just like the bacterial counterparts of Shh. Still, the observation that substitution of the Shh calcium/zinc sequences with those of BacHh results in a protein that does not enter the ECM, indicates that their substrates are not interchangeable.

Is Shh oligomerization preventing ECM association?

The zinc coordination center of Shh and in particular E177 are disadvantageous for Shh multimerization (Himmelstein et al., 2017). Zinc prevents oligomerization and we find that zinc is a potent agonist of ECM association and putative peptidase activity. Furthermore, while the E177A/V mutant prevents ECM association it enhances oligomerization (Himmelstein et al., 2017). These observations are consistent with the idea that the putative peptidase activity of Shh prevents or reverts multimerization. This notion is further supported by the structural observation that the cholesterol-modified C-terminus is in close proximity to the zinc coordination center, raising the hypothesis that Shh could have intermolecular autoproteolytic activity that prevents oligomerization (Hall et al., 1995). Indeed, multimer size has been reported to be negatively correlated with long-range signaling activity of Shh (Feng et al., 2004). This observation could explain why cholesterol-

unmodified Shh-C199*, which would be expected to form multimers less efficiently due to the absence of cholesterol, is more readily detectable in the ECM of transfected Hek293t cells and is an efficient non-cell autonomous ligand. Although an inter- or intramolecular autoproteolytic activity has not been demonstrated for ShhNp, many peptidases are produced as pro-proteins that undergo either an intra- or intermolecular activation event. The intramolecular activation events are often auto-catalyzed by the intrinsic peptidase domain (Bitar, Cao, & Marquis, 2008). If Shh has retained these bacterial characteristics it is possible that the autocatalytic de-oligomerization event results in a form of ShhN with a peptidase activity that can modify ECM components. In addition, Shh is subject to further N-terminal processing, or "shedding", prior or concomitant to its release from the cell (Dierker, Dreier, Petersen, Bordych, & Grobe, 2009), but this event can be mediated by a family of zinc-metalloproteases called a disintegrin and metalloprotease (ADAM), in concert with the scaffolding protein Scube2 (Jakobs et al., 2014). These metalloproteases share overlapping functions and are therefore sufficient, but not essential, for Shh shedding (Kheradmand & Werb, 2002), hinting at the variety of paths Shh can go to enter the extracellular space.

Although mutations of the central zinc coordinating triad are unstable and thus cannot be easily assessed for loss of peptidase function, mutations of several other catalytically important residues (E177, H135 and H181) are not destabilized and show a loss in the ability of Shh to enter the ECM. Together with the observation by Himmelstein and colleagues (Himmelstein et al., 2017) that ShhE177A cannot signal from the notochord to the overlying neural plate strongly supports the idea that a Shh-associated peptidase activity is required for non-cell autonomous signaling by promoting its distribution away from the source cells. Our findings challenge the dogma of the so called "pseudo catalytic domain", and we provide a function for the apparent peptidase activity intrinsic to ShhN. None of our observations are in conflict with previous reports, as we confine the activity of the Shh-associated peptidase upstream of the interaction between Shh and its receptors.

Conclusions

Our observations support the notion that the remarkable sequence similarity between the BacHhs and Shh reflects to a conserved function as a glycopeptidase. All ShhN mutants that are predicted to abolish its intrinsic peptidase activity fail to bind to the ECM and have an impaired ability to signal non-cell autonomously. However, BacHh cannot mediate the activities of ShhN, indicating that the substrates for BacHh are not conserved in metazoans.

Material and Methods

Sequence analysis

Bacterial Hedgehogs, Hedglings and Hedglets were identified via protein-protein BLAST (NCBI) and HMMER (ensemble) searches (Gish & States, 1993) using the peptide sequence of the Shh N-terminal domain as the initial query sequence. Conserved sequences were manually curated to contain only the calcium and zinc coordination motifs (around 105 residues). Sequences (supplemental file) were aligned in Clustal Omega (EMBL-EBI). An average distance tree and a PCA plot were generated in Jalview (Waterhouse, Procter, Martin, Clamp, & Barton, 2009), using the BLOSUM62 algorithm. Visualizations of the ShhN structure were generated in UCSF Chimera using Protein Database (PDB) ID 3D1M (McLellan et al., 2008).

Materials

MG-132 and Concanamycin A were from Calbiochem, Chloroquine and $ZnCl_2$ from Sigma, $CaCl_2$ from Fisher Scientific, and Dynasore from Abcam.

Cell culture

Ptch1$^{-/-}$;*Ptch2*$^{-/-}$ fibroblasts were derived from mouse embryonic stem cells and are described elsewhere (Casillas & Roelink, 2018) . All cells were cultured in DMEM (Invitrogen) supplemented with 10% FBS (Atlas Biologicals). Mouse embryonic stem cells were cultured in DMEM (Invitrogen) supplemented with 20% FBS (Atlas Biologicals), 2 mM L-Glutamine (Gibco), 1X MEM non-essential amino acids (Gibco), 0.001% 2-Mercaptoethanol (Gibco), and 0.001% Leukemia Inhibitory Factor (LIF). Cells were transfected using Lipofectamine2000 reagent (Invitrogen) according to the manufacturer's protocol.

DNA constructs

The following mutations were created via site-directed mutagenesis: *Shh-C199*/E177V, Shh-C199*/H135A, Shh-C199*/H135Y, Shh-C199*/H181A, Shh-C199*/H181Y, Shh-C199*/H135A/H181A, Shh-C199*/H135Y/H181Y, Shh-C199*/E90A/E91D/D96A/D130N/D132L, Shh-C199*/E90A/E91D/D96A/E127A/D130N/D132L. Bradyrhizobium paxllaer*i *BacHh* (EnsemblBacteria: LMTR21_38280, NCBI: WP_065756078.1) was codon optimized for eukaryotic expression using the IDT DNA Codon Optimization Tool, ordered as a gBlocks gene fragment from IDT DNA, and cloned into pcDNA3.1(+). Both the *Shh-C199** vector backbone including the Shh N- and C-terminus as well as the calcium and zinc coordination motifs of *Bradyrhizobium paxllaeri BacHh* were PCR amplified, separated on a 1% agarose gel, and extracted with MinElute columns (QIAGEN). The fragments were cut with *BsaI* and ligated with T4 DNA ligase according to the Golden Gate cloning protocol (New England Biolabs).

Immunostaining

Ptch1$^{-/-}$;*Ptch2*$^{-/-}$ fibroblasts were plated on 12mm glass cover slips and transfected with *Shh-C199** the following day and subsequently allowed to recover for 24h. The transfected cells

were then incubated for 24h in serum-free DMEM containing varying concentrations of $CaCl_2$ or $ZnCl_2$, the cells were detached from the cover slip with PBS. The cover slips were washed with PBS at least 5 times and blocked with 10% heat-inactivated goat serum in PBS with 0.1% TritonX (PBS-T). Mouse α-Shh (5E1, Developmental Studies Hybridoma Bank) was used at 1:30 in blocking solution and goat α-mouse Alexa568 secondary antibody (Invitrogen) at 1:1,000 in blocking solution. Shh distribution was visualized with a Zeiss Observer at 10x and 63x magnification.
For live staining, transfected cells were incubated in serum-free medium for 20h. An α-HA antibody 3F10 (Sigma) was added for another 4 hours (1:1,000) before cells were fixed with 4% PFA in PBS and blocked in 10% heat-inactivated goat serum in PBS. A goat α-rat Alexa488 secondary antibody (Invitrogen) was used at 1:1,000 in blocking solution and nuclei stained with DAPI.

Western Blot/SYPRO ruby staining
Hek293t cells were plated in 12 well plates and transfected with Shh mutants as indicated the next day. 24h after transfection, the medium was switched to serum free DMEM with the indicated calcium and zinc concentrations overnight. Cells were then detached from the plate with PBS and lysed in a microcentrifuge tube with RIPA buffer (150 mM NaCl, 50 mM Tris-HCl, 1% Igepal, 0.5% Sodium Deoxycholate, and protease inhibitors). The lysate was incubated for 30 min on ice and cleared by centrifugation. For isolation of ECM-bound Shh, the decellularized tissue culture dish was washed with PBS and deionized water at least 5 times and scraped with a cell scraper and 5X SDS sample buffer heated to 95°C, as described (Hellewell et al., 2017). A fifth of the sample was run on a 12% SDS-PAGE gel and transferred to a 0.45μ nitrocellulose membrane. Membranes were blocked in 5% milk in Tris-buffered saline with 0.1% Tween-20 (TBS-T) and incubated with a polyclonal rabbit α-Shh antibody (H2, 1:10,000) (Roelink et al., 1995) in blocking solution, followed by incubation with a goat α-rabbit Alexa647 secondary antibody (Invitrogen, 1:10,000) in blocking solution. GAPDH was used as a loading control (Rabbit α-GAPDH, 14C10, Cell Signaling Technologies). Western Blots were visualized with a ChemiDoc visualization system (Bio-Rad).
Alternatively, the SDS-PAGE gel was stained with SYPRO-Ruby gel stain (Thermo-Fisher) according to the manufacturer's instructions and visualized with a ChemiDoc visualization system (BioRad).

ELISA
Hek293t cells were plated in 96 well plates and transfected with *Shh-C199** and *Shh-C199*/E90A/E91D/D96A/E127A/D130N/D132L* in triplicates the next day. 24 h after transfection, the medium was replaced with DMEM containing 0.18 mM or 1.8 mM Calcium and Zinc concentrations ranging from 0.001 to 1 μM for 48 h. The cells were removed from the plate with PBS and deionized water. The plates were blocked with PBS + 5% heat-inactivated goat serum, incubated with mAB5E1, followed by an HRP conjugated α-mouse secondary antibody (Invitrogen). Western-Lightning Plus-ECL (Perkin Elmer) was added to the wells and luminescence was measured in a Wallac Victor3 plate reader (Perkin Elmer).

ECM signaling assay

Hek293t cells were plated in 24 well plates and transfected with the indicated *Shh-C199** variants the next day. 24h after transfection, cells were washed off with PBS and each well washed with PBS extensively to remove residual cells. LightII reporter cells (Taipale et al., 2000) were added and the medium was switched to DMEM as soon as the cells were adherent. 48h later, the cells were lysed and luciferase activity was measured using the Dual Luciferase Reporter Assay System (Promega). Firefly luciferase measurements were normalized against Renilla luciferase measurements for each technical replicate to control for differences in cell growth. Firefly/Renilla luciferase values were then normalized to the mock control average for each experiment.

Non-cell autonomous signaling assays

For the non-cell autonomous signaling assay in chimeric three-dimensional aggregates, Hek293t cells were plated in 12 well plates and transfected with *Shh-C199** constructs the next day. 24h after transfection, cells were washed off the culture dish with PBS and mixed with four times as many mESC *Ptch1*$^{LacZ/+}$;*Shh*$^{-/-}$ reporter cells in non-treated tissue culture plates. Cells were placed in DFNB medium on a rotating platform at 1 Hz for 48h and 2 µM Retinoic Acid (RA) was added for another 48h. The cells were then collected, washed once in PBS, and lysed in 100 mM potassium phosphate, pH 7.8, 0.2% Triton X-100. The lysates were cleared by centrifugation and 20 µl analyzed in triplicates for Ptch1:LacZ expression using the Galacto-Light chemiluminescent kit (Applied Biosciences). Lysates were normalized for total protein using the Bradford reagent (BioRad).

For the long-range signaling assay, Hek293t cells were plated in 12 well plates and transfected with the indicated *Shh-C199** constructs the next day. 24h after transfection, cells were washed off with PBS and collected in a conical tube. Aggregates were allowed to form for 48h in DFNB medium in non-treated tissue culture plates rotated at 1 Hz. Similarly, four times as many mESC *Ptch1*$^{LacZ/+}$;*Shh*$^{-/-}$ reporter cells as Hek293t cells were aggregated in DFNB medium for 48h rotated at 1 Hz. Hek293t aggregates and 2 µM Retinoic Acid (RA) were added to the mESC organoids for another 48h. Ptch1:LacZ expression was measured as described above.

Genome editing

Ptch1$^{LacZ/LacZ}$;*Ptch2*$^{-/-}$;*Boc*$^{-/-}$;*Cdo*$^{-/-}$;*Gas1*$^{-/-}$;*Shh*$^{-/-}$ were derived from *Ptch1*$^{LacZ/LacZ}$;*Ptch2*$^{-/--}$;*Shh*$^{-/-}$ cells (Roberts, Casillas, Alfaro, Jägers, & Roelink, 2016). TALEN constructs targeting the first exon of mouse *Cdo* and *Gas1* were designed and cloned into the pCTIG expression vectors containing IRES puromycin and IRES hygromycin selectable markers (Cermak et al., 2011). The following repeat variable domain sequences were generated: Cdo, 5' TALEN: NN HD NI NG HD HD NI NN NI HD HD NG HD NN NN ; 3' TALEN: HD NI HD NI NI NN NI NI HD NI NG NI HD NI NN; Gas1, 5' TALEN: NN NI NN NN NI HD NN HD HD HD NI NG NN HD HD; 3' TALEN: NN NN NI NI NI NI NN NG NG NG NN NG HD HD NN NI. Two CRISPR constructs targeting a double strand break flanking the first exon of mouse Boc were cloned into pSpCas9 vector with an IRES puromycin selectable marker (Ran et al., 2013). The Boc CRISPRs targeted the following forward genomic sequences (PAM sequences underlined): Upstream of first exon 5' <u>CCT</u>GTCCTCGCTGTTGGTCCCTA 3';

Downstream of first exon 5' CCCACAGACTCGCTGAAGAGCTC 3'. *Ptch1*$^{LacZ/LacZ}$;*Ptch2*$^{-/-}$;*Shh*$^{-/-}$ mouse embryonic stem cells (Roberts et al., 2016) were transfected with 6 genome editing plasmid. One day after transfection, ES medium with 100 μg/mL hygromycin and 0.5 μg/mL puromycin was added for 4 days. Surviving mESC colonies were isolated, expanded and genotyped by sequence PCR products spanning TALEN and CRISPR-binding sites. PCR screening was performed on cell lysates using primers flanking the TALEN or CRISPR binding sites for the *Boc*, *Cdo*, and *Gas1* loci. *Boc*, (5') CATCTAACAGCGTTGTCCAACAATG and (3') CAAGGTGGTATTGTCCGGATC; *Cdo*, (5') CACTTCAGTGTGATCTCCAG and (3') CCTTGAACTCACAGAGATTCG; Gas1, (5') ATGCCAGAGCTGCGAAGTGCTA and (3') AGCGCCTGCCAGCAGATGAG. PCR products were sequenced to confirm allele sequences. A *Ptch1*$^{LacZ/LacZ}$;*Ptch2*$^{-/-}$;*Boc*$^{-/-}$;*Cdo*$^{-/-}$;*Gas1*$^{-/-}$;*Shh*$^{-/-}$ mESC clone was identified harboring a 50 bp deletion in Cdo exon 1, a heteroallelic 480 bp insertion and a 200 bp deletion in Gas1 exon1 resulting in a premature stop codon in the reading frame, and a 450 bp deletion of Boc exon 1. These cells were transfected with *LargeT* and *myc*, and deprived of Lif to generate immortalized fibroblasts.

Data Analysis: Single Factor ANOVA was used to analyze more than two conditions, followed by a Student's *t*-test with a two-tailed distribution assuming unequal variance comparing two conditions. **p*<0.05, ***p*<0.01, ****p*<0.001, *****p*<0.0001.

Acknowledgements.
This work was supported by NIH grant 1R01GM117090 to HR. We thank Drs. N. King and D. Rokhsar for discussions on Hh evolution, and Dr. C. Casillas for help with the receptorless cell line.

Author contributions.
All experiments were performed by CJ. Experiments were designed by CJ and HR. The manuscript was written by CJ and HR.

Conflict of interest.
The authors declare no conflict of interest.

Supplemental Figure 1

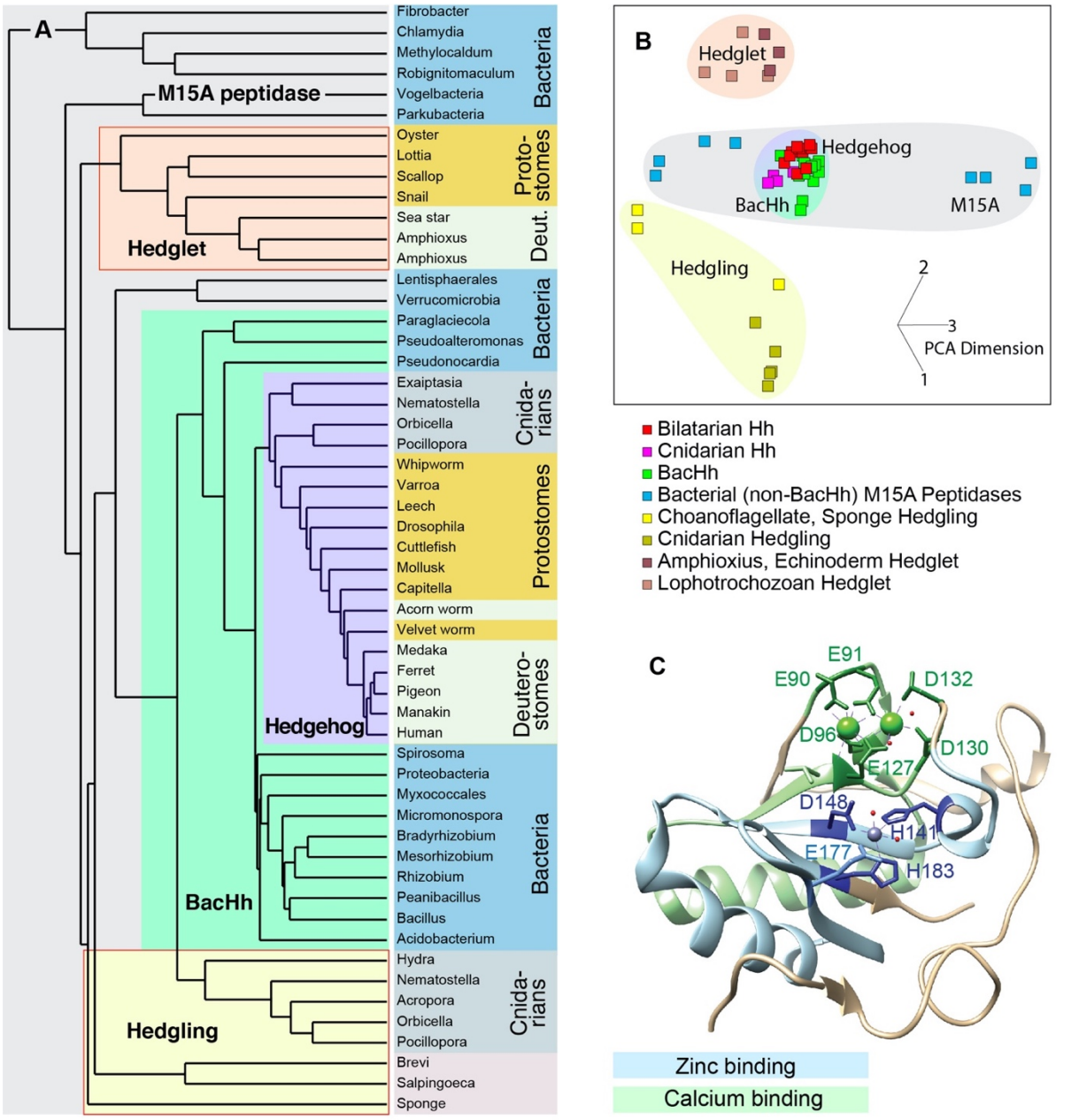

Figure S1. Sequence similarities between Hh, Hedgling, and Hedglet. **A:** a similarity tree of Hh sequences encompassing the calcium and zinc coordinating motifs. All Hhs are closely related and root from within the BacHhs. Hedglings (present in Choanoflagellates, Sponges, and Cnidarians) and Hedglets (present in Lophotrochozoans, Amphioxus and Echinoderms) form outgroups, but all are related to bacterial M15 peptidases. Organisms in the same phylum or clade are color coded, and common names of the organisms are used. Sequences and accession numbers can be found as a supplemental file. Hedglings and Hedglets (red borders) are predicted to be unable to mediate catalysis.

B: PCA plot of the tree presented in A. **C:** Structure of Shh with salient residues and domains indicated. **D:** Sequence lineup of Mesorhizobium BacHh, human Dhh, and Choanoflagellate Hedgling. Identical residues are indicated in amber. Salient residues are color coded and color coordinated with C.

Supplemental Figure 2

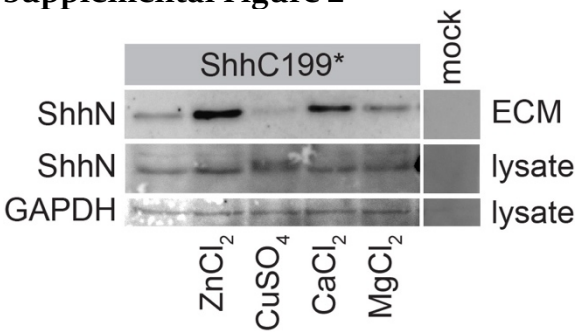

Figure S2: Association of Shh with the ECM is enhanced specifically in response to zinc. Western blot analysis of the lysate and ECM of Hek293t cells transfected with *Shh-C199** and cultured in medium containing 0.18 mM calcium and 5 μM zinc, 5 μM copper, 1.8 mM magnesium or 1.8 mM calcium as indicated.

References

Alonso, M. T., Rojo-Ruiz, J., Navas-Navarro, P., Rodríguez-Prados, M., & García-Sancho, J. (2017). Measuring Ca2+ inside intracellular organelles with luminescent and fluorescent aequorin-based sensors. *Biochimica Et Biophysica Acta. Molecular Cell Research*, *1864*(6), 894–899. http://doi.org/10.1016/j.bbamcr.2016.12.003

Bellaiche, Y., The, I., & Perrimon, N. (1998). Tout-velu is a Drosophila homologue of the putative tumour suppressor EXT-1 and is needed for Hh diffusion. *Nature*, *394*(6688), 85–88. http://doi.org/10.1038/27932

Bitar, A. P., Cao, M., & Marquis, H. (2008). The metalloprotease of Listeria monocytogenes is activated by intramolecular autocatalysis. *J Bacteriol*, *190*(1), 107–111. http://doi.org/10.1128/JB.00852-07

Bochtler, M., Odintsov, S. G., Marcyjaniak, M., & Sabala, I. (2004). Similar active sites in lysostaphins and D-Ala-D-Ala metallopeptidases. *Protein Sci*, *13*(4), 854–861. http://doi.org/10.1110/ps.03515704

Bosanac, I., Maun, H. R., Scales, S. J., Wen, X., Lingel, A., Bazan, J. F., et al. (2009). The structure of SHH in complex with HHIP reveals a recognition role for the Shh pseudo active site in signaling. *Nat Struct Mol Biol*, *16*(7), 691–697.

Capurro, M. I., Xu, P., Shi, W., Li, F., Jia, A., & Filmus, J. (2008). Glypican-3 inhibits Hedgehog signaling during development by competing with patched for Hedgehog binding. *Dev Cell*, *14*(5), 700–711. http://doi.org/10.1016/j.devcel.2008.03.006

Carrasco, H., Olivares, G. H., Faunes, F., Oliva, C., & Larraín, J. (2005). Heparan sulfate proteoglycans exert positive and negative effects in Shh activity. *J Cell Biochem*, *96*(4), 831–838. http://doi.org/10.1002/jcb.20586

Casillas, C., & Roelink, H. (2018). Gain-of-function Shh mutants activate Smo cell-autonomously independent of Ptch1/2 function. *Mech Dev*, *153*, 30–41. http://doi.org/10.1016/j.mod.2018.08.009

Cermak, T., Doyle, E. L., Christian, M., Wang, L., Zhang, Y., Schmidt, C., et al. (2011). Efficient design and assembly of custom TALEN and other TAL effector-based constructs for DNA targeting. *Nucleic Acids Res*, *39*(12), e82. http://doi.org/10.1093/nar/gkr218

Day, E. S., Wen, D., Garber, E. A., Hong, J., Avedissian, L. S., Rayhorn, P., et al. (1999). Zinc-dependent structural stability of human Sonic hedgehog. *Biochemistry*, *38*(45), 14868–14880. http://doi.org/10.1021/bi9910068

Dierker, T., Dreier, R., Petersen, A., Bordych, C., & Grobe, K. (2009). Heparan sulfate-modulated, metalloprotease-mediated sonic hedgehog release from producing cells. *J. Biol. Chem.*, *284*(12), 8013–8022. http://doi.org/10.1074/jbc.M806838200

Echelard, Y., Epstein, D. J., St-Jacques, B., Shen, L., Mohler, J., McMahon, J. A., & McMahon, A. P. (1993). Sonic hedgehog, a member of a family of putative signaling molecules, is implicated in the regulation of CNS polarity. *Cell*, *75*(7), 1417–1430.

Esko, J. D., & Selleck, S. B. (2002). Order out of chaos: assembly of ligand binding sites in heparan sulfate. *Annu. Rev. Biochem.*, *71*(1), 435–471. http://doi.org/10.1146/annurev.biochem.71.110601.135458

Farshi, P., Ohlig, S., Pickhinke, U., Höing, S., Jochmann, K., Lawrence, R., et al. (2011). Dual roles of the Cardin-Weintraub motif in multimeric Sonic hedgehog. *J. Biol. Chem.*, *286*(26), 23608–23619. http://doi.org/10.1074/jbc.M110.206474

Feng, J., White, B., Tyurina, O. V., Guner, B., Larson, T., Lee, H. Y., et al. (2004). Synergistic and antagonistic roles of the Sonic hedgehog N- and C-terminal lipids. *Development*, *131*(17), 4357–4370.

Filmus, J., Shi, W., Wong, Z. M., & Wong, M. J. (1995). Identification of a new membrane-bound heparan sulphate proteoglycan. *Biochem. J.*, *311 (Pt 2)*(2), 561–565. http://doi.org/10.1042/bj3110561

Fuse, N., Maiti, T., Wang, B., Porter, J. A., Hall, T. M., Leahy, D. J., & Beachy, P. A. (1999). Sonic hedgehog protein signals not as a hydrolytic enzyme but as an apparent ligand for patched. *Proceedings of the National Academy of Sciences of the United States of America*, *96*(20), 10992–10999.

Gish, W., & States, D. J. (1993). Identification of protein coding regions by database similarity search. *Nat Genet*, *3*(3), 266–272. http://doi.org/10.1038/ng0393-266

Gong, X., Qian, H., Cao, P., Zhao, X., Zhou, Q., Lei, J., & Yan, N. (2018). Structural basis for the recognition of Sonic Hedgehog by human Patched1. *Science*, *112*, eaas8935. http://doi.org/10.1126/science.aas8935

González, V., Santamaría, R. I., Bustos, P., Pérez-Carrascal, O. M., Vinuesa, P., Juárez, S., et al. (2019). Phylogenomic Rhizobium Species Are Structured by a Continuum of Diversity and Genomic Clusters. *Frontiers in Microbiology*, *10*, 910. http://doi.org/10.3389/fmicb.2019.00910

Guo, W., & Roelink, H. (2019). Loss of the Heparan Sulfate Proteoglycan Glypican5 facilitates long-range Shh signaling. *Stem Cells*. http://doi.org/10.1002/stem.3018

Hall, T. M., Porter, J. A., Beachy, P. A., & Leahy, D. J. (1995). A potential catalytic site revealed by the 1.7-A crystal structure of the amino-terminal signalling domain of Sonic hedgehog. *Nature*, *378*(6553), 212–216. http://doi.org/10.1038/378212a0

Hellewell, A. L., Rosini, S., & Adams, J. C. (2017). A Rapid, Scalable Method for the Isolation, Functional Study, and Analysis of Cell-derived Extracellular Matrix. *J Vis Exp*, (119). http://doi.org/10.3791/55051

Himmelstein, D. S., Cajigas, I., Bi, C., Clark, B. S., Van Der Voort, G., & Kohtz, J. D. (2017). SHH E176/E177-Zn(2+) conformation is required for signaling at endogenous sites. *Dev. Biol.*, *424*(2), 221–235. http://doi.org/10.1016/j.ydbio.2017.02.006

Huang, H., Liu, S., & Kornberg, T. B. (2019). Glutamate signaling at cytoneme synapses. *Science*, *363*(6430), 948–955. http://doi.org/10.1126/science.aat5053

Incardona, J. P., Lee, J. H., Robertson, C. P., Enga, K., Kapur, R. P., & Roelink, H. (2000). Receptor-mediated endocytosis of soluble and membrane-tethered Sonic hedgehog by Patched-1. *Proceedings of the National Academy of Sciences of the United States of America*, *97*(22), 12044–12049. http://doi.org/10.1073/pnas.220251997

Jakobs, P., Exner, S., Schürmann, S., Pickhinke, U., Bandari, S., Ortmann, C., et al. (2014). Scube2 enhances proteolytic Shh processing from the surface of Shh-producing cells. *Journal of Cell Science*, *127*(Pt 8), 1726–1737. http://doi.org/10.1242/jcs.137695

Jakobs, P., Schulz, P., Ortmann, C., Schürmann, S., Exner, S., Rebollido-Rios, R., et al. (2016). Bridging the gap: heparan sulfate and Scube2 assemble Sonic hedgehog release complexes at the surface of producing cells. *Scientific Reports*, *6*(1), 26435–14. http://doi.org/10.1038/srep26435

Jakobs, P., Schulz, P., Schürmann, S., Niland, S., Exner, S., Rebollido-Rios, R., et al. (2017). Ca2+ coordination controls sonic hedgehog structure and its Scube2-regulated release. *Journal of Cell Science*, *130*(19), 3261–3271. http://doi.org/10.1242/jcs.205872

Kheradmand, F., & Werb, Z. (2002). Shedding light on sheddases: role in growth and development. *Bioessays*, *24*(1), 8–12. http://doi.org/10.1002/bies.10037

Kunjithapatham, R., Geschwind, J.-F., Devine, L., Boronina, T. N., O'Meally, R. N., Cole, R. N., et al. (2015). Occurrence of a multimeric high-molecular-weight glyceraldehyde-3-phosphate dehydrogenase in human serum. *Journal of Proteome Research*, *14*(4), 1645–1656. http://doi.org/10.1021/acs.jproteome.5b00089

Lee, D. H., & Goldberg, A. L. (1998). Proteasome inhibitors: valuable new tools for cell biologists. *Trends Cell Biol*, *8*(10), 397–403. http://doi.org/10.1016/s0962-8924(98)01346-4

Macia, E., Ehrlich, M., Massol, R., Boucrot, E., Brunner, C., & Kirchhausen, T. (2006). Dynasore, a cell-permeable inhibitor of dynamin. *Dev Cell*, *10*(6), 839–850. http://doi.org/10.1016/j.devcel.2006.04.002

Matthews, B. W. (2002). Structural basis of the action of thermolysin and related zinc peptidases. *Accounts of Chemical Research*, *21*(9), 333–340. http://doi.org/10.1021/ar00153a003

Maun, H. R., Wen, X., Lingel, A., de Sauvage, F. J., Lazarus, R. A., Scales, S. J., & Hymowitz, S. G. (2010). Hedgehog pathway antagonist 5E1 binds hedgehog at the pseudo-active site. *J. Biol. Chem.*, *285*(34), 26570–26580.

McCarthy, R. A., Barth, J. L., Chintalapudi, M. R., Knaak, C., & Argraves, W. S. (2002). Megalin functions as an endocytic sonic hedgehog receptor. *J. Biol. Chem.*, *277*(28), 25660–25667.

McLellan, J. S., Zheng, X., Hauk, G., Ghirlando, R., Beachy, P. A., & Leahy, D. J. (2008). The mode of Hedgehog binding to Ihog homologues is not conserved across different phyla. *Nature*, *455*(7215), 979–983.

Nüsslein-Volhard, C., & Wieshaus, E. (1980). Mutations affecting segment number and polarity in Drosophila. *Nature*, *287*, 795–801.

Ohlig, S., Pickhinke, U., Sirko, S., Bandari, S., Hoffmann, D., Dreier, R., et al. (2012). An emerging role of Sonic hedgehog shedding as a modulator of heparan sulfate interactions. *J. Biol. Chem.*, *287*(52), 43708–43719. http://doi.org/10.1074/jbc.M112.356667

Qi, X., Schmiege, P., Coutavas, E., & Li, X. (2018a). Two Patched molecules engage distinct sites on Hedgehog yielding a signaling-competent complex. *Science*, *112*(6410), eaas8843. http://doi.org/10.1126/science.aas8843

Qi, X., Schmiege, P., Coutavas, E., Wang, J., & Li, X. (2018b). Structures of human Patched and its complex with native palmitoylated sonic hedgehog. *Nature*, *15*, 3059. http://doi.org/10.1038/s41586-018-0308-7

Ran, F. A., Hsu, P. D., Wright, J., Agarwala, V., Scott, D. A., & Zhang, F. (2013). Genome engineering using the CRISPR-Cas9 system. *Nat Protoc*, *8*(11), 2281–2308. http://doi.org/10.1038/nprot.2013.143

Rawlings, N. D., & Barrett, A. J. (2013). Chapter 77 - Introduction: Metallopeptidases and Their Clans. In N. D. Rawlings & G. Salvesen (Eds.), *Handbook of Proteolytic Enzymes (Third Edition)* (Third Edition, pp. 325–370). Academic Press. http://doi.org/https://doi.org/10.1016/B978-0-12-382219-2.00077-6

Rebollido-Rios, R., Bandari, S., Wilms, C., Jakuschev, S., Vortkamp, A., Grobe, K., & Hoffmann, D. (2014). Signaling domain of Sonic Hedgehog as cannibalistic calcium-regulated zinc-peptidase. *PLoS Computational Biology*, *10*(7), e1003707. http://doi.org/10.1371/journal.pcbi.1003707

Roberts, B., Casillas, C., Alfaro, A. C., Jägers, C., & Roelink, H. (2016). Patched1 and Patched2 inhibit Smoothened non-cell autonomously. *eLife*, *5*, e17634. http://doi.org/10.7554/eLife.17634

Roelink, H. (2018). Sonic Hedgehog Is a Member of the Hh/DD-Peptidase Family That Spans the Eukaryotic and Bacterial Domains of Life. *Journal of Developmental Biology*, *6*(2), 12. http://doi.org/10.3390/jdb6020012

Roelink, H., Porter, J. A., Chiang, C., Tanabe, Y., Chang, D. T., Beachy, P. A., & Jessell, T. M. (1995). Floor plate and motor neuron induction by different concentrations of the amino-terminal cleavage product of sonic hedgehog autoproteolysis. *Cell*, *81*(3), 445–455.

Roessler, E., Belloni, E., Gaudenz, K., Jay, P., Berta, P., Scherer, S. W., et al. (1996). Mutations in the human Sonic Hedgehog gene cause holoprosencephaly. *Nat Genet*, *14*(3), 357–360.

Siekmann, A. F., & Brand, M. (2005). Distinct tissue-specificity of three zebrafish ext1 genes encoding proteoglycan modifying enzymes and their relationship to somitic Sonic hedgehog signaling. *Dev Dyn*, *232*(2), 498–505. http://doi.org/10.1002/dvdy.20248

Taipale, J., Chen, J. K., Cooper, M. K., Wang, B., Mann, R. K., Milenkovic, L., et al. (2000). Effects of oncogenic mutations in Smoothened and Patched can be reversed by cyclopamine. *Nature*, *406*(6799), 1005–9.

Tian, H., Jeong, J., Harfe, B. D., Tabin, C. J., & McMahon, A. P. (2005). Mouse Disp1 is required in sonic hedgehog-expressing cells for paracrine activity of the cholesterol-modified ligand. *Development*, *132*(1), 133–142.

Traiffort, E., Dubourg, C., Faure, H., Rognan, D., Odent, S., Durou, M.-R., et al. (2004). Functional characterization of sonic hedgehog mutations associated with holoprosencephaly. *Journal of Biological Chemistry*, *279*(41), 42889–42897. http://doi.org/10.1074/jbc.M405161200

Tronrud, D. E., Roderick, S. L., & Matthews, B. W. (1992). Structural basis for the action of thermolysin. *Matrix (Stuttgart, Germany). Supplement*, *1*, 107–111.

Tukachinsky, H., Kuzmickas, R. P., Jao, C. Y., Liu, J., & Salic, A. (2012). Dispatched and scube mediate the efficient secretion of the cholesterol-modified hedgehog ligand. *Cell Reports*, *2*(2), 308–320. http://doi.org/10.1016/j.celrep.2012.07.010

Tukachinsky, H., Petrov, K., Watanabe, M., & Salic, A. (2016). Mechanism of inhibition of the tumor suppressor Patched by Sonic Hedgehog. *Proc. Natl. Acad. Sci. U. S. a.*, *113*(40), E5866–E5875. http://doi.org/10.1073/pnas.1606719113

Vollmer, W., & Bertsche, U. (2008). Murein (peptidoglycan) structure, architecture and biosynthesis in Escherichia coli. *Biochim. Biophys. Acta*, *1778*(9), 1714–1734. http://doi.org/10.1016/j.bbamem.2007.06.007

Waterhouse, A. M., Procter, J. B., Martin, D. M. A., Clamp, M., & Barton, G. J. (2009). Jalview Version 2--a multiple sequence alignment editor and analysis workbench. *Bioinformatics (Oxford, England)*, *25*(9), 1189–1191. http://doi.org/10.1093/bioinformatics/btp033

Wilson, C. W., & Chuang, P. T. (2010). Mechanism and evolution of cytosolic Hedgehog signal transduction. *Development*, *137*(13), 2079–2094. http://doi.org/10.1242/dev.045021

Witt, R. M., Hecht, M.-L., Pazyra-Murphy, M. F., Cohen, S. M., Noti, C., van Kuppevelt, T. H., et al. (2013). Heparan sulfate proteoglycans containing a glypican 5 core and 2-O-sulfo-iduronic acid function as Sonic Hedgehog co-receptors to promote proliferation. *J. Biol. Chem.*, *288*(36), 26275–26288. http://doi.org/10.1074/jbc.M112.438937

Yan, D., & Lin, X. (2009). Shaping morphogen gradients by proteoglycans. *Cold Spring Harbor Perspectives in Biology*, *1*(3), a002493–a002493. http://doi.org/10.1101/cshperspect.a002493

Chapter 4

Non-cell autonomous inhibition of the Shh pathway due to impaired cholesterol biosynthesis requires Ptch1/2

Carina Jägers and Henk Roelink
Department of Molecular and Cell Biology, University of California, Berkeley

Manuscript available on BioRxiv (uploaded on December 11th, 2020)
https://doi.org/10.1101/2020.12.10.420588

Abstract

Birth defects due to congenital errors in enzymes involved in cholesterol synthesis like Smith-Lemli-Opitz syndrome (SLOS) and lathosterolosis cause an accumulation of cholesterol precursors and a deficit in cholesterol. The phenotype of both SLOS and lathosterolosis have similarities to syndromes associated with abnormal Sonic hedgehog (Shh) signaling during development, consistent with the notion that impaired cholesterol signaling can cause reduced Shh signaling. Two multipass membrane proteins play central roles in Shh signal transduction, the putative Resistance, Nodulation and Division (RND) antiporters Ptch1 and Ptch2, and the G-protein coupled receptor Smoothened (Smo). Sterols have been suggested as cargo for Ptch1, while Smo activity can affected both positively and negatively by steroidal molecules. We demonstrate that mESCs mutant for *7-dehydroxycholesterol reductase* (*7Dhcr*) or *sterol-C5-desaturase* (*Sc5d*) reduce the Hh response in nearby wildtype cells when grown in mosaic organoids. This non-cell autonomous inhibitory activity of the mutant cells required the presence of both Ptch1 and Ptch2. These observations support a model in which late cholesterol precursors that accumulate in cells lacking 7DHCR are the cargo for Ptch1 and Ptch2 activity that mediates the non-cell autonomous inhibition of Smo.

Introduction

Hedgehog (Hh) signaling is critically important during embryonic development and patterning in most animals. In the absence of Shh, Ptch1 inhibits Smo non-stoichiometrically via a mechanism that remains poorly understood (Taipale, Cooper, Maiti, & Beachy, 2002). Binding of the ligand to the 12-transmembrane receptor Patched 1 (Ptch1) blocks Ptch1 function and releases a Ptch1-dependent inhibition of the putative G-protein coupled receptor Smoothened (Smo) (Izzi et al., 2011; Marigo, Davey, Zuo, Cunningham, & Tabin, 1996; Taipale et al., 2002).

Vertebrates have two Ptch homologs, Ptch1 and Ptch2 (Ptch1/2) that share overlapping functions (Alfaro, Roberts, Kwong, Bijlsma, & Roelink, 2014; B. Roberts, Casillas, Alfaro, Jägers, & Roelink, 2016). Ptch1/2 are members of the Resistance-Nodulation Division (RND) family of antiporters that are present in all domains of life. RND antiporters export their cargo in exchange for protons (Tseng et al., 1999) although it is possible that Ptch1/2 can utilize a sodium gradient (Myers, Neahring, Zhang, Roberts, & Beachy, 2017). In bacteria, RND transporters pump small lipophilic and amphiphilic molecules to the outside and eukaryotic RNDs could have a similar function.

Although the nature of the cargo of Ptch1/2 antiporter activity remains unknown, several observations suggest that it is a steroidal molecule (Hausmann, Mering, & Basler, 2009). The secretion of vitamin D/calcitriol and its precursor, vitamin D3/cholecalciferol, both derivatives of the cholesterol precursor 7-Dehydrocholesterol (7DHC), is Ptch1-dependent and these sterols repress Smo activity (Bijlsma et al., 2006; Linder et al., 2015). Furthermore, several known Smo modulators have a steroidal backbone, including the steroidal alkaloid cyclopamine (Incardona, Gaffield, Kapur, & Roelink, 1998; Keeler, 1969; H. J. Sharpe, Wang, Hannoush, & de Sauvage, 2015).

All animal sterols are derived from lanosterol. Cholesterol is produced from lanosterol in a series of nineteen enzymatic reactions, called the postsqualene pathway (Bloch, 1965; Kandutsch & Russell, 1960). Vitamin D is a product of the direct cholesterol precursor, 7DHC (Holick & Clark, 1978). Several congenital syndromes are caused by the loss of enzymes that catalyze the last steps in the cholesterol synthesis pathway. Smith-Lemli-Opitz syndrome (SLOS) is caused by mutations in the gene encoding the 3β-hydroxysterol Δ7-reductase (7DHCR) (Fitzky et al., 1998), which catalyzes the reduction of the 7-double bond in 7-Dehydrocholesterol (7DHC) (Figure 1A) (Kandutsch & Russell, 1960). In SLO, a distinctive facial appearance including cleft palate, microcephaly, a small upturned nose, micrognathia, and ptosis is common (Smith, Lemli & Opitz, 1964). Furthermore, limb malformations like postaxial polydactyly, syndactyly of the second and third toe, and proximally placed thumbs are observed in most patients. This syndrome has some overlap with the malformations caused by reduced Shh signaling (Chiang et al., 1996; Roessler et al., 1996; Smith et al., 1964). Biochemically, elevated levels of 7DHC and its isomer, 8-Dehydrocholesterol (8DHC), are found besides decreased cholesterol in serum and tissue of SLOS patients as well as in the mouse model (Tint, 1993; Wassif et al., 2001). 7DHC levels are used for the diagnosis of SLO and are typically increased more than 50-fold (F. D. Porter & Herman, 2011).

Lathosterolosis is caused by mutations in the gene encoding the 3β-hydroxysteroid-Δ5-desaturase (SC5D) which desaturates lathosterol to 7DHC in the second to last step of cholesterol synthesis (Figure 1A) (Brunetti-Pierri et al., 2002). Symptoms of lathosterolosis have similarities with those observed in SLOS, including postaxial polydactyly, microcephaly, micrognathia, and toe syndactyly (Brunetti-Pierri et al., 2002). In the lathosterolosis mouse model, lathosterol levels are elevated 60 fold whereas levels of cholesterol were decreased similar to the SLOS mouse model (Krakowiak et al., 2003; Wassif et al., 2001). To this point, it has not been resolved unambiguously if a reduction of cholesterol levels or the accumulation of its precursors constitute the phenotype of the malformation syndromes caused by inborn errors in the synthesis of cholesterol (Blassberg, Macrae, Briscoe, & Jacob, 2016; Cooper et al., 2003). Circulating maternal cholesterol can be transported to the fetus, making it unlikely that SLOS and lathosterolosis are predominantly caused by low fetal cholesterol. Instead, the accumulation of late sterol precursors seems to contribute to these birth defects, possibly by suppressing Shh signaling (Cooper et al., 2003).

Cell types in the developing neural tube arise in at stereotypic position in response to Shh signaling. An effective in vitro model of the neural tube are neuralized embryoid bodies (nEBs), also called spinal cord organoids (SCOs), which are aggregates of approximately 10^4 embryonic stem cells (ESCs) (Wichterle, Lieberam, Porter, & Jessell, 2002). Mosaic SCOs can be generated by mixing cells with genotypically diverse cell lines in varying ratios. This approach allows us to address the non-cell autonomous effects caused by genetic alterations.

Here, we provide evidence that accumulation of late sterol precursors can inhibit Shh signaling both cell autonomously, as well as non-cell autonomously even in cells with an intact cholesterol synthesis pathway. Importantly, this increased non-cell autonomous inhibition requires the presence of Ptch1/2 function in those cells that accumulate the cholesterol precursors. These observations are consistent with a model that late sterol precursors are the cargo of Ptch1/2 antiporter activity in its ability to inhibit Smo non-cell autonomously.

Results

The loss of 7-Dehydrocholesterol reductase and/or Lathosterol 5-desaturase changes the cellular distribution of sterols

We have shown before that Ptch1/2 activity can inhibit Smo non-cell autonomously, supporting the notion that Ptch1/2 functions in the distribution or secretion of a Smo inhibitor (B. Roberts et al., 2016). To assess if this inhibitor could be a late sterol precursor, we made *Shh*$^{-/-}$;*7Dhcr*$^{-/-}$ cells and found that these cells have reduced amounts of cholesterol after three days of serum starvation as compared to the parental *Shh*$^{-/-}$ cells (Figure 1B). To assess more global changes in the distribution of sterols, we stained serum-starved SCOs with Filipin, a fluorescent stain (Blanchette-Mackie, 2000) used in the diagnosis of Niemann-Pick disease type C (Sokol et al., 1988). Similar to SLOS, the phenotype of lathosterolosis overlaps with that of congenital Shh malformations, raising the question if similar mechanisms impair the Shh signal transduction. Besides *Shh*$^{-/-}$;*7Dhcr*$^{-/-}$ cells, we also stained *Shh*$^{-/-}$;*Sc5d*$^{-/-}$ cells as well as the triple mutant *Shh*$^{-/-}$;*7Dhcr*$^{-/-}$;*Sc5d*$^{-/-}$ cells, cultured as SCOs in the absence of serum for up to 72 hours. Cells lacking only Shh had surface and wrinkle-like accumulations of sterols on the cell surface on the first and second day of serum deprivation (Figure 1C). However, few cells appeared with small circular-shaped structures on the cell surface as well as inside the cell that accumulated on day 3. Whereas cells missing either 7Dhcr or Sc5d had a wild-type like distribution of sterols, *Shh*$^{-/-}$;*7Dhcr*$^{-/-}$;*Sc5d*$^{-/-}$ cells appeared to have a reduced amount of sterols (Figure 1C). These results indicate that a lack of Sc5d is not epistatic to a lack of 7Dhcr, which are thought to act in sequence in the cholesterol synthesis pathway, but in fact has an additive effect.

Accumulation of late sterol precursors inhibit the Hh response

The loss of DHCR7 in SLOS is known to suppress Shh signaling, and the prevailing hypothesis is that this is caused by the accumulation of a late sterol precursor inhibiting Smo (Cooper et al., 2003). To discern whether the accumulation of the direct cholesterol precursor 7DHC or the lack of cholesterol can inhibit Shh signaling, SCOs constituting of *Ptch1*$^{LacZ/LacZ}$;*Ptch2*$^{-/-}$;*Shh*$^{-/-}$ were treated with 13 µM 7DHC, 13 µM cholesterol, or a combination of both sterols, and the amount of Ptch1:LacZ was measured as a proxy for the Hh pathway response (Figure 1D). The reporter cells are devoid of both Ptch1 and Ptch2 with the result that Smo is constitutively active and the *Ptch1:LacZ* expression levels are highly increased compared to heterozygous reporter cells (*Ptch1*$^{+/LacZ}$;*Shh*$^{-/-}$, (Roberts et al., 2016). 7DHC significantly reduced the Shh pathway activity in *Ptch1*$^{LacZ/LacZ}$;*Ptch2*$^{-/-}$;*Shh*$^{-/-}$ SCOs by 30 % (Figure 1D). Cholesterol had no effect on the Hh response, neither when added alone nor in combination with 7DHC. This indicates that the accumulation of cholesterol precursors is the inhibitory event and not a lack of cholesterol and that additional cholesterol cannot compensate the inhibitory effect of 7DHC. These results suggest that the inhibitory cholesterol precursor can be found in the medium, and we therefore tested the inhibitory potential of conditioned supernatants. We transferred medium of SCOs consisting of *Ptch*$^{-/-}$ and/or *7Dhcr*$^{-/-}$ cells to *Ptch1*$^{LacZ/LacZ}$;*Ptch2*$^{-/-}$;*Shh*$^{-/-}$ reporter cells and found that in addition to a Ptch1/2-mediated inhibition, the conditioned medium of *7Dhcr*$^{-/-}$ cells decreased the Hh response in reporter cells by 40% (Figure 1E).

These results support the idea that a cholesterol precursor can inhibit the Hh response non-cell autonomously.

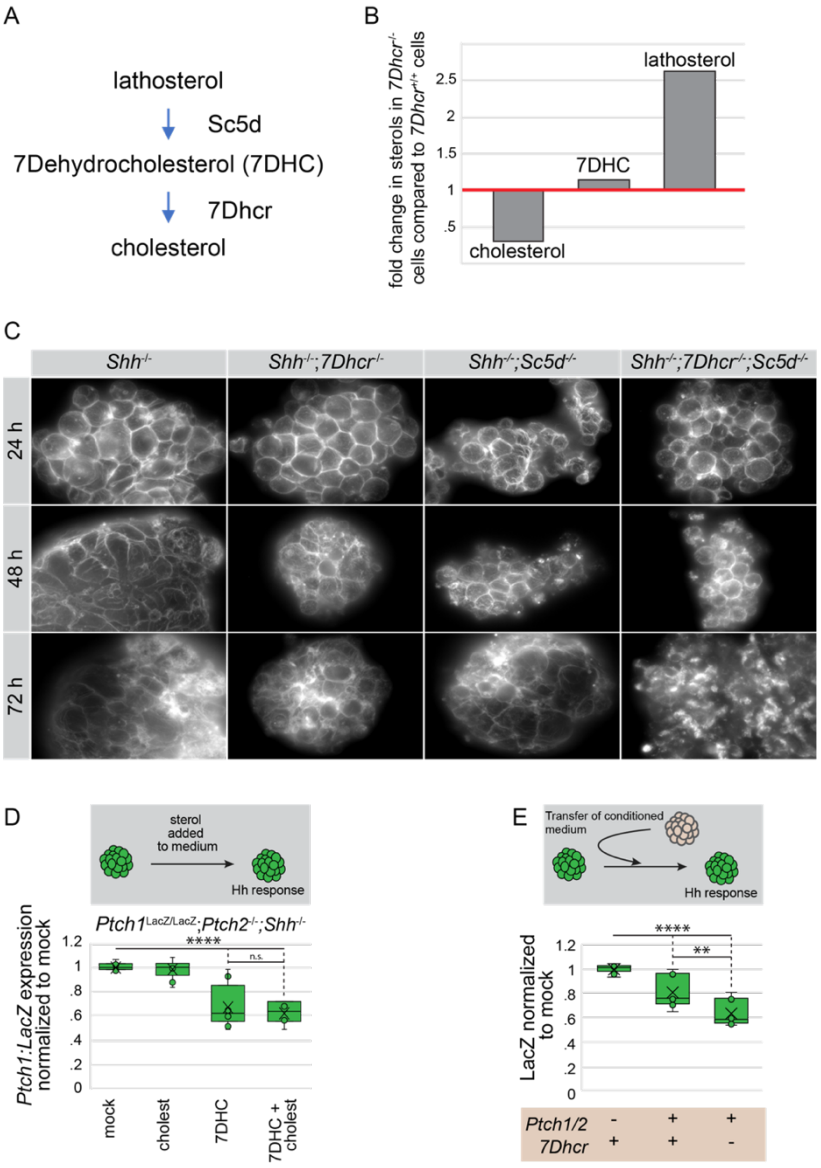

Figure 1: Late sterol precursors accumulate in *Shh*$^{-/-}$;*7Dhcr*$^{-/-}$ cells and inhibit the Hh response non-cell autonomously.
A: Schematic of the last enzymatic reactions in cholesterol synthesis. Lathosterol is converted to 7DHC by the desaturase Sc5d, and 7DHC to cholesterol by the desaturase 7Dhcr. **B:** Cholesterol, 7DHC, and lathosterol levels were measured in *7Dhcr*$^{-/-}$ cells 3 days after serum starvation by gas chromatography mass spectrometry (GC-MS) and compared to *7Dhcr*$^{+/+}$ cells. **C:** Staining of unesterified sterols in *Shh*$^{-/-}$, *Shh*$^{-/-}$;*7Dhcr*$^{-/-}$, *Shh*$^{-/-}$;*Sc5d*$^{-/-}$, and *Shh*$^{-/-}$;*7Dhcr*$^{-/-}$;*Sc5d*$^{-/-}$ SCOs with the fluorescent dye Filipin 3 days after serum starvation. **D:** *Ptch1:LacZ* measurement of *Ptch1*$^{LacZ/LacZ}$;*Ptch2*$^{-/-}$;*Shh*$^{-/-}$ reporter cells in SCOs that were treated with mock, 13 μM 7DHC, 13 μM cholesterol, or 13 μM 7DHC and 13 μM cholesterol for 3 days under serum starvation. Box-and-Whisker plot, n ≥ 3. **E:** *Ptch1:LacZ* measurement of *Ptch1*$^{LacZ/LacZ}$;*Ptch2*$^{-/-}$;*Shh*$^{-/-}$ reporter cells in SCOs that were cultured in medium conditioned by *Ptch1*$^{LacZ/LacZ}$;*Ptch2*$^{-/-}$;*Shh*$^{-/-}$, *Shh*$^{-/-}$, or *Shh*$^{-/-}$;*7Dhcr*$^{-/-}$ SCOs. Box-and-Whisker plot, n=3. ****p<0.0001, **p<0.01, n.s. not significant.

Loss of 7-Dehydrocholesterol reductase and/or lathosterol 5-desaturase inhibit the Shh pathway non-cell autonomously

To test if endogenous early cholesterol precursors like 7DHC or lathosterol can inhibit Shh signaling non-cell autonomously, we measured *Ptch1:LacZ* expression in our *Ptch1*$^{LacZ/LacZ}$;*Ptch2*$^{-/-}$;*Shh*$^{-/-}$ reporter cells in mosaic SCOs with 50% *Shh*$^{-/-}$;*7Dhcr*$^{-/-}$, *Shh*$^{-/-}$;*Sc5d*$^{-/-}$ or the triple mutant *Shh*$^{-/-}$;*7Dhcr*$^{-/-}$;*Sc5d*$^{-/-}$ mESCs (Figure 2A). Both *Shh*$^{-/-}$;*7Dhcr*$^{-/-}$ and *Shh*$^{-/-}$;*Sc5d*$^{-/-}$ cells inhibited Shh pathway activity in the neighboring reporter cells (Figure 2B). The inhibition by *Shh*$^{-/-}$;*7Dhcr*$^{-/-}$ cells, however, was significantly more potent than the one caused by *Shh*$^{-/-}$;*Sc5d*$^{-/-}$ mESCs, suggesting that 7DHC could be a major component of the inhibitory cholesterol precursors. Interestingly, a combination of the two

mutations further decreased the *Ptch1:LacZ* expression in SCOs composed of even amounts of *Ptch1*$^{LacZ/LacZ}$;*Ptch2*$^{-/-}$;*Shh*$^{-/-}$ and *Shh*$^{-/-}$;*7Dhcr*$^{-/-}$;*Sc5d*$^{-/-}$ mESCs. This additive effect, as mentioned earlier, contradicts the idea of a linear pathway with Sc5d and 7Dhcr being enzymes acting in sequence. The differences in the inhibitory potential of the different cell lines could not be explained by shifted ratios of reporter and repressor cells as lineage tracers showed even numbers of reporter and repressor cells in all 4 different types of mosaic SCOs 48 h after aggregation (Figure 2C).

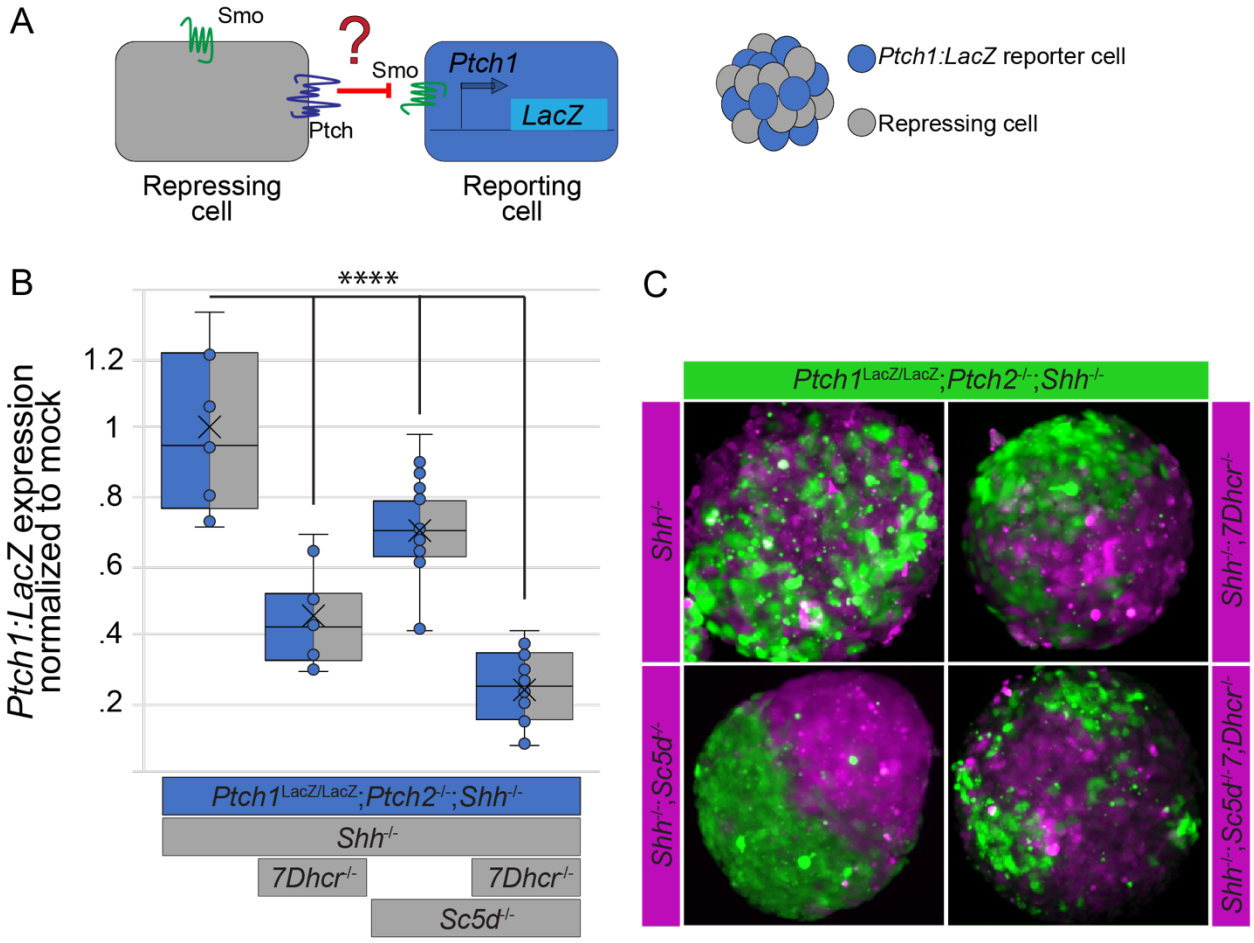

Figure 2: Non-cell autonomous inhibition of the Hh response by cells mutant for enzymes of cholesterol synthesis. A: Experimental setup: In mosaic SCOs consisting of equal amounts of reporter and repressor cells, repressor cells have Ptch1/2 but lack varying enzymes of cholesterol synthesis. The reporter cells with a *Ptch1:LacZ* reporter gene lack Ptch1/2 and therefore have an upregulated transcriptional Hh response. **B:** *Ptch1:LacZ* expression *Ptch1*$^{LacZ/LacZ}$;*Ptch2*$^{-/-}$;*Shh*$^{-/-}$ reporter cells in mosaic SCOs after 3 days of serum starvation. Box-and-Whisker plot, n=5, **** p<0.0001. **C:** Fluorescent images of mosaic SCOs consisting of reporter and repressor cells (genotypes indicated) that were loaded with lineage tracing dyes (CellTracker^{TM} Green and Blue). Images are pseudo-colored to enhance contrast.

These results suggest that a variety of early cholesterol precursors can inhibit Shh signaling non-cell autonomously. Moreover, the additive inhibitory effect of *Shh*$^{-/-}$;*7Dhcr*$^{-/-}$;*Sc5d*$^{-/-}$ on the Shh pathway contradicts the linear cholesterol biosynthesis pathway of textbooks.

Ptch1/2 is required for non-cell autonomous inhibition

We tested if Ptch1/2 is required for non-cell autonomous inhibition by cells deficient for 7Dhcr or Sc5d and compared the response to 7DHC in homogenous *Ptch1*$^{LacZ/LacZ}$;*Ptch2*$^{-/-}$;*Shh*$^{-/-}$ reporter SCOs to mosaic SCOs consisting of 50% *Ptch1*$^{LacZ/LacZ}$;*Ptch2*$^{-/-}$;*Shh*$^{-/-}$ reporter and 50% Ptch1/2-containing cells (Figure 3A). Exogenous 7DHC decreased the Hh response in reporter cells to a much greater extend when Ptch1/2-containing cells were present, additionally to the inhibitory function of Ptch1/2 alone (both types of SCOs were normalized to their respective mock-treatment). This suggests that 7DHC from the medium can be acted upon and potentiated in its Smo-inhibitory potential by Ptch1/2. This effect of Ptch1/2 on 7DHC was not observed for the Smo antagonist cyclopamine, suggesting that cyclopamine inhibits Smo directly without the need for Ptch1/2 function (Figure S1).

We next sought to assess if Ptch1/2 function can be rescued and if both paralogs contribute to Smo-inhibition. As overexpression experiments in mESCs usually suffer from poor transfection efficiencies, we overexpressed Ptch1 or Ptch2 in Ptch1/2- or 7Dhcr-deficient fibroblasts (*Ptch1*$^{LacZ/LacZ}$;*Ptch2*$^{-/-}$ and *Ptch1*$^{LacZ/LacZ}$;*Ptch2*$^{-/-}$;$^{7Dhcr-/-}$) and transferred their supernatant onto Light2 reporter cells (Taipale et al., 2000). Conditioned medium from Ptch1- and Ptch2-expressing cells inhibited the Shh pathway response in the presence of SAG equally and independent of 7Dhcr in the conditioning cells (Figure 3B).

To further assess the role of Ptch1/2 in non-cell autonomous inhibition of Shh signaling by cholesterol precursors, we mixed Ptch1/2-deficient *Ptch1*$^{LacZ/LacZ}$;*Ptch2*$^{-/-}$;*Shh*$^{-/}$ and *Ptch1*$^{LacZ/LacZ}$;*Ptch2*$^{-/-}$;*Shh*$^{-/-}$;*7Dhcr7*$^{-/-}$ mESCs in mosaic SCOs and compared their *Ptch1:LacZ* expression to SCOs consisting of either genotype alone. While the Hh response is constitutively high in *Ptch1*$^{LacZ/LacZ}$;*Ptch2*$^{-/-}$;*Shh*$^{-/-}$ cells, the loss of 7Dhcr decreases *Ptch1:LacZ* expression by approximately 70 % (Figure 3C). If Ptch1/2 are indeed required for non-cell autonomous Shh pathway inhibition, 7Dhcr- and Ptch1/2 deficient cells should not be able to inhibit the Shh pathway response and the *Ptch1:LacZ* expression of the mosaic SCOs should be exactly half of the difference between *Ptch1*$^{LacZ/LacZ}$;*Ptch2*$^{-/-}$;*Shh*$^{-/}$ and *Ptch1*$^{LacZ/LacZ}$;*Ptch2*$^{-/-}$;*Shh*$^{-/-}$;*7Dhcr*$^{-/-}$ SCOs. The null hypothesis would therefore be H_0 = 1 – ½ (average *Ptch1*$^{LacZ/LacZ}$;*Ptch2*$^{-/-}$;*Shh*$^{-/-}$- average *Ptch1*$^{LacZ/LacZ}$;*Ptch2*$^{-/-}$;*Shh*$^{-/-}$;*7Dhcr*$^{-/-}$), indicated by a red line in Figure 3C. Indeed, the average of Ptch1/2-deficient mosaic SCOs was only 2 percent points higher than H_0, suggesting that Ptch1/2 facilitates the non-cell autonomous inhibition of cholesterol precursors (Figure 3C).

To further confirm the role of Ptch1/2 in repressing cells, we mixed 5% *Hb9:gfp* mESCs with a panel of Ptch1/2-containing/deficient and/or 7Dhcr-containing/deficient mESCs (Figure 3D). The Hh pathway response was activated in the reporter cells with the Smoothened agonist SAG and the inhibitory potential of the interspersed cells was assessed by counting the number of *Hb9:gfp*-positive nuclei as a measure of Hh pathway activation. Compared to uninhibited *Hb9:gfp* reporter cells in Ptch1/2 -deficient mosaic SCOs, Ptch1/2 alone decreased the number of positive nuclei by more than half (Figure 3E). Consistent with our results described earlier, Ptch1/2 containing but 7Dhcr deficient cells decreased the number of positive nuclei even further. In the absence of Ptch1/2 and 7Dhcr, however, *Hb9:gfp* expression was uninhibited, similar to the level of Ptch1/2-deficient mosaic SCOs. This suggests that a loss of Ptch1/2 is epistatic to a loss of 7Dhcr in repressing cells and that

Ptch1/2 is required for non-cell autonomous inhibition. As the addition of SAG increased the number of *Hb9:gfp* positive nuclei in every condition, the inhibitory factor in the *7Dhcr*$^{-/-}$ cells is likely a competitive inhibitor to SAG, meaning that it acts at the level of Smo.

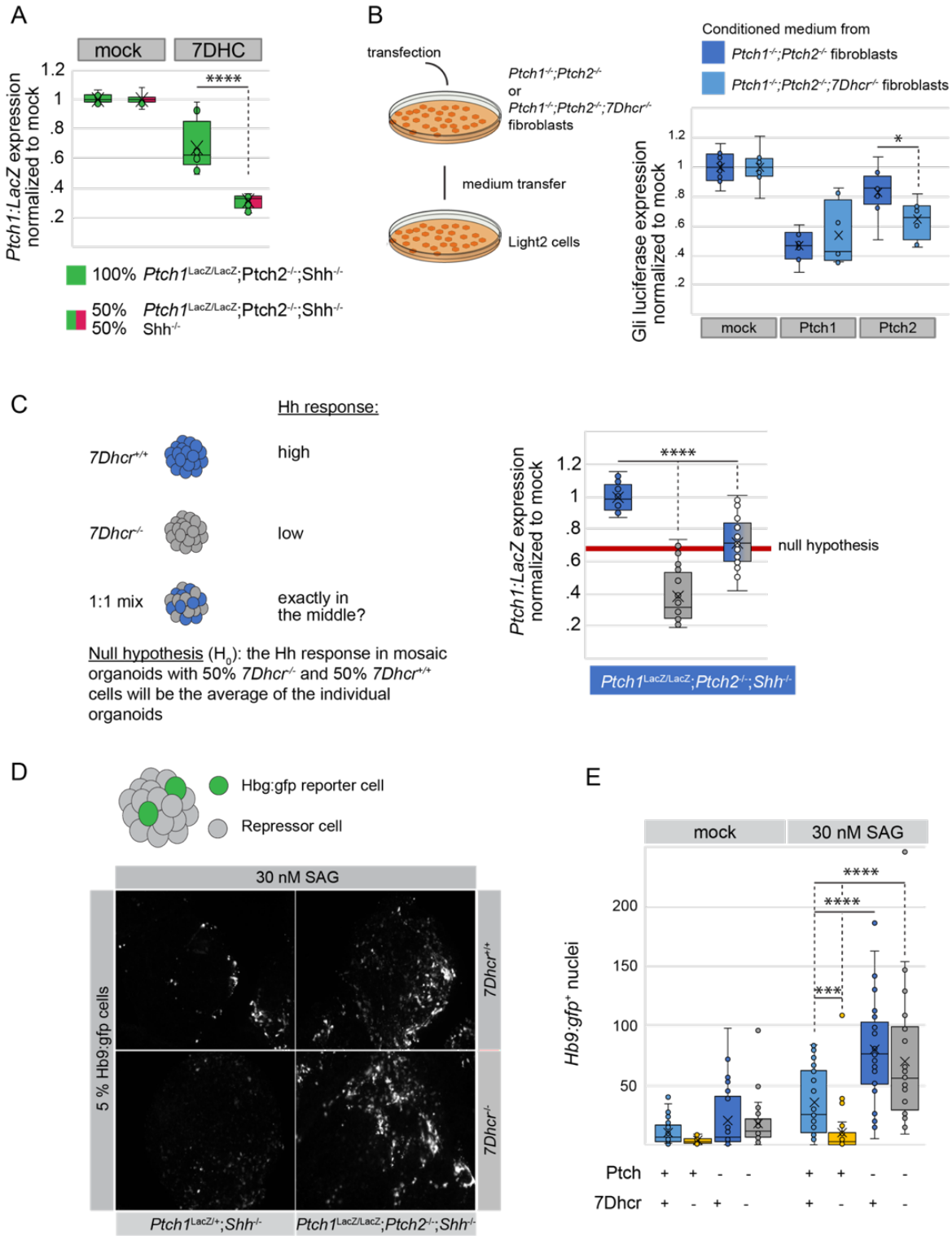

Figure 3: Non-cell autonomous inhibition by late cholesterol precursors requires Ptch1/2.
A: *Ptch1:LacZ* measurement of *Ptch1*$^{LacZ/LacZ}$*;Ptch2*$^{-/-}$*;Shh*$^{-/-}$ reporter cells in SCOs or in mosaic SCOs with 50 % *Shh*$^{-/-}$ mESCs after 3 days of serum starvation. 13 µM 7DHC was added after the first night of SCO aggregation. Ptch1:LacZ levels are normalized to the respective mock treatment to account for lower numbers of reporter cells and inhibition by Ptch1/2 in mosaic SCOs. Box-and-Whisker plot, n=4. **B:** Experimental setup and Gli luciferase measurements of Hh responsive Light2 cells. *Ptch1*$^{-/-}$*;Ptch2*$^{-/-}$ or *Ptch1*$^{-/-}$*;Ptch2*$^{-/-}$*;7Dhcr*$^{-/-}$ fibroblasts were transfected with mock, *Ptch1*, or *Ptch2* and their conditioned medium was filtered and transferred onto Light2 cells with 30 nM SAG. Gli luciferase levels were normalized to Renilla luciferase and all conditions to their respective mock transfection. Box-and-Whisker plot, n=4. **C:** Graphic representation of the null hypothesis (indicated by red line): If Ptch1/2 is not required for non-cell autonomous inhibition, *Ptch1:LacZ* expression in mosaic SCOs will be the average of the individual SCOs. *Ptch1:LacZ* measurement of *Ptch1*$^{LacZ/LacZ}$*;Ptch2*$^{-/-}$*;Shh*$^{-/-}$*,* *Ptch1*$^{LacZ/LacZ}$*;Ptch2*$^{-/-}$*;Shh*$^{-/-}$*7Dhcr*$^{-/-}$*,* and mosaic SCO consisting of equal amounts of the two reporter lines 3 days after serum starvation. Box-and-Whisker plot, n=4. **D:** Mosaic SCOs with 5% *Hb9:gfp* reporter cells and the indicated repressor cells were serum starved for 3 days and treated with 30 nM SAG for the last 24 hours. SCOs were fixed and *Hb9:gfp* expression imaged. Shown are representative images of mosaic SCOs for each condition. **E:** Quantification of *Hb9:gfp* positive nuclei of the experiment shown in D, shown in a Box-and-Whisker plot, n=3.* $p<0.05$, *** $p<0.001$, ****$p<0.0001$

Discussion

Mutations in the *DHCR7* gene encoding the 3β-hydroxysteroid Δ^7-reductase are associated with the Smith-Lemli-Opitz Syndrome (SLOS), a congenital multiple malformation syndrome (Fitzky et al., 1998). Malformations resemble birth defects observed with reduced Hedgehog signaling during embryogenesis, and the accumulating cholesterol precursor 7DHC were found to reduce Shh signaling (Cooper et al., 2003; Roessler et al., 1996). In addition to the known cell autonomous inhibition of the Hh response, we show here that *Shh*$^{-/-}$;*7Dhcr*$^{-/-}$ mESCs inhibit the Shh pathway non-cell autonomously. Importantly, Ptch1/2 was found to enhance the inhibitory effect of exogenously added 7DHC on reporter cells devoid of Ptch1/2, arguing for 7DHC being an endogenous cargo of Ptch1/2. Furthermore, Ptch1/2 are required for non-cell autonomous inhibition as *7Dchr*$^{-/-}$ cells also deficient for Ptch1/2 were not able to inhibit the Hh response in adjacent cells.

Possible scenario for the Ptch1/2-dependent inhibition of Smo by cholesterol precursors

The following model based on the data presented here evolved (Figure 4): Ptch1/2 is able to inhibit Smo non-cell autonomously and its inhibitory function is even enhanced when the cells are deficient for one or more enzymes of the cholesterol synthesis pathway. This is likely due to the transport of inhibitory cholesterol precursors like 7DHC, increasing their inhibitory potential by a yet unknown mechanism (Bijlsma et al., 2006; Cortes et al., 2015; Linder et al., 2015). To this point, we cannot exclude that a derivative of 7DHC like vitamin D3/cholecalciferol or vitamin D/calcitriol inhibits Smo. To be inhibitory non-cell autonomously, 7DHC and other cholesterol precursors need Ptch1/2 activity, as Ptch1/2-deficient cells had no inhibitory potential, independent of the presence of 7Dhcr or Sc5d.

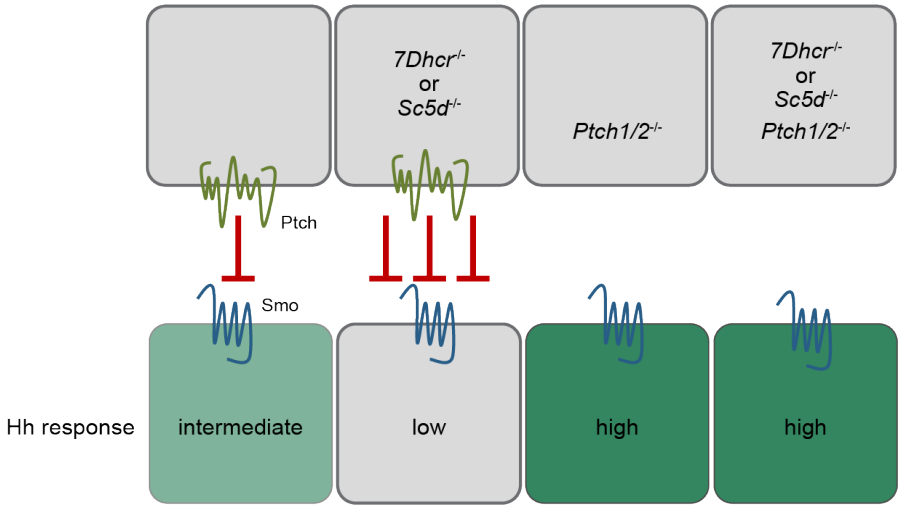

Figure 4: Model of non-cell autonomous Smo inhibition by Ptch1/2. Ptch1/2 inhibits Smo non-cell autonomously and does so more potently when the Ptch1/2-containing cells lack enzymes of cholesterol synthesis, resulting in a decreased transcriptional Hh response. In the absence of Ptch1/2 and independent of the absence or presence of enzymes of cholesterol synthesis, Smo in uninhibited and the transcriptional Hh response is high.

Does Ptch1/2 transport a Smo-inhibitory sterol?

Many Smo-modulating small molecules, both endogenous and exogenous as well as activating and inhibiting, are known (H. J. Sharpe et al., 2015). Some of those have a steroidal structure, that, together with evidence originating from Ptch1/2, suggests that Ptch1/2 uses a sterol to inhibit Smo in the absence of the Hh ligand. We find that Ptch1/2 does not exacerbate Smo inhibition by cyclopamine, arguing against it being a cargo of Ptch1/2. Cholesterol on the other hand would be a welcome endogenous candidate as a Ptch1/2 cargo due to its ubiquitous presence but definitive evidence, especially for a Smo inhibitory function, is scarce.

Besides cholesterol, vitamin D/calcitriol can be synthesized from 7DHC via photolysis. When 7DHC accumulates in the absence of 7Dhcr, the synthesis of vitamin D is increased (Prabhu, Luu, Sharpe, & Brown, 2016). Vitamin D3/cholecalciferol, the precursor of vitamin D, is capable of inhibiting Smo more efficiently than 7DHC and is secreted by Ptch1 (Bijlsma et al., 2006; Tang et al., 2011). Similarly, the hormonally active form of vitamin D3, calcitriol, was reported to be released into the extracellular space by Ptch1 and efficiently inhibit the translocation of Smo to the primary cilium (Cortes et al., 2015; Linder et al., 2015), further supporting the notion that a cholesterol precursor or derivative thereof could be the Ptch1/2 cargo that inhibits Smo.

Evidence for alternative pathways in the cholesterol biosynthesis pathway

Cholesterol synthesis begins with acetyl-CoA and has a multiplicity of intermediates, each requiring catalyzation by unique enzymes to progress to the next precursor molecule. Kandutsch and Russell proposed a linear but bifurcated pathway in 1960 for the synthesis of cholesterol that only differ in an additional double bond in the alkyl side chain appended to the CD-ring. This double bond can be resolved at any time by the 3β-hydroxysterol Δ^{24}-reductase. Sc5d acts upstream of 7Dhcr and a mutation would therefore logically be epistatic to a mutation in the *7Dhcr* gene. Contrary, we observed an additive inhibitory effect of the two mutations in combination on the Shh pathway. Thus, additional functions of enzymes or additional, Sc5d and/or 7Dhcr circumventing pathways are conceivable. Porter et. al proposed, with reservation, that 8-Dehydrocholesterol (8DHC), an isomer of 7DHC, can be synthesized from the precursor of lathosterol (cholesta-8(9)-en-3ß-ol) by Sc5d (F. D. Porter, 2002). 8DHC and 7DHC differ in the position of a double bond that can be swapped in both directions by the enzyme that synthesizes lathosterol from its precursor, 3β-hydroxysterol Δ8,Δ7-isomerase (EBP). Although this alternative pathway does not explain the additive inhibitory effect of combinatorial Sc5d and 7Dhcr knock-outs - a lack of Sc5d would still terminate the synthesis of cholesterol at the level of lathosterol - it still strengthens the likelihood that cholesterol synthesis is not as linear as textbooks impart and that enzymes of cholesterol synthesis can exhibit additional, unknown functions.

The mechanism of Smo inhibition by Ptch1/2

The hypothesis that the non-cell autonomous inhibition of the Shh pathway by Ptch1/2 is mediated by its antiporter function originates from the observation that a mutation in the antiporter channel (Ptch1D499A) blocks Ptch1 activity (Alfaro et al., 2014; Taipale et al.,

2002). As a member of the RND family of proton driven antiporters, Ptch1/2 is thought to require a proton gradient to transport molecules across membranes (Tseng et al., 1999). Sodium has been proposed as an alternative ion that would be transported across the cell membrane in exchange for the Smo inhibitory molecule (Myers et al., 2017). Besides the question of "what" Ptch1/2 transports, the "how/where" has been the point of more recent discussion. The Ptch1 monomer revealed a hydrophobic pore-like structure in cryo-electron microscopy (cryo-EM) models, oftentimes with sterols in the vicinity of the pore opening. Transport of sterols through that pore, however, are difficult to reconcile with a simultaneous antiport of an ion through the seemingly narrow diameter of the pore. Furthermore, the palmitoylated N-terminus of Shh inserts into this pore, thereby blocking Ptch1 function in a similar fashion to the antiporter channel mutant (Qi, Schmiege, Coutavas, Wang, & Li, 2018; Tukachinsky, Petrov, Watanabe, & Salic, 2016). Dispatched, another member of the RND superfamily, is a homotrimer, suggesting that Ptch1, too, could form a trimer with a large opening in the center (Etheridge, Crawford, Zhang, & Roelink, 2010). This central pore could transport the Smo-inhibitory sterol, leaving the pores in the individual monomers for ion antiport.

Conclusions

Our findings suggest that 7DHC and other cholesterol precursors are endogenous cargos of Ptch1/2. Similar to other (bacterial) members of the RND transporter family, Ptch1/2 can mediate the efflux of substrates that inhibit Smo and thus the downstream transcriptional response.

Materials and Methods

CRISPR/Cas9 mediated mutagenesis

The CRISPR/Cas9 genome editing technique was used to knock out the *7Dhcr* and *Sc5d* gene (Ran et al. 2013). The pX458/ pSpCas9(BB)-2A-Puro and pX459/ pSpCas9(BB)-2A-GFP expression plasmids were a gift from the Doudna lab (University of California, Berkeley, USA). sgRNAs were designed using the online tool provided by the Zhang lab (http://tools.genome-engineering.org, MIT, Massachusetts, USA) and ordered from IDT DNA Technologies (Iowa, USA). Cloning of sgRNA and Cas9 expressing plasmids was performed according to (Ran et al., 2013)

Tissue culture

Ptch1$^{LacZ/LacZ}$;*Ptch2*$^{-/-}$;*Shh*$^{-/-}$ and *Shh*$^{-/-}$ mESCs were generated using TALEN mediated mutagenesis and are described elsewhere (B. Roberts et al., 2016). The *Ptch1*$^{LacZ/LacZ}$;*Ptch2*$^{-/-}$;*Shh*$^{-/-}$ line originates from the *Ptch1*$^{LacZ/LacZ}$ line (Goodrich, Milenkovic, Higgins, & Scott, 1997). All cell lines were cultured under standard conditions in ES medium (DMEM/Gibco, 15 % FBS/Gibco, 2mM L-glutamine/Thermo Fisher Scientific, 1X Penicillin Streptomycin/ Thermo Fisher Scientific, 1X MEM Non-Essential Amino Acids Solution/Thermo Fisher Scientific, 1X Nucleosides for ES cells/EMD Millipore, 1X ß-Mercaptoethanol, 1X GST-LIF/Millipore) in tissue culture dishes coated with gelatin.

For generation of SCOs, 2 x 10^5 – 4 x 10^5 mESCs were cultured in 60mm Petri dishes in DFNB medium (Neurobasal medium/Gibco, DMEM F12 1:1/Gibco, 1.5 mM L-glutamine/ Thermo Fisher Scientific, 1X Penicillin Streptomycin/Thermo Fisher Scientific, 1X B27® Supplement/Gibco, 0.1 mM ß-Mercaptoethanol) on a rotating platform. After 48 h, 10 µM Retinoic Acid (Sigma/Aldrich) was added.

7DHC, cholesterol, and lathosterol (all Sigma/Aldrich) were dissolved in ethanol and used at 13 µM. All reagents were added directly to aggregating SCOs.

Fibroblasts were grown in DMEM + 10% FBS (Atlas Biologicals) and transfected with Lipofectamine2000 according to the manufacturer's instructions. The medium was exchanged with DMEM 24h after transfection for medium conditioning (24h). The conditioned medium was then removed, filtered, and transferred onto Light2 cells for another 48h with 30 nM SAG. Gli- and Renilla-luciferase levels in the Light2 cells were measured with the Dual luciferase kit according to the manufacturer's instructions. Gli luciferase/Renialla luciferase levels were normalized to the respective mock-transfected control.

Cell tracking

For cell lineage tracking experiments, cells were incubated with 500 µM CMFDA Green or CMAC Blue (both Invitrogen) in DFNB medium for 45 min at 37 °C and seeded as described above. After 48 h (or respective time points), SCOs were fixed in 4 % paraformaldehyde (Thermo Fisher Scientific) in 1X PBS for 10 min and mounted directly in Fluoromount G Mounting Medium (Thermo Fisher Scientific). Images were taken with a Zeiss Observer fluorescence microscope with a 20X and 10X objective.

Filipin staining
For filipin staining, SCOs were fixed in 4 % paraformaldehyde (Thermo Fisher Scientific) in 1X PBS for 10 min after one, two, or three days. SCOs were stained in 30 µM filipin III (Sigma/Aldrich) in 1X PBS for 30 min in the dark and mounted in Fluoromount G Mounting Medium (Thermo Fisher Scientific) after washing once with 1X PBS. Images were taken with a Zeiss Observer fluorescence microscope with a 63X objective and oil immersion.

Reporter Gene Assay for *Ptch1:LacZ* induction
Ptch1:LacZ expression levels were quantified 72 h after aggregation of SCOS using the Galacto-Light Plus™ system (Applied Biosciences) according to the manufacturer's instructions. Shortly, SCOs were collected in plastic tubes, washed with 1X PBS, and lysed using lysis buffer (100 mM potassium phosphate pH 7.8, 0.2% Triton X-100). Lysates were incubated with 70 µl Reaction buffer for 30 min in a 96 well plate, followed by an incubation with Accelerator-II for 15 min. Signal was read in a microplate luminometer for 5 s per well. *Ptch1:LacZ* levels were normalized to total protein using the Bradford reagent (BioRad).

Statistics
Single Factor ANOVA was used to analyze more than two conditions, followed by a Student's *t*-test with a two-tailed distribution assuming unequal variance comparing two conditions. *p<0.05, **p<0.01, ***p<0.001, ****p<0.0001

Acknowledgements
This work was supported by NIH grant R01GM117090 to HR. We thank Dr. Anthony T. Iavarone at the QB3/Chemistry Mass Spectrometry Facility (UC Berkeley) for help with obtaining the mass spectrometry data.

Author contributions
All experiments were performed by CJ. Experiments were designed by CJ and HR. The manuscript was written by CJ and HR.

Conflict of interest
The authors declare no conflict of interest.

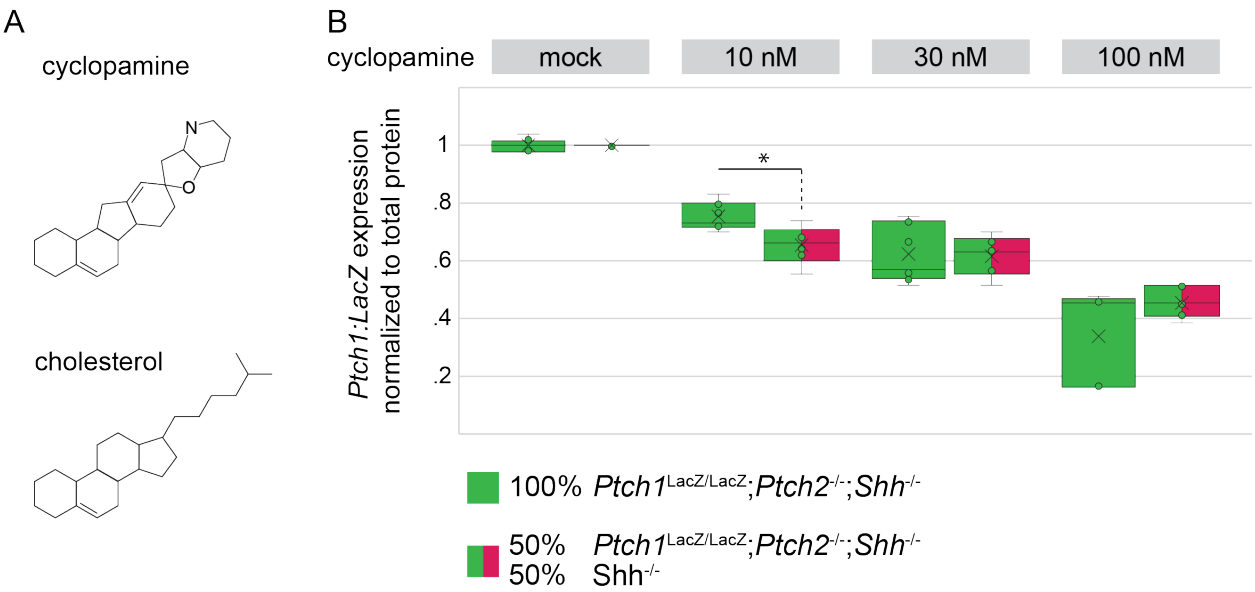

Figure Sl: Ptch1/2 does not exacerbate the inhibition of Smo by cyclopamine. A: Structural comparison of the steroidal molecules cyclopamine and cholesterol. **B:** *Ptch1:LacZ* measurement of *Ptch1*$^{LacZ/LacZ}$;*Ptch2*$^{-/-}$;*Shh*$^{-/-}$ reporter cells in SCOs or in mosaic SCOs with 50 % *Shh*$^{-/-}$ mESCs after 3 days of serum starvation. The indicated concentrations of cyclopamine were added after the first night of SCO aggregation. *Ptch1:LacZ* levels are normalized to the respective mock treatment to account for lower numbers of reporter cells and inhibition by Ptch1/2 in mosaic SCOs. Box-and-Whisker plot, n=6, *p<0.05.

References

Alfaro, A. C., Roberts, B., Kwong, L., Bijlsma, M. F., & Roelink, H. (2014). Ptch2 mediates the Shh response in Ptch1-/- cells. *Development*, *141*(17), 3331–3339. http://doi.org/10.1242/dev.110056

Bijlsma, M. F., Spek, C. A., Zivkovic, D., van de Water, S., Rezaee, F., & Peppelenbosch, M. P. (2006). Repression of smoothened by patched-dependent (pro-)vitamin D3 secretion. *PLoS Biol*, *4*(8), e232.

Blanchette-Mackie, E. J. (2000). Intracellular cholesterol trafficking: role of the NPC1 protein. *Biochim. Biophys. Acta*, *1486*(1), 171–183.

Blassberg, R., Macrae, J. I., Briscoe, J., & Jacob, J. (2016). Reduced cholesterol levels impair Smoothened activation in Smith-Lemli-Opitz syndrome. *Hum Mol Genet*, *25*(4), 693–705. http://doi.org/10.1093/hmg/ddv507

Bloch, K. (1965). The biological synthesis of cholesterol. *Science*, *150*(3692), 19–28. http://doi.org/10.1126/science.150.3692.19

Brunetti-Pierri, N., Corso, G., Rossi, M., Ferrari, P., Balli, F., Rivasi, F., et al. (2002). Lathosterolosis, a novel multiple-malformation/mental retardation syndrome due to deficiency of 3beta-hydroxysteroid-delta5-desaturase. *American Journal of Human Genetics*, *71*(4), 952–958. http://doi.org/10.1086/342668

Chiang, C., Litingtung, Y., Lee, E., Young, K. E., Corden, J. L., Westphal, H., & Beachy, P. A. (1996). Cyclopia and defective axial patterning in mice lacking Sonic hedgehog gene function. *Nature*, *383*(6599), 407–413.

Cooper, M. K., Wassif, C. A., Krakowiak, P. A., Taipale, J., Gong, R., Kelley, R. I., et al. (2003). A defective response to Hedgehog signaling in disorders of cholesterol biosynthesis. *Nat Genet*, *33*(4), 508–513.

Cortes, M., Liu, S. Y., Kwan, W., Alexa, K., Goessling, W., & North, T. E. (2015). Accumulation of the Vitamin D Precursor Cholecalciferol Antagonizes Hedgehog Signaling to Impair Hemogenic Endothelium Formation. *Stem Cell Reports*, *5*(4), 471–479. http://doi.org/10.1016/j.stemcr.2015.08.010

Etheridge, L. A., Crawford, T. Q., Zhang, S., & Roelink, H. (2010). Evidence for a role of vertebrate Disp1 in long-range Shh signaling. *Development*, *137*(1), 133–140. http://doi.org/10.1242/dev.043547

Fitzky, B. U., Witsch Baumgartner, M., Erdel, M., Lee, J. N., Paik, Y. K., Glossmann, H., et al. (1998). Mutations in the Delta7-sterol reductase gene in patients with the Smith-Lemli-Opitz syndrome. *Proc. Natl. Acad. Sci. U. S. a.*, *95*(14), 8181–8186.

Goodrich, L. V., Milenkovic, L., Higgins, K. M., & Scott, M. P. (1997). Altered neural cell fates and medulloblastoma in mouse patched mutants. *Science*, *277*, 1109–1113.

Hausmann, G., Mering, von, C., & Basler, K. (2009). The hedgehog signaling pathway: where did it come from? *PLoS Biol*, *7*(6), e1000146. http://doi.org/10.1371/journal.pbio.1000146

Holick, M. F., & Clark, M. B. (1978). The photobiogenesis and metabolism of vitamin D. *Fed Proc*, *37*(12), 2567–2574.

Incardona, J. P., Gaffield, W., Kapur, R. P., & Roelink, H. (1998). The teratogenic Veratrum alkaloid cyclopamine inhibits sonic hedgehog signal transduction. *Development*, *125*(18), 3553–3562.

Izzi, L., Lévesque, M., Morin, S., Laniel, D., Wilkes, B. C., Mille, F., et al. (2011). Boc and Gas1 each form distinct Shh receptor complexes with Ptch1 and are required for Shh-mediated cell proliferation. *Dev Cell*, *20*(6), 788–801. http://doi.org/10.1016/j.devcel.2011.04.017

Kandutsch, A. A., & Russell, A. E. (1960). Preputial gland tumor sterols. 3. A metabolic pathway from lanosterol to cholesterol. *Journal of Biological Chemistry*, *235*, 2256–2261.

Keeler, R. F. (1969). Teratogenic compounds of Veratrum californicum (Durand). VI. The structure of cyclopamine. *Phytochemistry*, *8*, 223–225.

Krakowiak, P. A., Wassif, C. A., Kratz, L., Cozma, D., Kovárová, M., Harris, G., et al. (2003). Lathosterolosis: an inborn error of human and murine cholesterol synthesis due to lathosterol 5-desaturase deficiency. *Hum Mol Genet*, *12*(13), 1631–1641.

Linder, B., Weber, S., Dittmann, K., Adamski, J., Hahn, H., & Uhmann, A. (2015). A Functional and Putative Physiological Role of Calcitriol in Patched1/Smoothened Interaction. *J. Biol. Chem.*, *290*(32), 19614–19628. http://doi.org/10.1074/jbc.M115.646141

Marigo, V., Davey, R. A., Zuo, Y., Cunningham, J. M., & Tabin, C. J. (1996). Biochemical evidence that patched is the Hedgehog receptor. *Nature*, *384*(6605), 176–179.

Myers, B. R., Neahring, L., Zhang, Y., Roberts, K. J., & Beachy, P. A. (2017). Rapid, direct activity assays for Smoothened reveal Hedgehog pathway regulation by membrane cholesterol and extracellular sodium. *Proc. Natl. Acad. Sci. U. S. a.*, *114*(52), E11141–E11150. http://doi.org/10.1073/pnas.1717891115

Porter, F. D. (2002). Malformation syndromes due to inborn errors of cholesterol synthesis. *J. Clin. Invest.*, *110*(6), 715–724. http://doi.org/10.1172/JCI16386

Porter, F. D., & Herman, G. E. (2011). Malformation syndromes caused by disorders of cholesterol synthesis. *J. Lipid Res.*, *52*(1), 6–34. http://doi.org/10.1194/jlr.R009548

Prabhu, A. V., Luu, W., Sharpe, L. J., & Brown, A. J. (2016). Cholesterol-mediated Degradation of 7-Dehydrocholesterol Reductase Switches the Balance from Cholesterol to Vitamin D Synthesis. *J. Biol. Chem.*, *291*(16), 8363–8373. http://doi.org/10.1074/jbc.M115.699546

Qi, X., Schmiege, P., Coutavas, E., Wang, J., & Li, X. (2018). Structures of human Patched and its complex with native palmitoylated sonic hedgehog. *Nature*, *15*, 3059. http://doi.org/10.1038/s41586-018-0308-7

Ran, F. A., Hsu, P. D., Wright, J., Agarwala, V., Scott, D. A., & Zhang, F. (2013). Genome engineering using the CRISPR-Cas9 system. *Nat Protoc*, *8*(11), 2281–2308. http://doi.org/10.1038/nprot.2013.143

Roberts, B., Casillas, C., Alfaro, A. C., Jägers, C., & Roelink, H. (2016). Patched1 and Patched2 inhibit Smoothened non-cell autonomously. *eLife*, *5*, e17634. http://doi.org/10.7554/eLife.17634

Roessler, E., Belloni, E., Gaudenz, K., Jay, P., Berta, P., Scherer, S. W., et al. (1996). Mutations in the human Sonic Hedgehog gene cause holoprosencephaly. *Nat Genet*, *14*(3), 357–360.

Sharpe, H. J., Wang, W., Hannoush, R. N., & de Sauvage, F. J. (2015). Regulation of the oncoprotein Smoothened by small molecules. *Nat Chem Biol*, *11*(4), 246–255. http://doi.org/10.1038/nchembio.1776

Smith, D. W., Lemli, L., & Opitz, J. M. (1964). A Newly Recognized Syndrome of Multiple Congenital Anomalies. *J. Pediatr.*, *64*(2), 210–217. http://doi.org/10.1016/s0022-3476(64)80264-x

Sokol, J., Blanchette Mackie, J., Kruth, H. S., Dwyer, N. K., Amende, L. M., Butler, J. D., et al. (1988). Type C Niemann-Pick disease. Lysosomal accumulation and defective intracellular mobilization of low density lipoprotein cholesterol. *J. Biol. Chem.*, *263*(7), 3411–3417.

Taipale, J., Chen, J. K., Cooper, M. K., Wang, B., Mann, R. K., Milenkovic, L., et al. (2000). Effects of oncogenic mutations in Smoothened and Patched can be reversed by cyclopamine. *Nature*, *406*(6799), 1005–9.

Taipale, J., Cooper, M. K., Maiti, T., & Beachy, P. A. (2002). Patched acts catalytically to suppress the activity of Smoothened. *Nature*, *418*(6900), 892–897.

Tang, J. Y., Xiao, T. Z., Oda, Y., Chang, K. S., Shpall, E., Wu, A., et al. (2011). Vitamin D3 inhibits hedgehog signaling and proliferation in murine Basal cell carcinomas. *Cancer Prevention Research (Philadelphia, Pa.)*, *4*(5), 744–751. http://doi.org/10.1158/1940-6207.CAPR-10-0285

Tint, G. S. (1993). Cholesterol defect in Smith-Lemli-Opitz syndrome. *Am.J.Med.Genet.*, *47*(4), 573–574. http://doi.org/10.1002/ajmg.1320470429

Tseng, T. T., Gratwick, K. S., Kollman, J., Park, D., Nies, D. H., Goffeau, A., & Saier, M. H. J. (1999). The RND permease superfamily: an ancient, ubiquitous and diverse family that includes human disease and development proteins. *J Mol Microbiol Biotechnol*, *1*(1), 107–125.

Tukachinsky, H., Petrov, K., Watanabe, M., & Salic, A. (2016). Mechanism of inhibition of the tumor suppressor Patched by Sonic Hedgehog. *Proc. Natl. Acad. Sci. U. S. a.*, *113*(40), E5866–E5875. http://doi.org/10.1073/pnas.1606719113

Wassif, C. A., Zhu, P., Kratz, L., Krakowiak, P. A., Battaile, K. P., Weight, F. F., et al. (2001). Biochemical, phenotypic and neurophysiological characterization of a genetic mouse model of RSH/Smith--Lemli--Opitz syndrome. *Hum Mol Genet*, *10*(6), 555–564. http://doi.org/10.1093/hmg/10.6.555

Wichterle, H., Lieberam, I., Porter, J. A., & Jessell, T. M. (2002). Directed differentiation of embryonic stem cells into motor neurons. *Cell*, *110*(3), 385–397.

Chapter 5

Conclusions and Open Questions

Since its discovery in late 1970s, Hh signaling has been extensively studied (Nüsslein-Volhard & Wieshaus, 1980). Nevertheless, several key questions remain largely unresolved. Two of these open questions were the focus of this dissertational research: Does Shh have a peptidase activity that facilitates its release from the cell, and how does the Hh receptor Ptch1/2 inhibit the GPCR and signal transducer Smo?

What does Ptch1/2 transport?

The holy grail in the field of Shh signaling has been the cargo for the Shh receptor and putative RND transporter Ptch1/2. The consensus is that the cargo is a sterol, but the exact nature of the Smo-inhibitory molecule has not been conclusively demonstrated. Among possible candidates are cholesterol, cholesterol precursors, and their derivatives. Ptch1 can transport cholesterol from the cytosol into the extracellular space as well as from the inner to the outer leaflet in a fashion reminiscent of membrane lipid flippases (Bidet et al., 2011; Y. Zhang et al., 2018b). Neither cholesterol in the extracellular space nor its removal from the inner leaflet, however, was directly shown to inhibit Smo. In addition, the changes in sterol composition of the cell membrane cannot account for non-cell autonomous signaling that I describe in this thesis (Chapter 4). A possible Smo-inhibitory cholesterol precursor addressed in this thesis, 7DHC, is a candidate as a cargo of Ptch1/2, as it inhibits Smo non-cell autonomously and its potency is increased in the presence of Ptch1/2. We cannot, however, exclude that 7DHC is modified spontaneously or enzymatically to a different sterol.

Given the variety of cargos known for other RND transporters and the numerous examples of Smo-modulating molecules it is likely that Ptch1/2 can flux several related sterols that can inhibit Smo.

The structure of Ptch1 and binding to ShhNp

Ptch1/2 belong to a family of RND transporters, a large family present in all domains of life. Some possible properties of Ptch1/2 are inferred from observations of other members of this family (Tseng et al., 1999). RND transporters like the bacterial AcrB, vertebrate Disp, and *Drosophila* Ptc function as trimers (Lu, Liu, & Kornberg, 2006), but trimerization of vertebrate Ptch1/2 has not been demonstrated. Due to its size and large number of hydrophobic transmembrane domains, early crystallographic studies of Ptch1 contained only monomers, often incomplete or assembled from two or more pieces. With the advent of more advanced methods, not requiring the packaging of proteins into crystals, like cryo-electron microscopy (cryoEM), more complex structural models including most of the protein sequence of Ptch1 have emerged. A structure of two Ptch1 molecules shows that dimerization is feasible and can be happen simultaneous to Shh binding (Qi, Schmiege, Coutavas, & Li, 2018a; Qi, Schmiege, Coutavas, Wang, & Li, 2018b). It does not, however, explain any advantages for its transporter function. Ptch1 molecules assembled into a homotrimer based on the model of known RNDs would elegantly explain ion transport through the channel of individual molecules with the transport of bigger molecules like sterols through the pore formed in the center of the trimer (Figure 1). When modeled *in silico* on existing structures of other RND trimers like AcrB, 3 Ptch1 monomers (PDB: 6OEU) fit seamlessly into a trimer without producing any apparent clashes. Nevertheless,

when ShhN is included in this model, the structure of ShhN partially overlaps with the extracellular domains of Ptch1, indicating that the model of the trimer and its binding to ShhN needs refinement.

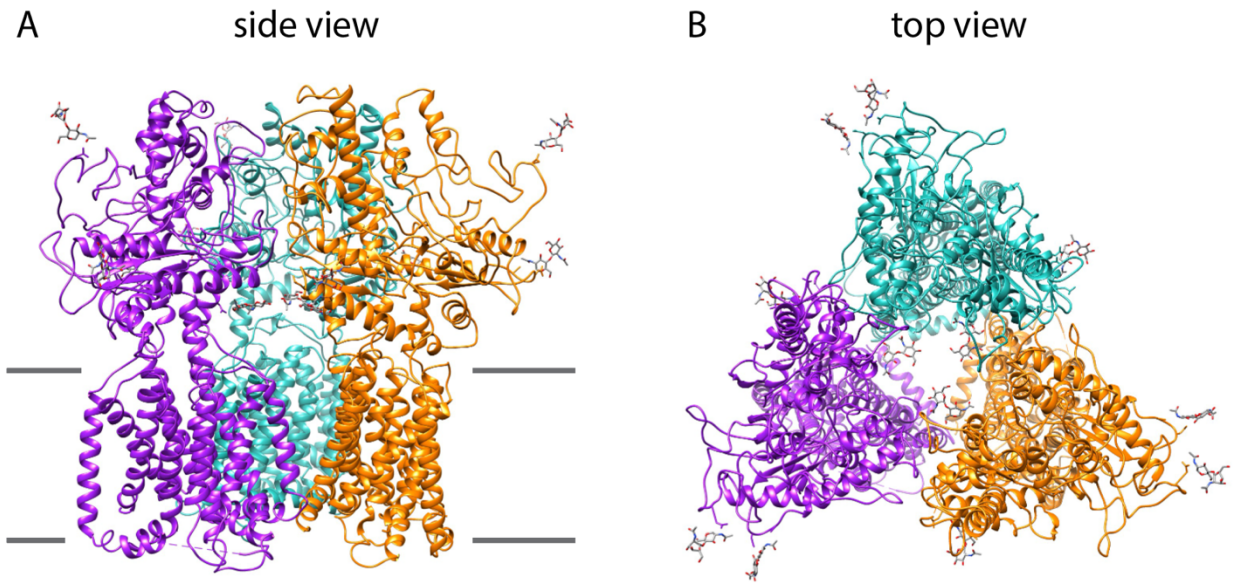

Figure 1. Reconstruction of a putative Ptch1 trimer. Three Ptch1 monomers (PDB 6OEU) were modeled *in silico* on an existing AcrB trimer structure (PDB 2DHH).

Shh appears to bind to Ptch1 with two different sites, the palmitoylated N-terminus and the zinc coordination center (Qi, Schmiege, Coutavas, & Li, 2018a; Qi, Schmiege, Coutavas, Wang, & Li, 2018b). The N-terminal 22 amino acids including the palmitoyl are sufficient to insert into the putative proton channel of Ptch1 (Qi, Schmiege, Coutavas, Wang, & Li, 2018b; Tukachinsky, Petrov, Watanabe, & Salic, 2016). This is presumably achieved through insertion and blocking of the proton channel of Ptch1 by the Shh N-terminus, abrogating the proton-driven antiporter function of the putative Smo inhibitor.

The second site of Shh binding to Ptch1 is the zinc coordination center, which binds to the two extracellular domains (ECD) of Ptch1. A mutant form of Ptch1 missing the second ECD (Ptch1Δloop2) acts in a dominant negative fashion in the developing chicken neural tube whose inhibitory function cannot be blocked by Shh, suggesting that this domain and binding site is required for Shh-mediated blocking of Ptch1 function (Briscoe et al., 2001). The interaction of the Shh zinc coordination center with the extracellular domains of Ptch1 causes an internalization of the complex (Incardona et al., 2000). N-terminally truncated Shh can bind Ptch1 with similar affinity as untruncated Shh, and N-terminal truncation does not affect Ptch1 internalization, suggesting that the N-terminus of Shh is dispensable for Ptch1 internalization (Williams et al., 1999). The monoclonal antibody 5E1 binds Shh at the zinc coordination center and blocks internalization, supporting the notion that access to the zinc coordination domain is required for internalization. When the zinc coordination center of Shh is already bound to 5E1, however, the large alpha helix of Shh on the opposite side of the protein seems to substitute as an alternative Ptch1 binding site

(Qi, Schmiege, Coutavas, Wang, & Li, 2018b). Furthermore, the structure of 2 Ptch1 molecules in complex with ShhN showed the morphogen being intercalated between the two Ptch1 monomers with both possible Ptch1 binding sites of ShhN being in contact with Ptch1 (Qi, Schmiege, Coutavas, & Li, 2018a). Intriguingly, the structure showed insertion of the Shh N-terminus into the pore of one Ptch1 molecule and binding of the zinc coordination center to the other, further strengthening the idea that the mode and function of Shh binding to Ptch1 is two-pronged.

It was recently demonstrated that the extracellular domain 1 (ECD1) of Ptch1 has a V-shaped hydrophobic cavity that can accommodate the ShhNp-linked cholesterol, offering a third binding site for Shh (Rudolf et al., 2019). This interaction enhances the ability of Shh to inactivate Ptch1 and trigger a Hh response. Furthermore, the cholesterol modified C-terminal 7 amino acids of Shh are sufficient to enhance the Hh response to the palmitoylated N-terminal 15 amino acids without the need for the globular core protein, indicating that the two lipid binding sites in Ptch1 are allosterically linked. These observations indicate that Shh can block Ptch1 function in a pincer grasp mechanism (Rudolf et al., 2019). Interestingly, the connector peptide of Shh linking the globular core of the protein with cholesterol is evolutionarily conserved and required for insertion of the cholesterol moiety into the ECD1 of Ptch1 (Rudolf et al., 2019). BacHh lack this linker domain, further indicating that the C-terminal cholesterol modified tail of Shh is required for receptor interaction and not for the putative peptidase activity.

The functional implications for the two lipid- and the core protein-mediated interactions of Shh with Ptch1 are complex, as all of them are sufficient but none is essential to trigger the Hh response in target cells. This might reflect different signaling environments and is discussed in more detail below.

Does Shh maturation and release from the cell require self-cleavage?

Many BacHh proteins are modular and have large N- or C-terminal appendages to their peptidase domain like Ig-like repeats, integral membrane proteins, or other peptidases (Roelink, 2018). It is conceivable that BacHhs are zymogens and that these appendages are removed through self-cleaving events before the peptidase is fully activated to cleave intended targets. We and others observed the removal of a C-terminal portion of cholesterol-modified and unmodified Shh concurrent with the release of Shh to either the medium or the extracellular matrix (Jakobs et al., 2014; 2017). We estimate this cleavage to take place close to the equivalent of the bacterial stop codon in the evolutionarily conserved linker domain of Shh. An early crystallographic model of Shh reported the association of this linker domain of one molecule with the zinc coordination center of a second molecule, showing a conceivable mechanism for intermolecular self-cleavage akin to that of the Hh analog thermolysin (Gao et al., 2010; Hall, Porter, Beachy, & Leahy, 1995). Furthermore, the peptidase-dead mutant Shh-E177A forms more and bigger Shh oligomers (Himmelstein et al., 2017). Although the mechanism and function of oligomerization of Shh remains largely unresolved, it might hint at a possible environment for self-cleavage which Shh-E177A without peptidase function cannot resolve and escape.

Release of Shh from the producing cell may involve yet another removal of a part of Shh, either a short peptide sequence or a post-translational modification. When dynamin-mediated endocytosis is blocked with the small-molecule inhibitor Dynasore, we detected a slightly larger form of Shh in the cell-only fraction but not in the medium or the ECM (see Chapter 2, Figure 1F). This form of Shh probably represents a short-lived form on the cell membrane that rapidly disappears through endocytosis and associated trimming of the protein. Unstable versions of Shh like the zinc coordination mutants do not have this form, presumably due to their degradation prior to presentation on the cell membrane. In *Drosophila*, Hh travels to the apical cell membrane and is internalized by the same cell prior to its release at the basolateral side of the cell, a mechanism that could represent one possible exit route for Shh in mammalian cells as well (Callejo et al., 2011).

Does Shh cleave Heparan-Sulfate Proteoglycans?

Both bacterial peptidoglycans in the cell wall and proteoglycans in the ECM of multicellular organisms are large molecules where peptides are attached to glycans. HSPGs can bind Shh, thereby regulating the Hh response either positively or negatively (Capurro et al., 2008; Carrasco, Olivares, Faunes, Oliva, & Larraín, 2005). It is therefore possible that a functional conservation between BacHhs and Shh is reflected in the ability to cleave proteoglycans. As the peptide chains intercalating the long glycan chains in bacterial peptidoglycan are relatively short (3-5 amino acids), BacHhs presumably exert their peptidase function close to the glycan chains. The HSPG Glypican 5 emerged as a potential, albeit not unique, target for Shh-mediated cleavage as it is one of the more important HSPG core proteins affecting Shh distribution and signaling (Guo & Roelink, 2019). Shh can bind heparan sulfate at two distinct sites, the Cardin-Weintraub motif close to the N-terminus and at a region in the globular core, that would predict a potential cleavage site close to the glycosylation sites of the HSPG core protein (Farshi et al., 2011; Whalen et al., 2013). As multiple Shh molecules can bind a short stretch of heparan sulfate, the interaction of Shh and Glypican 5 is conceivably non-stochiometric (Whalen et al., 2013). Intriguingly, the glycosylated serine residues of the Glypican 5 core protein are conserved with other Glypicans and clustered near a stretch of acidic residues that can also be found in HS-modified Neurexins. In synapse formation, Neurexins have been hypothesized as potential targets for Shh function (Courchet & Polleux, 2012; P. Zhang et al., 2018a). Neurexin 3 is released from the cell as a soluble form through cleavage by the zinc-peptidases ADAM10 and -17 between the acidic residues and the glycosylated serine residues (Borcel et al., 2016). This suggests that Neurexins could also be targets for the Shh peptidase and that the cleavage site could be at a similar location between the acidic stretch and HS-modified serine residues.

The possibility of a peptidase function for Shh is of great significance not only for the elucidation of developmental and tumor-inducing mechanisms but also for a potential class of new Shh inhibitors with clinical relevance. Beta-lactam antibiotics like penicillin are highly efficient inhibitors of DD-peptidases and a similar class of molecules could be used in the treatment of cancers with underlying increased Shh peptidase activity (Tipper, 1985). Robotnikinin is a potent inhibitor of the transcriptional Hh response and is hypothesized to bind Shh at the zinc coordination center (Hitzenberger, Schuster, & Hofer,

2017; Stanton et al., 2009). It is also predicted to not interfere with Shh binding to Ptch1, suggesting that it might block the putative Shh peptidase activity.

The lipid modifications of Shh – functional requirements or accessories?

All Hh ligands receive two lipid modifications in the ER and Golgi, a palmitoyl moiety at the N-terminus and a cholesterol moiety at the C-terminus that tether them to the cell membrane. The palmitoylated N-terminal 22 amino acids can block Ptch1 activity, and the C-terminal cholesterol may have an auxiliary role in Ptch1/2 blocking via binding to an allosteric site in the extracellular domain of Ptch1 (Rudolf et al., 2019; Tukachinsky et al., 2016). Seemingly contradictory studies have shown that both the N- and C-terminus of Shh are removed in the process of releasing Shh from the producing cell, the shedding process (Jakobs et al., 2014; 2017). How can these observations be combined? The signaling context is presumably determinative on the form of Shh, meaning that different forms of Shh could exert different functions at different locations. Shh without lipid modifications is soluble and can either diffuse freely as a monomer or bind to HSPGs. Here, the putative peptidase activity could have a second role in releasing Shh from one HSPG so that it can move on to the next, similar to a conveyor belt. This form of Shh could potentially cover great distances. It can block Ptch1 activity and elicit a Hh pathway response, but the missing lipid modifications render it less potent (Tukachinsky et al., 2016). Shh in exosomes, liposomes, or cytonemes on the other hand is predicted to be dually lipid-modified and therefore a potent inhibitor of Ptch1/2 function. The distance that this form of Shh can travel, in particular on cytonemes, would only be several cell diameters, keeping it relatively close to the site of Shh expression. Hence, the different modes of transport and forms of Shh could provide additional information for responding cells and aid in the fine-tuning of the graded Hh response by increasing the difference in response to the morphogen gradient.

References
9

Bidet, M., Joubert, O., Lacombe, B., Ciantar, M., Nehmé, R., Mollat, P., et al. (2011). The hedgehog receptor patched is involved in cholesterol transport. *PLoS One*, *6*(9), e23834. http://doi.org/10.1371/journal.pone.0023834

Briscoe, J., Chen, Y., Jessell, T. M., & Struhl, G. (2001). A hedgehog-insensitive form of patched provides evidence for direct long-range morphogen activity of sonic hedgehog in the neural tube. *Mol Cell*, *7*(6), 1279–1291. https://doi.org/10.1016/S1097-2765(01)00271-4

Borcel, E., Palczynska, M., Krzisch, M., Dimitrov, M., Ulrich, G., Toni, N., & Fraering, P. C. (2016). Shedding of neurexin 3β ectodomain by ADAM10 releases a soluble fragment that affects the development of newborn neurons. *Scientific Reports*, *6*(1), 39310. http://doi.org/10.1038/srep39310

Callejo, A., Bilioni, A., Mollica, E., Gorfinkiel, N., Andrés, G., Ibáñez, C., et al. (2011). Dispatched mediates Hedgehog basolateral release to form the long-range morphogenetic gradient in the Drosophila wing disk epithelium. *Proc. Natl. Acad. Sci. U. S. a.*, *108*(31), 12591–12598. http://doi.org/10.1073/pnas.1106881108

Capurro, M. I., Xu, P., Shi, W., Li, F., Jia, A., & Filmus, J. (2008). Glypican-3 inhibits Hedgehog signaling during development by competing with patched for Hedgehog binding. *Dev Cell*, *14*(5), 700–711. http://doi.org/10.1016/j.devcel.2008.03.006

Carrasco, H., Olivares, G. H., Faunes, F., Oliva, C., & Larraín, J. (2005). Heparan sulfate proteoglycans exert positive and negative effects in Shh activity. *J Cell Biochem*, *96*(4), 831–838. http://doi.org/10.1002/jcb.20586

Courchet, J., & Polleux, F. (2012). Sonic hedgehog, BOC, and synaptic development: new players for an old game. *Neuron*, *73*(6), 1055–1058. http://doi.org/10.1016/j.neuron.2012.03.008

Farshi, P., Ohlig, S., Pickhinke, U., Höing, S., Jochmann, K., Lawrence, R., et al. (2011). Dual roles of the Cardin-Weintraub motif in multimeric Sonic hedgehog. *J. Biol. Chem.*, *286*(26), 23608–23619. http://doi.org/10.1074/jbc.M110.206474

Gao, X., Wang, J., Yu, D.-Q., Bian, F., Xie, B.-B., Chen, X.-L., et al. (2010). Structural basis for the autoprocessing of zinc metalloproteases in the thermolysin family. *Proc. Natl. Acad. Sci. U. S. a.*, *107*(41), 17569–17574. http://doi.org/10.1073/pnas.1005681107

Guo, W., & Roelink, H. (2019). Loss of the Heparan Sulfate Proteoglycan Glypican5 facilitates long-range Shh signaling. *Stem Cells*. http://doi.org/10.1002/stem.3018

Hall, T. M., Porter, J. A., Beachy, P. A., & Leahy, D. J. (1995). A potential catalytic site revealed by the 1.7-A crystal structure of the amino-terminal signalling domain of Sonic hedgehog. *Nature*, *378*(6553), 212–216. http://doi.org/10.1038/378212a0

Himmelstein, D. S., Cajigas, I., Bi, C., Clark, B. S., Van Der Voort, G., & Kohtz, J. D. (2017). SHH E176/E177-Zn(2+) conformation is required for signaling at endogenous sites. *Dev. Biol.*, *424*(2), 221–235. http://doi.org/10.1016/j.ydbio.2017.02.006

Hitzenberger, M., Schuster, D., & Hofer, T. S. (2017). The Binding Mode of the Sonic Hedgehog Inhibitor Robotnikinin, a Combined Docking and QM/MM MD Study. *Frontiers in Chemistry*, *5*, 76. http://doi.org/10.3389/fchem.2017.00076

Incardona, J. P., Lee, J. H., Robertson, C. P., Enga, K., Kapur, R. P., & Roelink, H. (2000). Receptor-mediated endocytosis of soluble and membrane-tethered Sonic hedgehog by Patched-1. *Proceedings of the National Academy of Sciences of the United States of America*, *97*(22), 12044–12049. http://doi.org/10.1073/pnas.220251997

Jakobs, P., Exner, S., Schürmann, S., Pickhinke, U., Bandari, S., Ortmann, C., et al. (2014). Scube2 enhances proteolytic Shh processing from the surface of Shh-producing cells. *Journal of Cell Science*, *127*(Pt 8), 1726–1737. http://doi.org/10.1242/jcs.137695

Jakobs, P., Schulz, P., Schürmann, S., Niland, S., Exner, S., Rebollido-Rios, R., et al. (2017). Ca2+ coordination controls sonic hedgehog structure and its Scube2-regulated release. *Journal of Cell Science*, *130*(19), 3261–3271. http://doi.org/10.1242/jcs.205872

Lu, X., Liu, S., & Kornberg, T. B. (2006). The C-terminal tail of the Hedgehog receptor Patched regulates both localization and turnover. *Genes and Development*, *20*(18), 2539–2551.

Nüsslein-Volhard, C., & Wieshaus, E. (1980). Mutations affecting segment number and polarity in Drosophila. *Nature*, *287*, 795–801.

Qi, X., Schmiege, P., Coutavas, E., & Li, X. (2018a). Two Patched molecules engage distinct sites on Hedgehog yielding a signaling-competent complex. *Science*, *112*(6410), eaas8843. http://doi.org/10.1126/science.aas8843

Qi, X., Schmiege, P., Coutavas, E., Wang, J., & Li, X. (2018b). Structures of human Patched and its complex with native palmitoylated sonic hedgehog. *Nature*, *15*, 3059. http://doi.org/10.1038/s41586-018-0308-7

Roelink, H. (2018). Sonic Hedgehog Is a Member of the Hh/DD-Peptidase Family That Spans the Eukaryotic and Bacterial Domains of Life. *Journal of Developmental Biology*, *6*(2), 12. http://doi.org/10.3390/jdb6020012

Rudolf, A. F., Kinnebrew, M., Kowatsch, C., Ansell, T. B., Omari, El, K., Bishop, B., et al. (2019). The morphogen Sonic hedgehog inhibits its receptor Patched by a pincer grasp mechanism. *Nat Chem Biol*, *15*(10), 975–982. http://doi.org/10.1038/s41589-019-0370-y

Stanton, B. Z., Peng, L. F., Maloof, N., Nakai, K., Wang, X., Duffner, J. L., et al. (2009). A small molecule that binds Hedgehog and blocks its signaling in human cells. *Nat Chem Biol*, *5*(3), 154–156.

Tipper, D. J. (1985). Mode of action of beta-lactam antibiotics. *Pharmacol Ther*, *27*(1), 1–35. http://doi.org/10.1016/0163-7258(85)90062-2

Tseng, T. T., Gratwick, K. S., Kollman, J., Park, D., Nies, D. H., Goffeau, A., & Saier, M. H. J. (1999). The RND permease superfamily: an ancient, ubiquitous and diverse family that includes human disease and development proteins. *J Mol Microbiol Biotechnol*, *1*(1), 107–125.

Tukachinsky, H., Petrov, K., Watanabe, M., & Salic, A. (2016). Mechanism of inhibition of the tumor suppressor Patched by Sonic Hedgehog. *Proc. Natl. Acad. Sci. U. S. a.*, *113*(40), E5866–E5875. http://doi.org/10.1073/pnas.1606719113

Whalen, D., Malinauskas, T., Gilbert, R. J. C., Siebold, C. (2013). Structural insights into proteoglycan-shaped Hedgehog signaling. *Proc. Natl. Acad. Sci. U. S. a.*, *110*(41), 16420–16425. http://doi.org/10.1073/pnas.1310097110

Williams, K. P., Rayhorn, P., Chi-Rosso, G., Garber, E. A., Strauch, K. L., Horan, G. S., et al. (1999). Functional antagonists of sonic hedgehog reveal the importance of the N terminus for activity. *J Cell Sci*, *112*(Pt 23), 4405–4414.

Zhang, P., Lu, H., Peixoto, R. T., Pines, M. K., Ge, Y., Oku, S., et al. (2018a). Heparan Sulfate Organizes Neuronal Synapses through Neurexin Partnerships. *Cell*, *174*(6), 1450–1464.e23. http://doi.org/10.1016/j.cell.2018.07.002

Zhang, Y., Bulkley, D. P., Xin, Y., Roberts, K. J., Asarnow, D. E., Sharma, A., et al. (2018b). Structural Basis for Cholesterol Transport-like Activity of the Hedgehog Receptor Patched. *Cell*, *175*(5), 1352–1364.e14. http://doi.org/10.1016/j.cell.2018.10.026